https://doi.org/10.15388/vu.thesis.183
https://orcid.org/0000-0002-8444-0403

VILNIUS UNIVERSITY

Arūnas
KRIKŠTAPONIS

Investigation of the catabolism of 7-hydroxycoumarin in *Pseudomonas mandelii* 7HK4 bacteria

DOCTORAL DISSERTATION

Natural sciences,
Biochemistry (N 004)

VILNIUS 2021

This dissertation was written between 2016 and 2020 at the Department of Molecular Microbiology and Biotechnology, Institute of Biochemistry, Life Sciences Center, Vilnius University. The research was supported by the European Union's Horizon 2020 research and innovation program [BlueGrowth: Unlocking the potential of Seas and Oceans] under grant agreement No. 634486 (project acronym INMARE) and by European Regional Development Fund (project No 01.2.2-LMT-K-718-03-0082) under grant agreement with the Research Council of Lithuania (LMTLT).

Academic supervisor:

Prof. Dr. Rolandas Meškys (Vilnius University, natural sciences, biochemistry – N 004).

https://doi.org/10.15388/vu.thesis.183
https://orcid.org/0000-0002-8444-0403

VILNIAUS UNIVERSITETAS

Arūnas
KRIKŠTAPONIS

7-Hidroksikumarino katabolizmo *Pseudomonas mandelii* 7HK4 bakterijose tyrimas

DAKTARO DISERTACIJA

Gamtos mokslai,
Biochemija (N 004)

VILNIUS 2021

Disertacija rengta 2016–2020 metais Vilniaus universiteto Gyvybės mokslų centro Biochemijos institute, Molekulinės mikrobiologijos ir biotechnologijos skyriuje. Mokslinius tyrimus rėmė ES bendroji mokslinių tyrimų ir inovacijų programa Horizon 2020 [BlueGrowth: Unlocking the potential of Seas and Oceans] pagal dotacijos sutartį Nr. 634486 (projekto akronimas INMARE) ir Europos regioninės plėtros fondas (projekto Nr. 01.2.2-LMT-K-718-03-0082) pagal dotacijos sutartį su Lietuvos mokslų taryba (LMTLT).

Mokslinis vadovas:

Prof. Dr. Rolandas Meškys (Vilniaus universitetas, gamtos mokslai, biochemija – N 004)

CONTENT

LIST OF ABBREVIATIONS

6HK	6-Hydroxycoumarin
67DHK	6,7-Dihydroxycoumarin
7HK	7-Hydroxycoumarin
7MK	7-Methylcoumarin
CYP	Cytochrome P_{450} monooxygenase
DCH	Dihydrocoumarin hydrolase
DHFP	3-(2,4-Dihydroxyphenyl) propionic acid
DPPH	2,2-Diphenyl-1-picrylhydrazyl-
ER	Ene-reductase
FMO	Flavin-binding monooxygenase
GLC	Glucose
IC_{50}	The half maximal inhibitory concentration
KUM	Coumarin
NADH	Nicotinamide adenine dinucleotide
NADPH	Nicotinamide adenine dinucleotide phosphate
MDR	Medium chain dehydrogenase/reductase
OYE	Old yellow enzyme
SDR	Short chain dehydrogenase/reductase

INTRODUCTION

Coumarin group compounds are naturally occurring heterocyclic compounds. For example, 7-hydroxycoumarin, also known as umbelliferone, is one of the most abundant plant-derived secondary metabolites, and is found in celery, cumin, parsley, fennel, and other plants [1–3]. When damaged, plants produce a high diversity of natural coumarins as a defence mechanism against insect herbivores as well as fungal and microbial pathogens [4]. For example, hydroxycoumarins have antibacterial activity against *Ralstonia solanacearum*, *Escherichia coli*, *Klebsiella pneumoniae*, *Staphylococcus aureus*, and *Pseudomonas aeruginosa* [4–8]. Notably, 7-hydroxycoumarin exhibits a wider spectrum of biological activities than any other homologous coumarin. Hence, 7-hydroxycoumarin shows not only antibacterial and antifungal properties, but it is also a good antioxidant, an effective chemotherapeutic agent against colon and laryngeal cancers, and a strong UV light absorber making it ideal for the production of sunscreens. In addition, 7-hydroxycoumarin is a parent compound of other, more complex pharmacologically active furanocoumarins and pyranocoumarins in higher plants [3]. Keeping in mind a wide spreading of coumarins in biosphere, there is a great interest in understanding of biodegradation of this group of compounds particularly in soil.

It has been shown previously that a number of soil microorganisms, such as *Pseudomonas*, *Arthrobacter*, *Aspergillus*, *Penicillium*, and *Fusarium* spp. can grow on coumarin as a sole source of carbon [9–16]. The key intermediate during coumarin catabolism in bacteria is 3-(2-hydroxyphenyl) propionic acid [10,11,16]. The bioconversion of coumarin to 3-(2-hydroxyphenyl) propionic acid can be achieved in two different metabolic pathways. Bacteria belonging to the *Arthrobacter* genus enzymatically hydrolyse the lactone moiety to give 3-(2-hydroxyphenyl)-2-propenoic acid, and then reduce a double bond by using a NADH-dependent enzyme to yield 3-(2-hydroxyphenyl) propionic acid [11]. In the case of *Pseudomonas* sp. 30-1 and *Aspergillus niger* ATCC 11394 cells, coumarin is initially reduced to dihydrocoumarin by a NADH-dependent oxidoreductase and only then is enzymatically hydrolysed [9,10,14]. *Arthrobacter* and *Pseudomonas* species are capable of oxidizing 3-(2-hydroxyphenyl) propionic acid to 3-(2,3-dihydroxyphenyl) propionic acid by using specific flavin-binding aromatic hydroxylases [16]. However, no data are available on further conversions of 3-(2,3-dihydroxyphenyl) propionic acid in these bacteria. Also, no microorganisms or enzymes implicated in the metabolism of any hydroxycoumarin including umbelliferone have been identified to date.

Thus, to expand the existing fundamental knowledge about bacterial degradation of hydroxycoumarins and to identify the unique enzymes that may be adapted to selective and specific bioconversion reactions of pharmacologically active compounds, **the aim of this work** was to identify genes encoding enzymes involved in degradation of 7-hydroxycoumarin, and to propose the catabolic pathway of hydroxycoumarins in bacteria.

The main tasks of this work were:

- Identify the genes encoding enzymes involved in degradation of 7-hydroxycoumarin in *Pseudomonas mandelii* 7HK4 bacteria.
- Characterize the enzymes responsible of 7-hydroxycoumarin degradation in *Pseudomonas mandelii* 7HK4 bacteria.
- Define the catabolic pathway of 7-hydroxycoumarin in *Pseudomonas mandelii* 7HK4 bacteria.

Scientific novelty

Notwithstanding the importance of coumarins and numerous attempts to elucidate the fate of such compounds in environment, only partially characterized metabolic pathways of coumarin were described in several soil bacteria. Moreover, even though the catabolic enzymes were partially purified and intermediate metabolites were identified, the genes responsible for the first stages of coumarin degradation were not identified. Particularly, a catabolism of 7-hydroxycoumarin was not explored at all.

Therefore, here we described a 7-hydroxycoumarin catabolic pathway in *Pseudomonas mandelii* 7HK4 bacteria. New metabolites and genes responsible for the degradation of 7-hydroxycoumarin have been isolated and identified. Our results show that the degradation of 7-hydroxycoumarin in *Pseudomonas mandelii* 7HK4 involves a distinct metabolic pathway, compared to the previously characterized catabolic routes for coumarin in *Pseudomonas*, *Arthrobacter* and *Aspergillus* species.

New gene responsible for the reduction of 7-hydroxycoumarin has been isolated and identified. Our results show that the reduction of 7-hydroxycoumarin in *Pseudomonas mandelii* 7HK4 involves a similar approach like in the previously characterized coumarin catabolic routes in *Pseudomonas* sp. 30-1 and *Aspergillus niger* ATCC 11394. However, 7HK4 bacteria employ a unique NADPH-dependent alcohol dehydrogenase family protein HcdE for the reduction of the C-3/C-4 double bond of 7-hydroxycoumarin lactone moiety forming 7-hydroxy-3,4-dihydrocoumarin.

HcdE dehydrogenase described in this work has a significantly distant sequence homology from the previously characterized enzyme implicated in the degradation of structurally similar substrate, such as 8-hydroxycoumarin in *Pseudomonas putida* 86. HcdE dehydrogenase is, to our best knowledge, the first ene-reductase of MDR family involved in the *in vivo* degradation of coumarin compounds.

Further, it has been shown that *Pseudomonas mandelii* 7HK4 bacteria employ another unique enzyme – a flavin-binding *ipso*-hydroxylase HcdA for the oxidation of the aromatic ring of 3-(2,4-dihydroxyphenyl) propionic acid. We showed that later compound is then converted to (2*E*,4*E*)-2,4-dihydroxy-6-oxonona-2,4-dienedioic acid by extradiol dioxygenase HcdB. Finally, we demonstrated that the ring cleavage product of HcdB protein is subsequently hydrolysed by the putative HcdC hydroxymuconic semialdehyde hydrolase. None of these proteins have substantial sequence homology to the previously characterized enzymes implicated in the degradation of structurally similar substrates, such as 3-(2-hydroxyphenyl) propionic acid in *Rhodococcus* sp. V49, 3-(3-hydroxyphenyl) propionic acid and 3-hydroxycinnamic acid in *E. coli* K-12, *Comamonas testosteroni* TA441, *Rhodococcus globerulus* PWD1, or even 4-hydroxyphenylacetate in *Escherichia coli* W.

Thus, our results provide a fundamentally new insight into the degradation of hydroxycoumarins by the soil microorganisms. In addition, the discovered new bacteria and enzymes can be further employed for the development of novel biocatalytic processes useful for industry.

The statements to be defended:

- A *hcd* gene cluster of *Pseudomonas mandelii* 7HK4 bacteria encodes enzymes required for the degradation of 7-hydroxycoumarin.
- NADPH-dependent alcohol dehydrogenase HcdE reduces 7-hydroxycoumarin to 7-hydroxy-3,4-dihydrocoumarin.
- *Ipso*-monooxygenase HcdA oxidizes 3-(2,4-dihydroxyphenyl) propionic acid to 3-(2,3,5-trihydroxyphenyl) propionic acid.
- HcdB extradiol dioxygenase oxidizes 3-(2,3,5-trihydroxyphenyl) propionic acid to (2*E*,4*E*)-2,4-dihydroxy-6-oxonona-2,4-dienedioic acid.
- Putative hydroxymuconic semialdehyde hydrolase HcdC hydrolyses (2*E*,4*E*)-2,4-dihydroxy-6-oxonona-2,4-dienedioic acid.

1. LITERATURE OVERVIEW

Coumarin is a naturally occurring benzopyran-2-one (Fig. 1). This compound was first discovered in 1820 in the plants of *Dipteryx odorata* [17], but the name originated only a century after the name of the genus *Coumarouna odorata*, because only then its physiological role in living organisms was clarified. More than a thousand coumarin derivatives are now known and described, from the simplest with hydroxy groups and alkyl side groups to the most complex ones with benzoyl, furanoyl, pyranoyl, or other larger side groups [18].

1.1. Occurrence and functions of coumarins in nature

Coumarins are found in grass, flowering, citrus, spice and other widespread plants in nature, and many structures have already been described [19]. They are detectable in the roots, stems, leaves, and fruits of plants [20]. There have been many reports on the effect of simple coumarin in plants, at the organ, tissue or cellular levels [21]. Many researches tend to demonstrate that coumarin acts as a plant hormone. However, until now there is a lack of evidence for a physiological or molecular function in plant tissues.

Ubiquitous hydroxylated coumarins are involved in plant responses to stressors like salicylic acid [22,23]. Some hydroxylated coumarins also demonstrate radical scavenging properties toward reactive oxygen species and may be involved in the reduction of oxidative stress in plant cells [24]. In addition, 7-hydroxy-8-methoxycoumarin, also known as hydrangetin (Fig. 1), had been described as a protein kinase inhibitor [25], thus functioning during cold acclimatization [26]. This might be the first illustration of a coumarin involved in hormone-like signalling [21].

There have been reports on many other minor coumarins in the phytochemical articles. Amongst this vast chemical variety, methylenedioxy-substituted coumarins (e.g., ayapin), prenylated coumarins (e.g., osthole and puberulin), the linear or angular types of furanocoumarins (e.g., psoralen, xanthotoxin, angelicin) and pyranocoumarins (e.g., xanthyletin) need to be mentioned [21] (Fig. 1). Such compounds are difficult to detoxify by phytopathogenic microorganisms [27], which supports their role as phytoalexins.

Due to the pleasant smell (e.g., vanilla-like odour), coumarins have been commonly used as flavouring agents in the past. However, their toxic properties were subsequently determined [20], therefore the use of coumarins as a food additive was banned. Still, the toxicity of coumarins allowed the use of coumarin derivatives in pesticide production [18,28]. For example, the addition

of the ethylene group into the benzene ring of 7-hydroxycoumarin produces psoralen, which is converted to a toxin when exposed to ionizing radiation. Psoralen binds to dsDNA and creates covalent cross-links primarily with thymidine residues, therefore interferes with DNA transcription and repair processes [29]. Other coumarins can also act as strong anticoagulants [30].

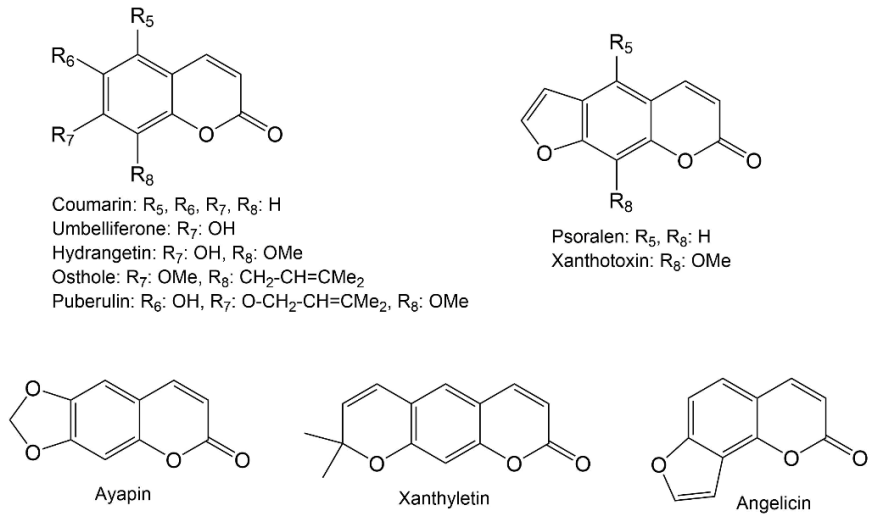

Figure 1. Types of coumarins found in higher plants.

Basic coumarin derivatives are found in plants in free form or as glucoside derivatives. Typically, there are 5 to 10 different coumarin derivatives of one type in one plant species. In addition, the amount of coumarin in the plant also depends on the growth stage of the plant. To date, there is only one possible explanation for why these compounds are so prevalent in plants. In the course of plant evolution, coumarin toxicity [20] and bitter taste are thought to have become the only weapon of plants against herbivores and phytopathogenic microorganisms. But it should be kept in mind that co-evolution of phytopathogenic microorganisms also took place: several metabolic pathways have been found in them, in which xenobiotics are processed and used as carbon and energy sources or removed from the body [18].

1.1.1. Important bioactivities of 7-hydroxycoumarin

7-Hydroxycoumarin, also known as umbelliferone, is one of the most abundant coumarin in plants. The umbelliferae family consists of many economically important herbs such as sanicle, alexanders, angelica, asafoetica, celery, cumin, fennel, parsley and giant hogweed. The name Umbelliferone was derived from the umbelliferae family of plants, however

latter they were named for their umbrella-shaped inflorescences phenomena [31,32]. It is a pharmacologically active compound, for example, it acts as an inhibitor of the 17β-hydroxysteroid dehydrogenases (17β-HSDs) to block the formation of active hydroxysteroids that stimulate estrogeno-sensitive pathologies (breast, ovarian, and endometrium cancers) and androgeno-sensitive pathologies (prostate cancer, benign prostatic hyperplasia, acne, hirsutism, etc). Its structural simplicity has been generally accepted as the parent compound for the more complex coumarins and is widely used as a synthon for a wider variety of coumarin-heterocycles [33,34].

It is widely thought that some coumarins, including umbelliferone and furanocoumarins are phytoalexins that play important fungicidal roles in plants. The antimicrobial and antifungal properties of umbelliferone were examined against different bacterial and fungal strains. It showed some inhibition levels against *Staphylococcus aureus*, *Pseudomonas aeruginosa*, *Escherichia coli*, *Fusarium culmorum* and *Byssochlamys fulva* microorganisms. However, umbelliferone usually display no antifungal activities and very weak antibacterial activities regardless the used concentrations [32].

Umbelliferone has been shown to exhibit antioxidant properties including radical scavenging, metal chelation and inhibition of lipid peroxidation. The 7-hydroxycoumarin is a moderate 2,2-diphenyl-1-picrylhydrazyl (DPPH) radical scavenger at a concentration of 50 µg/mL, demonstrating 59.6 % inhibition [35] while ascorbic acid shows 96 % DPPH radical inhibition [36]. Also, umbelliferone scavenges hydroxyl radicals at all concentration in a concentration-dependent manner [37]. Further, it inhibits superoxide anion formation during the oxidation of NADH by phenazine methosulphate showing IC_{50} value of 150 µM compared to ascorbic acid IC_{50} value of 86 µM. In addition, it was reported that umbelliferone causes the reduction of the Fe^{3+}/ferricyanide complex to the ferrous form monitoring by the formation of Perl's Prussian blue and bound Fe^{2+} ions by 58.8 % at 200 µg/mL [35]. Additionally, umbelliferone was assessed for the protection of *β*-carotene from linoleic acid induced bleaching. Linoleic acid is capable of producing aqueous free radicals by generating hydrogen peroxide. The presence of umbelliferone helps to neutralize hydroperoxide and inhibits the oxidation of *β*-carotene [38].

Further, antihyperglycemic effects of umbelliferone were also reported. Post-prandial hyperglycaemia is characterized as the earliest symptom of diabetes. It inhibits *α*-glucosidase (IC_{50} = 7.08 µg/mL) in a non-competitive mode of inhibition. *In vitro* glycation assays showed that umbelliferone

prevented each stage of protein glycation and exhibited a potent inhibition on aldose reductase (IC_{50} = 1.32–0.29 µg/mL) [32,39].

Even the anti-carcinogenic efficacy was reported for umbelliferone alone and in synergistic activity with 5-fluorouracil. These compounds are effective and potential chemotherapeutic agents against 1,2-dimethylhydrazine-induced colon carcinogenesis. Umbelliferone controls the side effects of 5-fluorouracil [40]. An anticancer activity against laryngeal cancer cells (RK33 LCC) by reducing their viability and cell migration was also reported by Kielbus and co-workers [41].

Umbelliferone absorbs strongly at 300, 305 and 325 nm, with logε values of 3.9, 3.95 and 4.15 respectively, and it fluoresces blue in both ultraviolet and visible light. The powerful absorption at three different wavelengths, coupled with the fact that the energy is dissipated safely as visible light, make umbelliferone a useful sunscreen agent. The fluorescent property of umbelliferone was also used to design a fluorescent probe for hydrogen peroxide which showed good selectivity over other reactive oxygen species [42].

1.2. Biosynthesis of coumarins in plants

The pathway of coumarin biosynthesis has been largely investigated during the ‘60s and ‘70s [21]. Radiolabelled cinnamic acid was incorporated into coumarin or 7-hydroxycoumarins *in vivo* [43]. It was discovered that the *ortho*-hydroxylation of cinnamic acid is a key step of coumarin biosynthesis [44]. A P_{450}-dependent hydroxylation mechanism was suggested; however, the *in vitro* results could not be reproduced, and the class of the enzyme involved as well as its subcellular site remain to be established [21].

The formation of umbelliferone proceeds from *p*-coumaric acid or its ester derivatives. It is synthesized from L-phenylalanine, which is produced via the shikimate pathway. Phenylalanine is lyased into cinnamic acid which later is converted to *p*-coumaric acid by cinnamate 4-hydroxylase, a cytochrome P_{450} monooxygenase from the CYP73A family [45]. Following the related literature, *p*-coumaric acid is *ortho*-hydroxylated by putative P_{450} enzyme to 2,4-dihydroxycinnamic acid [46]. Further, the formation of esculetin (6,7-dihydroxycoumarin) was examined in *Cichorium intybus*. These studies revealed that umbelliferone was an efficient precursor but not a caffeic acid, suggesting 6-hydroxylation of umbelliferone, probably by the action of a P_{450} monooxygenase [47].

While coumarin biosynthesis remains a mystery, several enzymes of the furanocoumarin pathway have been isolated and characterized. Umbelliferone rather than coumarin is the parent compound of furanocoumarins [21,48]. It is

biosynthesized by a coupling of dimethylallyl pyrophosphate (DMAPP) and 7-hydroxycoumarin.

1.3. Catabolism of coumarins

The electron charges of different atoms in a coumarin molecule vary greatly. Negative charges are distributed on 3, 5, 6, 7, and 8 carbon atoms, and positive charges only at positions 2 and 4 (Fig. 2). Quantitative differences in negative charges lead to a variety of theoretical metabolic pathways, as well as a variety of participations in different biological processes. Atoms with a positive charge will tend to attach to the nucleophile, and at positions where the charges are negative, there is a high probability of an electrophile attack. The most common modification of coumarin *in vivo* is hydroxylation, which usually occurs at positions 3, 7, and 8, while hydroxylation at positions 4 and 6 are very rare [18,28,49].

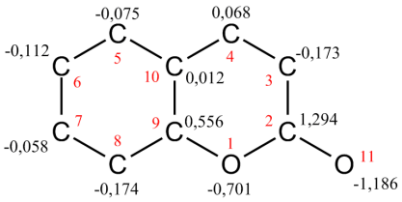

Figure 2. Electron charge distribution in the coumarin molecule.

Cytochrome P_{450} enzymes are usually involved in the hydroxylation of coumarins *in vivo* [28,49]. These monooxygenases are present in both microorganisms and animals; however, the metabolic routes differ. In microorganisms, cytochrome P_{450} enzymes usually perform hydroxylation of the coumarin benzene ring only. In animals, cytochrome P_{450} monooxygenases almost in all cases catalyze the epoxidation of the C3–C4 double bond and/or the hydroxylation of the C7 atom. The resulting coumarin 3,4-epoxide can be further conjugated to glutathione or converted to *o*-hydroxy-phenylacetaldehyde, which is immediately oxidized to *o*-hydroxyphenylacetic acid or reduced to *o*-hydroxyphenylethanol (Fig. 3) [28,49].

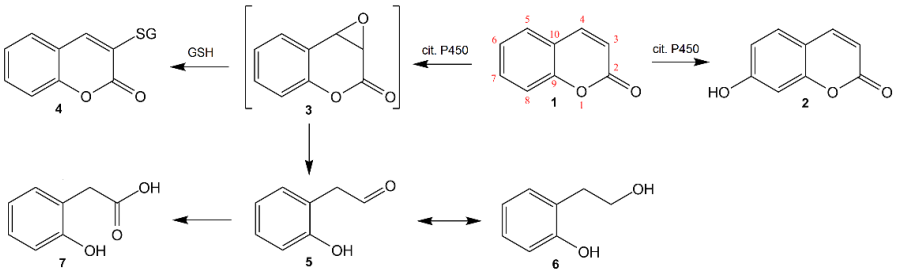

Figure 3. Metabolism of coumarin in animals. 1 – coumarin; 2 – 7-hydroxycoumarin; 3 – coumarin 3,4-epoxide; 4 – coumarin 3-glutathione; 5 – *o*-hydroxyphenylacetaldehyde; 6 – *o*-hydroxyphenylethanol; 7 – *o*-hydroxy-phenylacetic acid; GSH – glutathione.

In animals, P_{450} enzymes can also catalyze the dealkylation of alkylcoumarins, however coumarins are not fully metabolized but only modified and immediately eliminated from the organism [28,49]. Unlike animals, microorganisms (micromycetes and bacteria) can utilize coumarin and its derivatives as the sole sources of carbon and energy, and therefore the metabolic pathways are different from animals. The metabolic routes of coumarins in both bacteria and microscopic fungi are very similar.

1.3.1. Biotransformation of coumarin and its derivatives in fungi

After elucidating the physiological significance of coumarins, there has been a strong interest in the detoxification mechanisms of these compounds in living organisms. As early as the middle of the twentieth century, quite a lot was known about the metabolism of coumarin in plants and animals, but there was a lack of knowledge about the metabolic pathways in microorganisms [18,20].

The study of soil micromycetes (microscopic fungi), which use coumarin as the sole source of carbon and energy, quickly revealed that 3-(2-hydroxyphenyl) propionic acid (also known as melilotic acid) is one of the major intermediates of the coumarin metabolic pathway [9,13]. At that time, several fungal genera were found, such as *Fusarium*, *Aspergillus*, *Penicillium*, *Mucor*, in which coumarin is degraded to melilotic acid [9]. The latter compound can then be hydroxylated to form 3-(2,3-dihydroxyphenyl) propionic acid (Fig. 4). In the case of *Aspergillus niger*, very small amounts of *o*-coumaric acid, 4-hydroxycoumarin and catechol were also detected among the coumarin metabolites. When *A. niger* was grown with *o*-coumaric acid, as much as 72 % of the substrate was converted to 4-hydroxycoumarin, which was not further metabolized [13,50].

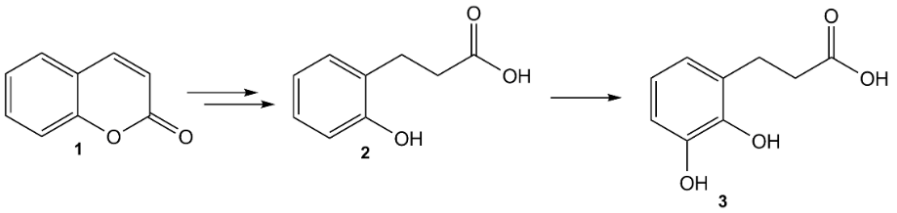

Figure 4. Intermediates of coumarin metabolism in micromycetes. 1 – coumarin; 2 – melilotic acid; 3 – 3-(2,3-dihydroxyphenyl) propionic acid.

Subsequent studies of biotransformation of coumarin in the plant pathogen *Colletotrichum capsici* revealed that coumarin and 6-methylcoumarin are converted to 2-(3'-hydroxypropyl)-phenol and 2-(3'-hydroxypropyl)-4-methylphenol, respectively (Fig. 5) [51].

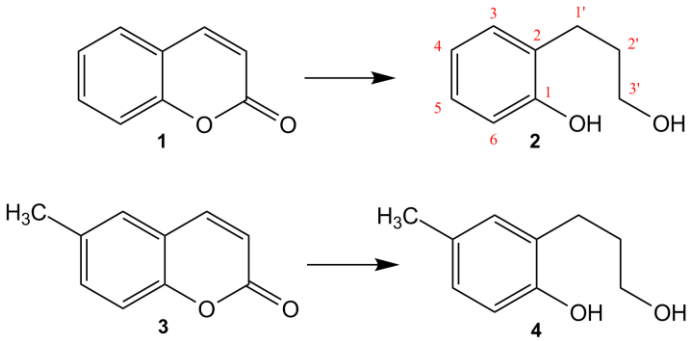

Figure 5. Metabolism of coumarin and 6-methylcoumarin in *Colletotrichum capsici* fungi. 1 – coumarin; 2 – (3'-hydroxypropyl)-phenol; 3 – 6-methylcoumarin; 4 – 2-(3'-hydroxypropyl)-4-methylphenol.

Fungi of the genus *Aspergillus* are still widely studied. It is already known that fungi of this genus have a very high synthesis of cytochrome P_{450} enzymes and are able to detoxify various xenobiotics. Coumarins are most actively metabolized by *A. niger*, *A. flavus*, and *A. ochraceus* [14].

Whole cells of *A. ochraceus* can consume coumarin as the sole source of carbon and energy, though biotransformation products are not detected. Meanwhile, in growing cells coumarin is not fully metabolized but only modified to form the sole metabolite 3,4-dihydrocoumarin (Fig. 6) [14].

Studies with *A. flavus* revealed a slightly different metabolism when coumarin was converted to a more polar compound. In experiments with both

whole cells and growing cells, 5-hydroxycoumarin was detected as the sole product of biotransformation (Fig. 6) [14].

In experiments with *A. niger* whole and growing cells, two different pathways of coumarin biotransformation were detected. It was found that *A. niger* primarily reduce the C3–C4 double bond of coumarin to form 3,4-dihydrocoumarin [14]. This is followed by two different metabolic pathways: (a) hydrolysis of the lactone ring between oxygen and carbonyl carbon atoms and reduction of the resulting melilotic acid to the primary alcohol 2-(3'-hydroxypropyl)-phenol, or (b) hydroxylation of 3,4-dihydrocoumarin aromatic ring at C6 position (Fig. 6). These metabolic pathways have been confirmed in biotransformation studies using 3,4-dihydrocoumarin as the substrate, which is thought to be the major intermediate of coumarin metabolism. The same resulting products were obtained. It is worth noting that the metabolic pathway of coumarin **a** in *A. niger* (Fig. 6) coincides with the metabolism of coumarin in previously studied *C. capsici* fungi [14].

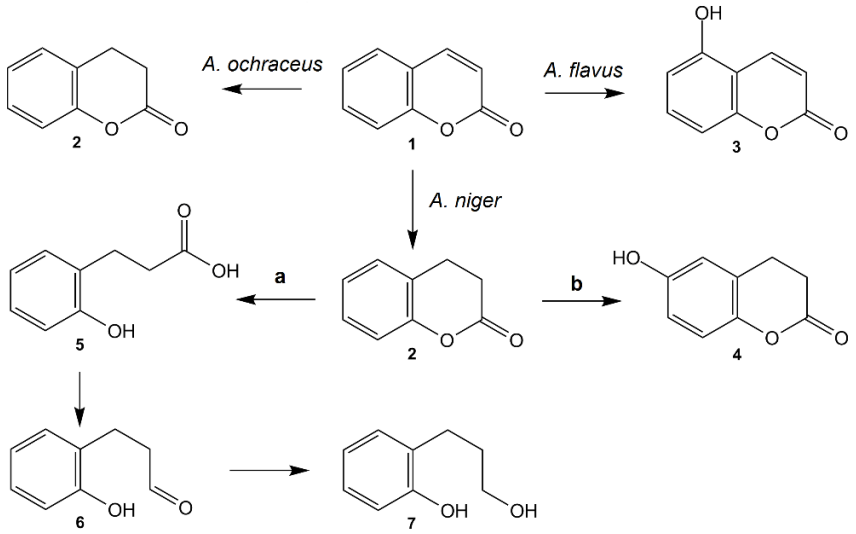

Figure 6. Biotransformation of coumarin in fungi of the genus *Aspergillus*. 1 – coumarin; 2 – 3,4-dihydrocoumarin; 3 – 5-hydroxycoumarin; 4 – 3,4-dihydro-6-hydroxycoumarin; 5 – melilotic acid; 6 – 3-(2-hydroxyphenyl) propanal; 7 – 2-(3'-hydroxypropyl) phenol.

A study of the influence of oxygen on coumarin conversion in *A. niger* showed that with better aeration of medium, the final products of coumarin metabolism were 3,4-dihydrocoumarin, 3,4-dihydro-6-hydroxycoumarin and 2-(3'-hydroxypropyl)-phenol. With less aeration, the final metabolites were

3,4-dihydrocoumarin, 3,4-dihydro-6-hydroxycoumarin, and melilotic acid only (Fig. 6) [14].

The metabolic pathways of coumarin derivatives were also studied in *A. niger* fungi. Coumarins that were monohydroxylated at positions 3, 4, and 6 were found not to be metabolized by *A. niger*, and only biotransformation of 6-methoxycoumarin were recorded, when the appropriate methoxy derivative was used as a substrate. First, 6-methoxycoumarin is converted to 3,4-dihydro-6-methoxycoumarin, which can then be demethylated to 3,4-dihydro-6-hydroxycoumarin or hydroxylated at the aromatic ring (Fig. 7) [14].

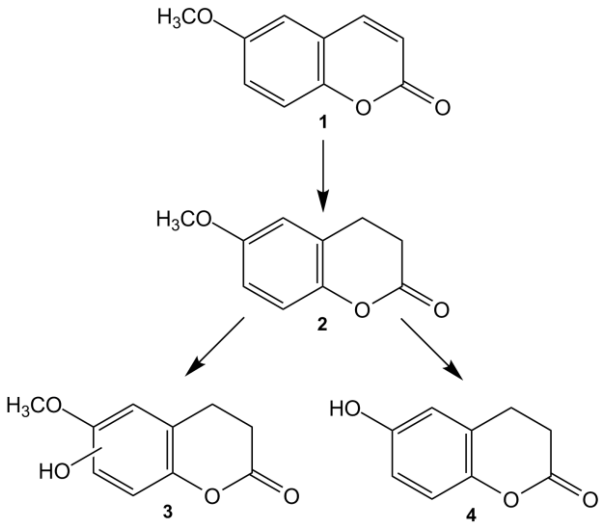

Figure 7. Biotransformation of 6-methoxycoumarin in *Aspergillus niger* fungi. 1 – 6-methoxycoumarin; 2 – 3,4-dihydro-6-methoxycoumarin; 3 – 3,4-dihydro-hydroxy-6-methoxycoumarin; 4 – 3,4-dihydro-6-hydroxycoumarin.

Metabolic studies of more complex coumarin derivatives such as furanocoumarins or pyranocoumarins have revealed the fungus *Glomerella cingulata*, which does not use coumarin as a source of carbon and energy but only metabolizes it to melilotic acid [15]. This microorganism performs biotechnologically interesting bioconversions: it transforms psoralen (7*H*-furo-[3,2-g]-chromen-7-one) and xanthyletin (8,8-dimethyl-2*H*,8*H*-pyrano-[3,2-g]-chromen-2-one). *G. cingulata* reduces and hydrolyses the pyrone ring of coumarin derivatives to form the corresponding acids and performs further reduction to alcohols [15].

1.3.2. Biotransformation of coumarin and its derivatives in bacteria

Like micromycetes, bacteria are able to use coumarin as their sole source of carbon and energy. Despite the fact that fungi are eukaryotic organisms and bacteria are prokaryotes, studied coumarin biotransformation and intermediates are very similar in both bacteria and fungi. The first bacteria in which coumarin metabolic routes were studied in detail belonged to the genera of *Arthrobacter* and *Pseudomonas* [10,16], and only later the metabolism of coumarin was described in genera of *Streptomyces* [52] and *Rhodococcus* [53].

Gram-positive bacteria of the genus *Arthrobacter* and gram-negative bacteria of the genus *Pseudomonas* metabolize coumarin to 3-(2,3-dihydroxyphenyl) propionic acid [10,16], but the first stage of biotransformation in these bacteria is different. Bacteria of the genus *Arthrobacter* primarily hydrolyse the pyrone ring of coumarin to form *o-trans*-coumaric acid via the intermediate *o-cis*-coumaric acid. Then the NADH:*o*-coumarate oxidoreductase enzyme reduces *o-trans*-coumaric acid to melilotic acid, which is oxidized by melilotate hydroxylase to 3-(2,3-dihydroxyphenyl) propionic acid in the presence of oxygen and NADH (Fig. 8) [16].

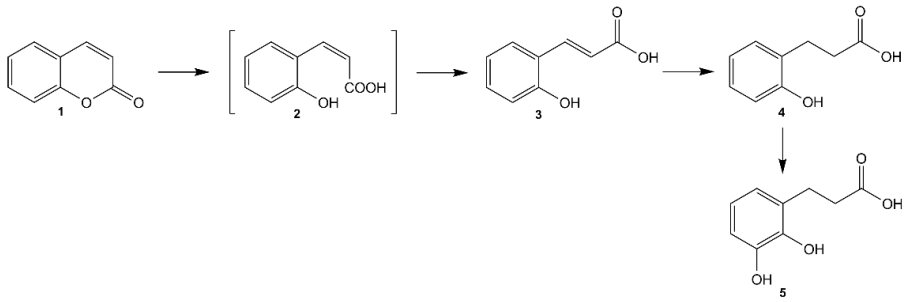

Figure 8. Biotransformation of coumarin in *Arthrobacter* bacteria. 1 – coumarin; 2– *o-cis*-coumaric acid; 3 – *o-trans*-coumaric acid; 4 – melilotic acid; 5 – 3-(2,3-dihydroxyphenyl) propionic acid.

Bacteria of the genus *Pseudomonas* first reduce the C3–C4 double bond of coumarin to form 3,4-dihydrocoumarin. This reaction is catalysed by NADH-dependent coumarin reductase. This coumarin reductase has a Zn^{2+} ion in the active site. The bond of 3,4-dihydrocoumarin between oxygen and carbonyl carbon atoms is hydrolysed to form melilotic acid. The latter compound is oxidized by melilotate hydroxylase in these bacteria (Fig. 9) [10].

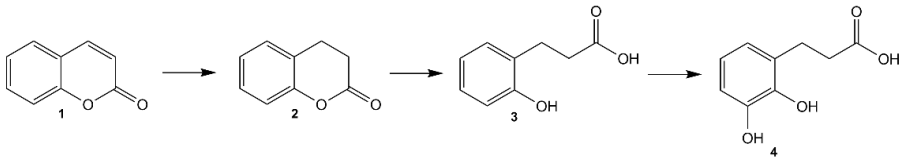

Figure 9. Biotransformation of coumarin in *Pseudomonas* bacteria. 1 – coumarin; 2 – 3,4-dihydrocoumarin; 3 – melilotic acid; 4 – 3-(2,3-dihydroxyphenyl) propionic acid.

During the metabolic studies of coumarin derivatives *Streptomyces griseus* bacteria were detected that did not use coumarin and its derivatives as the sole source of carbon and energy, however were able to modify the aromatic ring [52]. For example, coumarin was hydroxylated at the C7 position. In addition, the products obtained from 7-ethoxycoumarin as the sole carbon source were 7-hydroxycoumarin and 7-hydroxy-6-methoxycoumarin (Fig. 10).

It is believed that 7-ethoxycoumarin is primarily deethylated and then hydroxylated at the C6 position to form the intermediate 6,7-dihydroxycoumarin. However, the latter compound could not be detected in the experiments. Therefore, its formation was demonstrated by usage of 6,7-dihydroxycoumarin as the sole carbon source in bacteria, which yielded 7-hydroxy-6-methoxycoumarin and its isomer 6-hydroxy-7-methoxycoumarin (Fig. 10) [52].

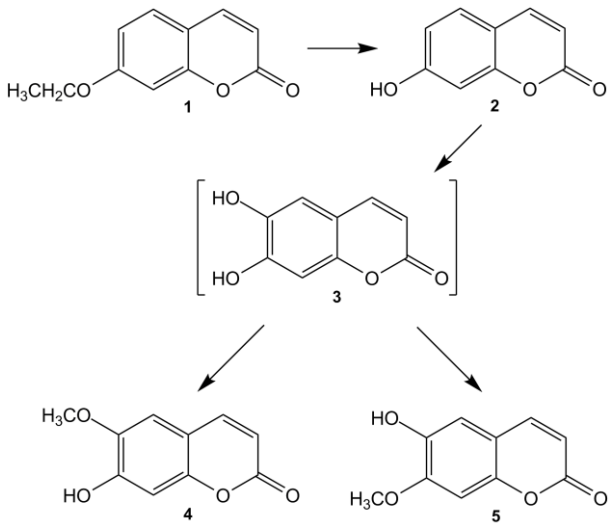

Figure 10. Biotransformation of 7-ethoxycoumarin in *Streptomyces griseus*. 1 – 7-ethoxycoumarin; 2 – 7-hydroxycoumarin; 3 – 6,7-dihydroxycoumarin; 4 – 7-hydroxy-6-methoxycoumarin; 5 – 6-hydroxy-7-methoxycoumarin.

New aerobic bacterial strains of the genera *Rhodococcus* and *Pseudomonas* that use coumarin and its derivatives as the only sources of carbon and energy have also recently been described [54]. *Rhodococcus* sp. K5 bacteria metabolize coumarin, 6-hydroxycoumarin, 7-hydroxycoumarin, 7-methylcoumarin and melilotic acid. The latter compound and coumarin are also degraded by *Rhodococcus* sp. TMP1 bacteria that has a hypothetical *kum* operon encoding a coumarin catabolic enzymes determined in their genome. Part of the proteins encoded by this operon coincide with proteins encoded by the *ohp* operon in *Rhodococcus* sp. V49 bacteria [53,54].

Two other novel bacterial strains are specific for C7-substituted coumarins. *Rhodococcus* sp. 7HK9 bacteria are able to metabolize 7-hydroxycoumarin and 7-methylcoumarin, and *Pseudomonas* sp. 7HK4 bacteria utilize 7-hydroxycoumarin only. These two strains cannot use melilotic acid as the sole source of carbon and energy [54]. Based on the literature, 3-(2,4-dihydroxyphenyl) propionic acid could be an intermediate in the metabolism of 7-hydroxycoumarin, further exposed to aromatic hydroxylases at the C3- or C5-positions, similar to melilotic acid in coumarin metabolism.

1.3.3. Catabolism of melilotic acid in bacteria

The first studies of coumarin metabolism in fungi and bacteria in which coumarin was used as the sole source of carbon and energy revealed that melilotic acid is the main intermediate in coumarin metabolism. In both *Arthrobacter* and *Pseudomonas* bacteria melilotic acid is oxidized to 3-(2,3-dihydroxyphenyl) propionic acid [10,16]. At that time, the same compound was also found in bacteria of the genus *Achromobacter*, which are able to use 3-phenylpropionic acid and 3-phenylpropenoic acid (also known as cinnamic acid) as the sole sources of carbon and energy [55]. *Achromobacter* bacteria have the enzymes responsible for the oxidative degradation of the benzene ring of 3-(2,3-dihydroxyphenyl) propionic acid and the conversion of the resulting yellow compound to succinate and 4-hydroxy-2-oxovalerate. After about two decades, results of 3-phenylpropionic acid metabolism in *Escherichia coli* were also published [56], which were analogous to 3-phenylpropionic acid metabolism in *Achromobacter* bacteria. Melilotic acid was not detected as an intermediate in the metabolism of 3-phenylpropionic acid in either *Achromobacter* or *E. Coli* bacteria. However, it was thought that the metabolism of 3-(2,3-dihydroxyphenyl) propionic acid in *Arthrobacter* and *Pseudomonas* bacteria grown on coumarin may be similar to that in *Achromobacter* [55] and *E. coli* [56].

The metabolism of melilotic acid was elucidated at the end of twentieth century when *Rhodococcus* sp. V49 bacterial strain capable of utilizing

melilotic acid as a source of carbon and energy was found [53]. Genetic analysis of this strain revealed an *ohp* operon consisting of the *ohpR*, *ohpA*, *ohpB*, *ohpC*, and *ohpD* genes encoding hypothetical regulatory and transport proteins, confirmed monooxygenase, hydroxymuconic semialdehyde hydrolase and catechol 2,3-dioxygenase, respectively. Biochemical analysis of the *ohpB*, *ohpC*, and *ohpD* gene products revealed that OhpB monooxygenase specifically oxidizes melilotic acid to 3-(2,3-dihydroxyphenyl) propionic acid. OhpD catechol 2,3-dioxygenase cleaves the benzene ring of 3-(2,3-dihydroxyphenyl) propionic acid between the acid and hydroxy groups (extradiol cleavage). The reaction yields a yellow 2-hydroxy-6-ketonona-2,4-dienedioic acid which is hydrolysed by OhpC hydroxymuconic semialdehyde hydrolase. Both ohpD and ohpC enzymes are specific for products of melilotic and *o*-coumaric acid metabolism only [53]. The proposed metabolic pathway for melilotic acid is shown in Figure 11.

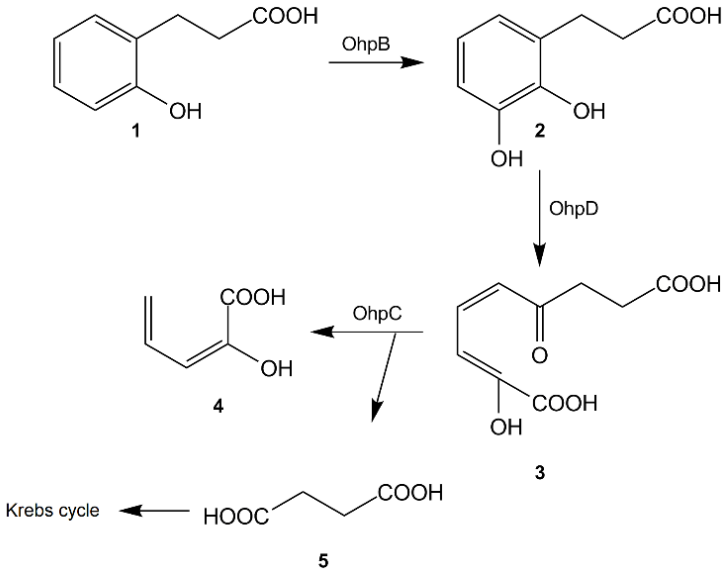

Figure 11. Metabolic pathway of melilotic acid in *Rhodococcus* sp. V49 bacterial strain. 1 – melilotic acid; 2 – 3-(2,3-dihydroxyphenyl) propionic acid; 3 – 2-hydroxy-6-ketonona-2,4-dienedioic acid; 4 – 2-keto-4-penteneoic acid; 5 – succinate; OhpB – monooxygenase; OhpD – catechol 2,3-dioxygenase; OhpC – hydroxymuconic semialdehyde hydrolase.

1.4. Catabolic enzymes and their mechanisms

Compounds containing the benzene ring constitute the second largest group of naturally occurring substances (after sugar residues). Aromatic compounds display resistance to environmental chemical degradation, owing to the inherent thermodynamic stability of the benzene ring. However, microorganisms possess a wide range of catabolic biodegradation pathways and, thus, use these hazardous xenobiotics as the sole source of carbon and energy [57–59]. In general, the microorganisms degrade xenobiotics either aerobically or anaerobically. The representative most common aerobic biodegradation pathway exhibited by microorganisms is depicted in Figure 12.

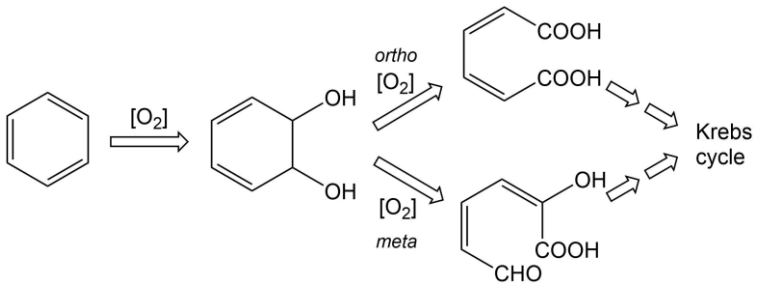

Figure 12. Schematic representation of the principal metabolic pathways involved in aerobic biodegradation of aromatic compounds by microorganisms.

In the case of aerobic biodegradation, the original substrate undergoes mostly oxygenation reactions and is converted to dihydroaromatic derivatives such as catechol, protocatechuate, gentisate, homoprotocatechuate, homogentisate, hydroquinone and hydroxyquinone. The key enzymes catalysing the reactions are monooxygenases and/or hydroxylating dioxygenases. These intermediates may act as substrates for enzymes that cleave the aromatic ring in reactions involving molecular oxygen. The aromatic ring may be opened by cleavage of the bond between two neighbouring carbon atoms carrying hydroxyls. In this case, the process is termed *ortho*-cleavage, and the enzymes involved are intradiol dioxygenases. On the other hand, if other bonds taking a *meta*-position are cleaved in order to open the aromatic ring, the term used is *meta*-cleavage with the enzymes extradiol dioxygenases involved in the process. Central metabolic pathways involve series of reactions that culminate in the formation of intermediates of the Krebs cycle [57–61].

1.4.1. Reduction of coumarin

Like previously described it is known that 3-(2-hydroxyphenyl) propionic acid is one of the major intermediates of the coumarin metabolic pathway [9,13]. Therefore, initial coumarin metabolic pathway stages must overcome reduction and hydrolysis of its lactone moiety. Studies have shown that microorganisms can harness two catabolic strategies for achieving this. Primarily hydrolysing the pyrone ring of coumarin to form *o-trans*-coumaric acid via the intermediate *o-cis*-coumaric acid, then reducing *o-trans*-coumaric acid to melilotic acid by the NADH:*o*-coumarate oxidoreductase enzyme [16]. On the other hand, bacteria of the genus *Pseudomonas* first reduce the C3–C4 double bond of coumarin to form 3,4-dihydrocoumarin. This reaction is catalysed by NADH-dependent coumarin reductase. Later, the bond of 3,4-dihydrocoumarin between oxygen and carbonyl carbon atoms is hydrolysed to form melilotic acid [10]. To this date, some enzymes having coumarin reducing activity have been biochemically characterized [10,62], however no genetic data or enzyme mechanisms have been presented.

Reduction of coumarin C=C-bond could be catalysed by ene-reductases (ERs) [63]. ERs are widely used in biocatalytic nicotinamide-dependent asymmetric reduction of activated C=C-bonds yielding chiral α-substituted and/or β-substituted reduction products. To date, four different classes of ERs have been investigated capable of reducing a broad variety of substrates including α,β-unsaturated aldehydes, ketones, carboxylic acids and derivatives (such as esters, lactones, cyclic imides), and nitro compounds [64–68]. The most extensively investigated family of ERs is the FMN-containing Old Yellow Enzyme (OYE) family of oxidoreductases [65]. Other families of ERs are the oxygen-sensitive FAD and [4Fe-4S]-containing clostridial Enoate Reductases (EnoR) [69], the leukotriene B4 dehydrogenase subfamily of medium chain dehydrogenases/reductases (MDR) [70] and the salutaridine/menthone reductase-like subfamily of short chain dehydrogenases/reductases (SDR) [71,72]. The last two families contain a less characterized NAD(P)H-dependent flavin-independent ERs that have been recently researched for their biocatalytic mechanisms [64,73].

It was reported that as a member of OYE family Xenobiotic Reductase A (XenA) from *Pseudomonas putida* 86 has the ability to reduce the C-3/C-4 double bond of coumarin and 8-hydroxycoumarin resulting in formation of 3,4-dihydrocoumarin and 3,4-dihydro-8-hydroxycoumarin, respectively [62]. Though *P. putida* strain is capable to reduce coumarin, it is quinoline degrading strain, and therefore do not grow with coumarin as a sole source of carbon and energy. XenA enzyme shares a generally low amino acid sequence

identity and similarity with other OYE enzymes and structural variation was observed in the active site of XenA compared to the OYE family [74]. However, this was the only coumarin reducing enzyme that has been genetically, structurally and biochemically described so far.

1.4.2. Lactonohydrolases

Despite the possible initial coumarin catabolic strategies either it starts with reduction or hydrolysis of coumarin lactone moiety, the latter metabolic step is also under-explored and little data are known so far. Two decades ago, a novel lactonohydrolase, 3,4-dihydrocoumarin hydrolase (DCH), from *Acinetobacter calcoaceticus* F46 growing on fluorene as sole carbon source was found and isolated [75]. It was shown that DCH can catalyze not only the hydrolysis of 3,4-dihydrocoumarin, 2-coumaranone and homogentisic acid lactone, but also the bromination of monochlorodimedon (2-chloro-5,5-dimethyl-1,3-cyclohexanedione) in the presence of H_2O_2. Analysis of the primary structure of this enzyme showed that it belongs to the esterase-haloperoxidase family. This was the first demonstration of 3,4-dihydrocoumarin hydrolase activity yielding phenylpropanoid in a bacterial strain. However, the enzyme is not coumarin or 3,4-dihydrocoumarin induced, and considered to participate in the metabolic pathway of polycyclic aromatic compounds only [75,76].

1.4.3. Hydroxylation of phenylpropanoids

At least several distinct pathways for the degradation of hydroxylated aromatic compounds have been described [77]. The specific route taken appears to be dictated in large part by the number of hydroxyl groups and their relative positions on the ring. A typical pathway for metabolizing phenylpropanoids is to hydroxylate the ring, by the enzyme hydroxylase, resulting in catechol formation [78]. At present, P_{450} monooxygenases, which belong to the family of prosthetic heme-binding monooxygenases, are most widely abundant in nature among various organisms. These enzymes have the unique property of catalysing the specific hydroxylation of inactivated carbon atoms of various organic compounds [79,80]. In addition to P_{450} monooxygenases, other classes of monooxygenases are known, such as heme-independent monooxygenase, copper ion-dependent monooxygenase and flavin-dependent monooxygenase [81]. It is the latter class that accounts for the largest proportion of naturally occurring monooxygenases, such as most of the aromatic compound hydroxylases found in aerobic bacteria [79,82].

1.4.3.1. Flavin-binding monooxygenases

Flavin-binding monooxygenases belong to the class of oxidative enzymes. These enzymes can perform a variety of reactions: hydroxylation, epoxidation, Baeyer-Villiger oxidation, sulfoxidation, and more. The specificity and selectivity of the oxidative reaction depend on the physical and chemical properties of the active site of the monooxygenase, which are determined by the primary and secondary structures of the protein [79].

Flavin monooxygenases are able to activate molecular oxygen, converting the molecule to the singlet state ($^1\Delta g$), which is higher energy and less stable, making it significantly more reactive. To achieve this goal, monooxygenase uses a cofactor - flavin. The reduced form of flavin is rich in electrons that can be donated to molecular oxygen to form superoxide and the flavin radical (Fig. 13) [83].

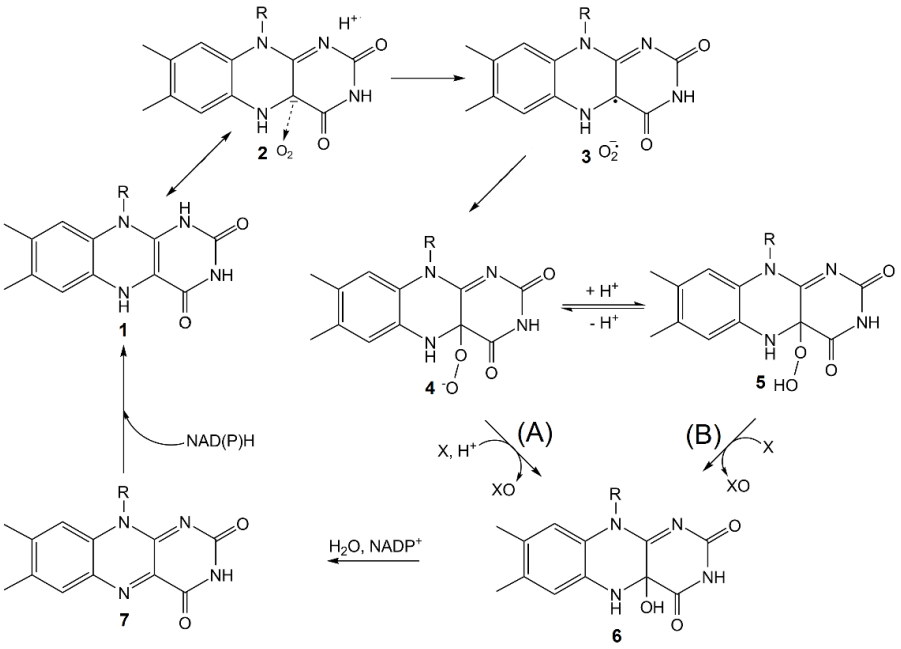

Figure 13. General mechanism of oxidative reaction catalysed by flavin monooxygenases. Flavin bound in the active site of the enzyme is reduced using NAD(P)H, reacts with O_2 to form (hydro)peroxyflavin, which can participate in both nucleophilic (A) and electrophilic (B) substrate hydroxylation reactions. 1(2) – reduced flavin; 3 – flavin semi-quinone radical; 4 – $C_{4\alpha}$-peroxyflavin; 5 – $C_{4\alpha}$-hydroperoxyflavin; 6 – $C_{4\alpha}$-hydroxyflavin; 7 – oxidized flavin.

During this reaction, the inversion of the O_2 electron spin occurs and a reduced singlet state O_2 molecule is formed [84]. In the case of most flavin monooxygenases, a reactive intermediate $C_{4\alpha}$-hydroperoxyflavin (Fig. 13) is formed in the active site, which is unstable and decomposes to form hydrogen peroxide and oxidized flavin. However, flavin monooxygenases can stabilize $C_{4\alpha}$-hydroperoxyflavin, which is used to introduce a single oxygen atom into organic compounds [85]. Depending on the level of peroxyflavin protonation, both nucleophilic (Fig. 13, A) and electrophilic reactions (Fig. 13, B) can occur [79].

Flavin-dependent monooxygenases can be classified according to the type of reaction catalysed, the substrate, the homology of the sequences, or the spatial structures [86]. In 2006, van Berkel and colleagues grouped flavin monooxygenases into six classes A–F. The classification was based on the similarities of primary and secondary protein structures [79]. However, class A oxygenases make up the largest proportion of all flavin monooxygenases. Oxygenases of this type are mainly responsible for the hydroxylation of aromatic compounds [87]. For more than forty years, enzymes in this class, especially *p*-hydroxybenzoate hydroxylase or phenol hydroxylase, have been extensively studied and have already become a paradigm against which new flavin-dependent monooxygenases are now compared [88].

1.4.3.2. *Ipso*-hydroxylation

Many aromatic compounds are degraded via hydroxylation of the aromatic moiety at unsubstituted positions with subsequent *ortho*-hydroxylation and cleavage of the aromatic ring by various dioxygenases [89]. However, more than twenty years ago reactions at the *ipso*-position of *para*-hydroxylated phenol derivatives were also discovered [90]. The term *ipso*-substitution describes two substituents sharing the same ring position in an intermediate compound in an electrophilic aromatic substitution. This discovery was unexpected, as a number of cases were subsequently reported where *ipso*-substitutions occurred after initializing attacks at positions which had previously been believed unfavourable [89].

Founded on reactions catalysed by CYP systems, it has been proposed to classify *ipso*-substitutions into two types, solely depending on the substrate and not on the catalysing enzyme. Type I *ipso*-substitution – the leaving group is detached from the substrate as an anion and the product will form a quinone. During a type II *ipso*-substitution, the leaving group is a cation, leading to the formation of a quinol (Fig. 14) [89,91].

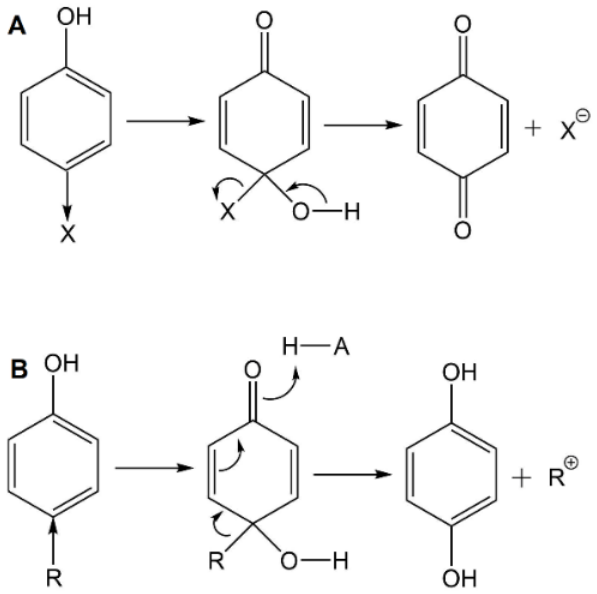

Figure 14. *Ipso*-substitution of phenolic compounds that have *para*-substituents with electron-donating (B) or electron-withdrawing (A) properties (as indicated by the direction of the arrow).

Several classes of enzymes are known to be capable of catalysing such aromatic *ipso*-hydroxylation: CYP, FMO, GST, laccases, peroxidases and dioxygenases. Laccases possess a broad substrate range [89]. The degradation of phenolic azo dyes by a laccase from *Pyricularia oryzae* is started through a type I *ipso*-hydroxylation. It is initiated by the oxidation of the phenolic moiety resulting in formation of a phenoxy radical and a carbenium radical at the C atom linked to the azo group. A following nucleophilic attack by water leads to the fade of the azo dye, releasing a benzoquinone derivative and 4-sulfophenyldiazene which is further oxidized to 4-sulfophenylhydroperoxide [92]. This reaction mechanism is characteristic for laccases, and it is involved in various biotransformations, for example, the cleavage of aryl–alkyl bonds from phenolic subunits in lignin backbones [93], 2,4,6-trimethoxyphenol demethylation [94] or tetrachloroguaiacol dechlorination [95].

The catabolism of the phenolic lignin compound arylglycerol-β-aryl ether by a manganese peroxidase follows the same mechanism and results in the same metabolites as described in the previous paragraph on laccases [96].

Another class of enzymes that are known to catalyze attacks at the *ipso*-position is dioxygenases. Two dioxygenases from *C. testosteroni* T2 and from *Sphingomonas* sp. strain RW1, respectively, were involved in the desulfonation of 4-sulfobenzoate by *ipso*-substitution [97,98]. In addition, a

dioxygenase from *Comamonas* sp. strain JS765 converted a wide range of isomers of mono-nitrotoluene and di-nitrotoluene to the corresponding catechols with the accompanying release of nitrite [99].

Further, cytochrome P_{450} dependent monooxygenases (CYP) are also known for their role in *ipso*-substitutions. A reconstituted rat-liver-CYP system was able to convert *p*-chloro, *p*-bromo, *p*-nitro, *p*-cyano, *p*-hydroxymethyl, *p*-formyl and *p*-acetyl phenols to hydroquinone by *ipso*-hydroxylation [100].

FMOs are responsible for a wide range of xenobiotic biotransformations with no exceptions in *ipso*-hydroxylation. An FMO from *Pseudomonas putida* is involved in nicotine degradation by hydroxylation of 6-hydroxy-3-succinoyl-pyridine at the carbon bearing the succinic semialdehyde moiety which leads to the fragmentation into 2,5-dihydroxypyridine and succinic semialdehyde [101]. An FMO from *Sphingomonas* sp. strain PWE1 attacks alkylphenols at the aromatic carbon bearing the alkyl chain, leading to the formation of hydroquinone and the detached alkyl chain [102]. What surprised the most is the attack adjacent to quaternary carbon atoms which previously thought to be improbable due to steric hindrances [103].

In rare cases, the reactions initiating *ipso*-hydroxylation can result in side-products where the initial *ipso*-group is not removed but shifted to adjacent position by intramolecular rearrangements (NIH-shift) (Fig. 15) [89].

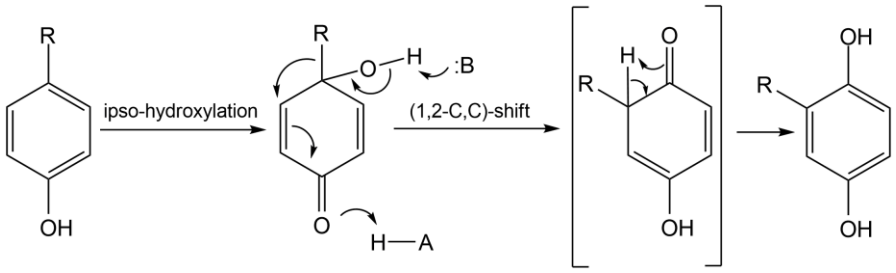

Figure 15. *Ipso*-substitution mechanism with NIH shift. *Para*-substituted hydroxybenzenes can undergo *ipso*-hydroxylation followed by internal rearrangement leading to NIH-shift products. R – alkyl group. H-A and B indicate proton donor and acceptor, respectively.

Investigations showed that NIH-shifts occur for fluorinated benzenes with CYP systems [104] and for 4-hydroxyarylaldehydes [105] and 4-alkylphenols with FMOs. Also, other rearrangements are possible when some alkyl substituents can be observed forming arylethers with the aromatic ring upon introduction of the hydroxyl group [103]. These side reactions are supposedly substrate-

specific and the rearrangements are not enzymatically catalysed but rather occurring spontaneously. However, these rearrangements have only been observed in the degradation of alkylphenols by FMOs [89].

1.4.4. Aromatic ring degrading enzymes

Cyclic aromatic products containing two hydroxyl substituents on adjacent carbon atoms of the ring are then converted to noncyclic products by ring-cleavage dioxygenases that cleave the C–C bond either between the hydroxylated carbons (*ortho* cleavage) or between a hydroxylated and non-hydroxylated carbon (*meta* cleavage) [106]. Here a few representative enzymes involved in activation and ring cleavage of aromatic hydrocarbons containing only carbon and hydrogen are examined. Ring-cleavage dioxygenases can be placed into two major classes, intradiol or extradiol, depending on the position of cleavage relative to that of the ring hydroxyl groups [106,107].

Intradiol ring-cleavage dioxygenases utilize non-heme Fe(III) as a cofactor to catalyze insertion of both atoms of molecular oxygen into catechols to break the bond between two adjacent ring carbon atoms bearing hydroxyl groups (*ortho* cleavage). The *ortho*-cleavage product of catechol is *cis,cis*-muconate. A broad diversity of bacterial species utilizes these enzymes but all of the proteins appear to be evolutionarily related and have similar properties. The main differences are in subunit composition and quaternary structure [106,107].

Extradiol ring-cleavage dioxygenases utilize non-heme Fe(II) as a cofactor to catalyze insertion of both atoms of molecular oxygen into catechols to break the bond between vicinal hydroxylated and non-hydroxylated carbons (*meta* cleavage). The *meta*-cleavage product of catechol is 2-hydroxy-6-oxo-hexa-2,4-dienoate, also called 2-hydroxy-*cis,cis*-muconic semialdehyde. As with the intradiol enzymes, extradiol dioxygenases are also found in a broad diversity of bacterial species. However, the two types of enzymes are evolutionary distinct from one another and extradiol dioxygenases utilize non-heme Fe(II) as a cofactor. Structurally many of the extradiol enzymes consist of one type of subunit with an α_2 to α_8 quaternary structure [106,107].

Following ring cleavage, subsequent reactions then yield products such as acetate, pyruvate and succinate that enter the Krebs tricarboxylic acid cycle or are used for biosynthesis.

In summary, degradation of hydroxycoumarins has been poorly studied. To fill many gaps existing in the understanding of catabolic pathways of coumarins, the aim of this work is to identify genes encoding enzymes involved in degradation of 7-hydroxycoumarin, and to propose the catabolic pathway of hydroxycoumarins in bacteria.

As a consequence, newly discovered enzymes could potentially be used as environmentally friendly biocatalysts in the organic synthesis in bioconversion of hydroxycoumarin-like compounds. In this field, there is a particular lack of oxidation enzymes, such as aromatic hydroxylases, which are attractive in drug synthesis. The benzene ring, whether phenyl or fused with other rings, is the most common hydrophobic pharmacophoric moiety in drug molecules. And through a pharmacokinetic effect, the aromatic hydroxy group enhances the water solubility and elimination of the drug metabolites, that is essential pharmacophoric status in some drug classes [175].

2. MATERIALS AND METHODS

2.1. Reagents and materials

2.1.1. Bacterial strains, plasmids and reagents

Pseudomonas mandelii 7HK4 bacterial strain from laboratory collection (DSMZ accession number DSM 107615) capable of using 7-hydroxycoumarin as the sole source of carbon and energy was isolated from Lithuanian soil by enrichment in mineral medium containing 0.05 % of 7-hydroxycoumarin. For cloning purposes, *E. coli* DH5α bacteria (ϕ80 *lacZ*ΔM15 Δ(*lacZY-argF*)*U169 deoR recA1 endA1 hsdR17*(r_K–m_K+) *supE44 thi-1 gyrA96 relA1*) (Thermo Fischer Scientific, Lithuania) were used. *E. coli* BL21 (DE3) bacteria (F^- ompT gal dcm lon hsdSB(rB^- mB^-) λ(DE3) [F^- *ompT gal dcm lon hsdS*$_B$(r_B^- m_B^-) λ(DE3) [*lacI lacUV5-T7* gene 1, *ind1*, *sam7*, *nin5*]) (Novagen, Germany) were used for gene expression studies.

All reagents used during this study are listed in Table 1 and plasmids are described in Table 2.

Table 1. Materials and reagents used in the study.

Chemicals and reagents	Source
7-Hydroxycoumarin, ethyl acetate, methanol, diethyl ether, dichloromethane	Merck, Germany
Ampicillin, streptomycin, 3-(2-hydroxyphenyl)-2-propenoic acid, 3-(4-hydroxyphenyl)-2-propenoic acid, 3-(3-hydroxyphenyl)-2-propenoic acid, pyrocatechol, coumarin, cinnamyl alcohol, 3-(2,4-dihydroxyphenyl) propionic acid, 2-ethylphenol, caffeic acid, Na_2CO_3, Na_2HPO_4, NaOH, glycerol, *β*-mercaptoethanol, ammonium acetate	Fluka, Germany
3-Hydroxycoumarin, 4-hydroxycoumarin, 7-methylcoumarin, 3-methylcatechol, 4-methylcatechol, iodoacetamide, trifluoroacetic acid, kanamycin sulphate, 3-(2-hydroxyphenyl) propionic acid, *trans*-2,4-dihydroxycinnamic acid, 3-(2-bromophenyl) propionic acid, 3-(2-nitrophenyl) propionic acid, 3-phenylpropionic acid, *trans*-cinnamic acid, 2-propylphenol, 2-propenylphenol, *o*-cresol, *o*-tyrosine, resorcinol, 2,3-dihydroxypyridine, 2-hydroxy-4-aminopyridine, *N*-methyl-2-pyridone, *N*-ethyl-2-pyridone, *N*-propyl-2-	Sigma-Aldrich (Merck), Germany

pyridone, *N*-butyl-2-pyridone, indoline, indole, pyrogallol, 3-methoxycatechol, 2',3'-dihydroxy-4'-methoxyacetophenone hydrate, gallacetophenone, 3,4-dihydroxybenzoic acid, 2,3,4-trihydroxybenzoic acid, 2,3,4-trihydroxybenzophenone, 1,2,4-benzentriol, 6,7-dihydroxycoumarin, acetonitrile, dimethyl sulfoxide, sodium dodecyl sulphate (SDS), quinoline, isoquinoline, 7-methoxycoumarin, 4-methyl-7-hydroxycoumarin, 7-ethoxycoumarin, 3,4-dihydroquinoline-(1H)-2-one, 2-hydroxyquinoline, 3,4-dihydro-7-hydroxyquinoline-(1H)-2-one	
E-2,4-dihydroxycinnamic acid, 3-(2,3-dihydroxyphenyl) propionic acid, 7-hydroxy-3,4-dihydrocoumarin	Synthesized in this study
Agar, Brain Heart Infusion Broth (Bhi), Lysogeny broth (LB)	Oxoid, UK
Restriction endonucleases, T4 DNA ligase, Phusion High-Fidelity PCR Master Mix with HF Buffer, Isopropyl β-D-1-thiogalactopyranoside (IPTG), PageRuler Prestained Protein Ladder, RiboPure™ Bacteria RNA Purification Kit, High-Capacity cDNA Reverse Transcription Kit, Fast SYBR™ Green Master Mix, Mass Ruler™ DNA Ladder (High Range)	Thermo Fischer Scientific Baltics, Lithuania
Rapid Clean Resin	Advansta, US
C_{18} Reverse-Phase column (12 g)	Grace, US
PCR primers	Metabion, Germany
Ethanol	Vilniaus degtinė, Lithuania
Tris(hydroxymethyl)aminomethane (Tris), succinic acid, glucose	AppliChem, Germany
Agarose, ethidium bromide, chloramphenicol	Serva, Germany
Acrylamide, ethylenediaminetetraacetic acid (EDTA), phenol-chloroform-isoamyl alcohol (25:24:1) solution	Roth, Germany
7-hydroxyquinoline-(1*H*)-2-one	Biosynth Carbosynth, UK

Table 2. Plasmids used in the study.

Plasmids	Properties	Source
pET21b(+)	Amp^R, *lacI*, P_{T7lac}, 5442 bp	Novagen, Germany
pET28b(+)	Kan^R, *lacI*, P_{T7lac}, 5368 bp	Novagen, Germany
pCDFDuet-1	Sm^R, *lacI*, P_{T7lac}, 3781 bp	Novagen, Germany
pACYCDuet-1	Cm^R, *lacI*, P_{T7lac}, 4008 bp	Novagen, Germany
pTHPPDO	The *hcdB* gene is cloned into pET28b(+), *Nco*I and *Hind*III restriction sites	This study
p4pmPmo	The *hcdA* gene is cloned into pET21b(+), *Nde*I and *Xho*I restriction sites	Previous study [108]
p4pmPmoH[c]	The *hcdA* gene is cloned into pET21b(+), with C-terminal His_6-tag, *Nde*I and *Hind*III restriction sites	Previous study [108]
p2K4PH	The *hcdC* gene is cloned into pET21b(+), *Nde*I and *Xho*I restriction sites	This study
pCDF-BC	The *hcdB* and *hcdC* genes are cloned into pCDFDuet-1, *Nco*I and *Hind*III, or *Nde*I and *Xho*I restriction sites, respectively	This study
p5Pmo	The gene of 3-(2-hydroxyphenyl) propionic acid monooxygenase from *Rhodococcus* sp. K5 is cloned into pET21b(+)	Previous study [108]
p4XenA38	The *4XenA38* gene is cloned into pET21b(+), *Nde*I and *Xho*I restriction sites	This study
p4XenA45	The *4XenA45* gene is cloned into pET21b(+), *Nde*I and *Xho*I restriction sites	This study
p4XenA205	The *4XenA205* gene is cloned into pET21b(+), *Nde*I and *Xho*I restriction sites	This study
pHP4-10	The 3kb region containing *hp4*, *hp7*, *hp9* and *hp10* genes is cloned into pACYCDuet-1, *Nde*I and *Xho*I restriction sites	This study
pHP7	The *hp7* gene is cloned into pET21b(+), *Nde*I and *Xho*I restriction sites	This study

2.1.2. Bacterial culture media

Mineral medium (pH 7.2): 5 g/L NaCl, 1 g/L $NH_4H_2PO_4$, 1 g/L K_2HPO_4, 0,4 g/L $MgSO_4 \cdot 7H_2O$.

Minimal C-750501 medium (pH 8.0) [109].

Lysogeny broth (LB) medium (pH 7.2): 20 g of powder in 1 L of water.

Brain Heart Infusion (BHI) medium (pH 7.4): 37 g of powder in 1 L of water.

For the production of agar plates 15 g of agar powder was added to 1 L of medium.

All media were sterilized for 30 minutes at 121 °C, 1 atm.

2.2. Organic synthesis methods

2.2.1. Synthesis of *E*-2,4-dihydroxycinnamic acid and 3-(2,3-dihydroxyphenyl) propionic acid

The starting material 7-hydroxycoumarin (3.24 g, 20 mmol) was dissolved in a 2 M KOH solution (50 mL) and stirred for 2 h at 80–90 °C temperature. Completion of the reaction was determined by thin layer chromatography (TLC, chloroform/methanol, 9/1). After the reaction was completed (TLC), the reaction mixture was diluted with water (100 mL) and then acidified to pH 3–4 with HCl. The acidic compounds were extracted with ethyl acetate. The organic solvent was dried (Na_2SO_4) and removed under reduced pressure. The residue was purified by column chromatography (silica gel, chloroform/methanol mixture). The solvents were removed under reduced pressure to afford 1.98 g (11 mmol, 55 % yield) of *E*-2,4-dihydroxycinnamic acid. MS (ESI+): *m/z* 181.00 $[M+H]^+$; 179.00 $[M-H]^-$. ^{1}H NMR (DMSO-d_6, 400 MHz): δ = 6.26 (dd, *J* = 8.5, 2.3 Hz, 2H, CH), 6.28 (d, *J* = 16.0 Hz, 1H, CH=CH), 6.36 (d, *J* = 2.3 Hz, 1H, CH), 7.38 (d, *J* = 8.6 Hz, 1H, CH), 7.71 (d, *J* = 16.1 Hz, 1H, CH=CH). ^{13}C NMR (DMSO-d_6, 100 MHz): δ = 102.58, 108.15, 113.23, 115.26, 129.36, 140.14, 158.72, 161.11, 168.41.

2.2.2. Synthesis of 7-hydroxy-3,4-dihydrocoumarin

The analytical sample of 7-hydroxy-3,4-dihydrocoumarin was synthesized in good yield by thermal cyclisation of 3-(2,4-dihydroxyphenyl) propionic acid [110]. In short, 3-(2,4-dihydroxyphenyl) propionic acid (182 mg, 1 mmol) was heated in an oven at 135 °C for 3 hours. Resulting brown coloured melt was cooled to room temperature and dissolved in a hot toluene (~50 °C). The solution was treated with silica, filtered and the solvent was removed under vacuum. The residue then was crystallized from small amount of toluene. The

product was filtered and vacuum dried. Yield: 112 mg (68 %). MS (ESI+): m/z 163 $[M-H]^-$ (see Figure S1 in Supplementary Material). ^{1}H NMR (400 MHz, DMSO-d_6): δ 9.61 (s, 1H), 7.05 (d, J = 8.2 Hz, 1H), 6.52 (dd, J = 8.2, 2.4 Hz, 1H), 6.43 (d, J = 2.4 Hz, 1H), 2.86–2.82 (m, 2H), 2.74–2.70 (m, 2H). ^{13}C NMR (100 MHz, DMSO-d_6): δ 168.5, 157.1, 152.3, 128.7, 113.2, 111.2, 103.2, 29.0, 22.1.

2.3. Biochemical methods

2.3.1. Biochemical characterization of bacteria

Bacteria were characterized by using API strips according user manuals (Biomerieux, USA). API 50 CH strip was used for carbohydrate fermentation test. *Pseudomonas mandelii* 7HK4 bacteria were grown overnight (~2 OD) in 10 mL of LB medium in conical tube (50 mL volume). Cells were centrifuged for 10 minutes at 3,220 × *g* and resuspended in 10 mL of API 50 CHB/E medium. 100 µL of resuspended culture was transferred into wells of API 50 CH strip and incubated at 30 °C for 48 h. Colour of the medium changes from red colour to yellow colour due to acid production, if the test is positive.

And API 20 ZYM strip was used to test enzyme activities. 10 mL of overnight bacterial culture was resuspended in 3 mL of mineral medium (without Mg^{2+}) and aliquoted into wells of API 20 ZYM strip. Incubated at 30 °C for 4 h. After incubation 1 drop of ZYM A and 1 drop of ZYM B reagents were added to each well. Colourless wells showed negative test results.

2.3.2. Whole-cell bioconversions

Pseudomonas mandelii 7HK4 bacteria were grown in mineral medium supplemented with 0.05 % (w/v) of 7-hydroxycoumarin or glucose, as the sole carbon and energy source, at 30 °C with rotary aeration (180 rpm) in conical flask (50 mL volume) for 48 h (~5 OD). *E. coli* BL21 (DE3) bacteria containing recombinant genes were grown in 30 mL of BHI medium at 30 °C and 180 rpm aeration in conical flask (50 mL volume) overnight. High density (15–20 OD) *E. coli* bacterial culture was centrifuged and resuspended in 30 mL of minimal C-750501 medium, in which the synthesis of proteins was induced with 1 mM of IPTG after 1.5 h of incubation at 20 °C and 180 rpm [109,111]. Incubation at 20 °C was continued for another 24 h. Both *Pseudomonas mandelii* 7HK4 and *E. coli* cells were sedimented by centrifugation (3,220 × *g*, 15 min, 20 °C). The collected cells were washed twice with 15 mL of 0.9 % NaCl solution. For whole-cell conversion experiments, cells from 20 mL of culture were resuspended in 1 mL of 50 mM potassium phosphate buffer (pH 7.2). All small-scale bioconversions with whole cells were made in 50 mM

potassium phosphate buffer, pH 7.2, which contained 0.5–2 mM of the substrate. The reaction mixtures were kept in a thermoblock at 30 °C and 500 rpm for 1–24 hours. Bioconversion mixtures were centrifuged for 2 min at 10,000 × *g* (20 °C), and 100 µL of the supernatant were analysed by UV-VIS spectroscopy (range 200–600 nm). Measurements were repeated to record the changes in the absorption intensity over time. All measurements were performed with PowerWave XS microplate reader.

2.3.3. Preparation of cell-free extracts

Cells were sedimented by centrifugation (3,220 × *g*, 15 min, 20 °C). The biomass was resuspended in 3 ml of 50 mM potassium phosphate buffer (pH 7.2). The cells were disrupted by pulse-mode sonication (3 min duration and 1 s cycles) at 4 °C. Cell debris was removed by centrifugation (4 °C, 16,100 × *g*, 15 min).

2.3.4. Protein purification

His_6-tagged proteins were purified with Äkta purifier 900 chromatography systems (GE Healthcare, Finland). Cell-free extracts were loaded onto a Ni^{2+} Chelating HiTrap™ HP column (1–5 mL) (GE Healthcare, Finland) equilibrated with 50 mM potassium phosphate buffer (pH 7.0–7.2), at 1.0 mL/min. The column was washed with at least 3 volumes of the same buffer. Then the bound proteins were eluted with 0.5 M imidazole in 50 mM potassium phosphate buffer (pH 7.0–7.2). The fractions containing the purified enzyme were combined and dialyzed against the 50 mM potassium phosphate buffer (pH 7.0–7.2), at 4 °C overnight or applied to HiTrap™ Desalting column with Sephadex G-25 resin (GE Healthcare, Finland) and eluted with 50 mM potassium phosphate buffer (pH 7.0–7.2). Protein concentration was determined by the Lowry method [112].

2.3.5. Gel filtration chromatography

The structure of the native HcdA protein was determined by gel filtration chromatography. The purified protein was applied to Superdex™ 200 10/300 GL column (GE Healthcare, Finland) using a 50 mM Tris-HCl buffer, pH 7.5, containing 0.1 M of NaCl at 0.3 mL/min. Protein molecular mass was determined using the calibration curve, constructed by the application of carbonic anhydrase (M=29 kDa), albumin (M=66 kDa) and apoferritin (M=443 kDa). 0.8–1 mg of all proteins was dissolved in 0.5 mL 50 mM Tris-HCl, pH 7.5 and 0.1 M NaCl buffer. The K_{av} values were calculated for 3 proteins using the equation $K_{av} = (V_e-V_0)/(V_c-V_0)$, where V_0 = column void

volume = 8.2 mL, V_c = geometric column volume = 23.6 mL and V_e = elution volume for each protein: carbonic anhydrase (29 kDa) V_e=16.9 mL, albumin (66 kDa) V_e=14.47 mL and apoferritin (443 kDa) V_e=10.6 mL. For the sample, the observed V_e was used to calculate the corresponding K_{av} value that was used to determine the molecular weight from the equation of the calibration curve. The term K_{av} indicates the ratio between the elution volume of a given molecule and the total available volume of the column.

2.3.6. SDS-polyacrylamide gel electrophoresis

Proteins were analysed by SDS-PAGE according to Laemmli [113], using a 14 % separating gel (pH=8.8) and 4.5 % stacking gel (pH=6.8). To visualize the protein bands, the gels were immersed for 1 min in a hot solution consisting of 0.1 % Coomassie Brilliant Blue R250, 10 % acetic acid, and 50 % methanol, followed by destaining in 7 % acetic acid.

2.3.7. Preparation of proteins from a polyacrylamide gel for mass spectrometric analysis

Proteins were fractionated on an SDS-polyacrylamide gel. After Coomassie blue R-250 staining, protein samples were extracted from the gel [114]. Protein bands were excised from the gel with a razor, and the gel was then destained twice with 200 µL of 25 mM ammonium bicarbonate and 50 % acetonitrile solution for 30 min at 37 °C. Protein disulphide bonds were reduced with 40 µL of 10 mM DTT for 45 min 60 °C, followed by incubation with 30 µL of 100 mM iodoacetamide for 1 h at room temperature in the dark to alkylate free cysteines. Gel slices were washed again twice with 100 µL 25 mM ammonium bicarbonate and 50 % acetonitrile solution for 15 min at 37 °C, dehydrated by adding 50 µL 100 % acetonitrile and dried using a vacuum centrifuge. Gel pieces were incubated with up to 40 µl of activated trypsin (10 ng/µL) at 37 °C overnight. The next day, the supernatant was saved and the peptides were extracted from the gel by incubating gel slices in two consecutive changes of 50 µL of 5 % trifluoroacetic acid and 50 % acetonitrile solution for 1 h at 37 °C. Combined supernatants were dried using a vacuum centrifuge at 30 °C. Lyophilized peptides were dissolved in 20 µL of 0.1 % trifluoroacetic acid solution. Peptides purified and concentrated using Millipore C18 ZipTips.

2.3.8. Enzyme assays

3-(2,4-dihydroxyphenyl) propionic acid hydroxylase activity was measured spectrophotometrically by monitoring absorption changes of the

reaction mixture at 340 nm wavelength due to the oxidation of either NADH or NADPH (ε_{340} = 6,220 $M^{-1}cm^{-1}$) after the addition of the substrate. The activity measurements were made with cell-free extracts or the purified protein. All measurements of the enzyme activity were carried out at 22 °C in 1 mL of reaction mixture, containing 25–50 mM tricine or potassium phosphate buffers (pH 7.8), 100 µM NAD(P)H, and 150 µM aromatic substrate. One unit of activity was defined as the amount of the enzyme that catalysed the oxidation of 1 µmol of NAD(P)H per minute in buffer of pH 7.8 at 22 °C.

Reducing activity of HcdE protein was measured spectrophotometrically by monitoring absorption changes of bimolecular reaction at 340 nm wavelength due to the oxidation of NADPH and reduction of various coumarin derivatives (ε_{340} = 5,580 $M^{-1}cm^{-1}$ (for 7-hydroxycoumarin), ε_{340} = 4,780 $M^{-1}cm^{-1}$ (for 6-hydroxycoumarin), ε_{340} = 4,440 $M^{-1}cm^{-1}$ (for 6-methylcoumarin), ε_{340} = 8,500 $M^{-1}cm^{-1}$ (for 6,7-dihydroxycoumarin), ε_{340} = 3,690 $M^{-1}cm^{-1}$ (for coumarin)) after the addition of the enzyme. The activity measurements were made with cell-free extracts or the purified protein. The standard measurements of the enzyme activity were carried out at 22 °C in 0.8 mL of reaction mixture, containing 50 mM potassium phosphate buffer (pH 7.0), 160 µM NADPH, and 60 µM aromatic substrate.

Kinetic characterization of HcdE protein was performed by monitoring absorption changes of reaction mixture at 365 nm wavelength due to the oxidation of NADPH only (ε_{365} = 3,500 $M^{-1}cm^{-1}$), after the addition of the enzyme. The measurements of the enzyme activity were carried out at 22 °C in 0.8 mL of reaction mixture, containing 50 mM potassium phosphate buffer (pH 7.0), 5–200 µM NADPH, 5–150 µM 7-hydroxycoumarin, and 99 nM HcdE protein. Each measurement was performed three times. Kinetic data were analysed using Wolfram Mathematica software (Wolfram Research, Inc).

2.3.9. *In vivo* bioconversion of 3-(2,4-dihydroxyphenyl) propionic acid

E. coli BL21 (DE3) bacteria, containing p4pmPmo and pTHPPDO plasmids, were grown in 200 mL of BHI medium at 30 °C and 180 rpm aeration in conical flask (500 mL volume) overnight. High density (15–20 OD) bacterial culture was centrifuged (3,220 × *g*, 20 °C) and resuspended in 200 mL of minimal C-750501 medium, in which synthesis of proteins was induced with 1 mM of IPTG at 20 °C and 180 rpm [115,116]. After 24 h of induction 3-(2,4-dihydroxyphenyl) propionic acid was added to the final concentration of 4 mM. Bioconversion mixture was incubated for another 3

days at 30 °C with shaking (180 rpm). Cells were removed by centrifugation for 30 min at 3,220 × *g* (20 °C) and the supernatants were kept at 4 °C.

2.3.10. Purification of 3-(2,4-dihydroxyphenyl) propionic acid bioconversion product

The supernatant containing the 3-(2,4-dihydroxyphenyl) propionic acid oxidation product was incubated with 1.2 M ammonium chloride at room temperature overnight [115,116]. Reaction mixture was concentrated to ~100 mL volume and adjusted to pH 1 with concentrated HCl. The remains of substrate were extracted by five consecutive changes of 25 mL of ethyl acetate, and then aqueous fraction was purified using a reverse phase C_{18} column, equilibrated with water. Column was washed with at least 100 ml of water and then eluted with linear gradient of 0–60 % methanol solution at a flow rate of 2 mL/min. Aqueous fractions were combined and evaporated (40 °C). Brownish crystals were dissolved in 0.1 % formic acid solution and again loaded onto a reverse phase C_{18} column, previously equilibrated with 0.1 % formic acid solution. Column was washed with at least 30 ml of 0.1 % formic acid solution and then eluted with 60 % methanol solution. Picolinic acid derivative was eluted with 0.1 % formic acid solution. Fractions containing the product were collected, combined and evaporated (40 °C). Picolinic acid yield from 145 mg of 3-(2,4-dihydroxyphenyl) propionic acid fermentation was 34 mg, 24 % of the theoretical yield. The product had traces of formic acid impurities, which aided the dissolution of the analyte in D_2O for NMR analysis.

2.3.11. *In vivo* bioconversion of 7-hydroxycoumarin

E. coli BL21 (DE3) cells, containing pHP7 plasmid, were grown in 6 × 200 mL of LB medium at 30 °C and 180 rpm aeration in conical flasks (500 mL volume) overnight. High density (15–20 OD) bacterial cultures were supplied with 0.5 mM of IPTG for induction of protein synthesis, and incubated at 20 °C and 180 rpm. After 48 hours of induction cells were centrifuged (3,220 × *g*, 20 °C) and resuspended in respective volumes of 50 mM potassium phosphate buffer (pH 7.2). Then, 7-hydroxycoumarin was added to the final concentration of 0.3 mM. Bioconversion mixture was incubated at 30 °C with shaking (180 rpm) overnight. Cells were removed by centrifugation for 40 min at 3,220 × *g* (20 °C) and the supernatants were used for product purification.

2.3.12. Purification of 7-hydroxycoumarin bioconversion product

Bioconversion product was purified as described in Serra et al. (2019) with minor changes [117]. The biotransformation broth was treated with concentrated

HCl aq. in order to bring the pH between 4 and 5. The solution was saturated with NaCl and extracted with CH_2Cl_2 (4 × 100 mL). The combined organic phases were dried (Na_2SO_4) and concentrated under reduced pressure resulting in 7-hydroxycoumarin residues (MS (ESI+): m/z 161 $[M-H]^-$). Ethyl acetate (100 mL) was then added to the aqueous solution and the mixture was filtered on a celite pad. The phases were separated and the aqueous phase was extracted with further solvent. The combined organic phases were dried (Na_2SO_4) and concentrated under reduced pressure. The obtained pale-yellow precipitates consisted of 3-(2,4-dihydroxyphenyl) propionic acid. MS (ESI+): m/z 181 $[M-H]^-$; ^{1}H NMR (DMSO-d_6, 400 MHz): δ 11.97 (s, 1H), 9.14 (s, 1H), 8.96 (s, 1H), 6.80 (d, *J* = 8.2 Hz, 1H), 6.26 (d, *J* = 2.4 Hz, 1H), 6.11 (dd, *J* = 8.1, 2.4 Hz, 1H), 2.63 (dd, *J* = 8.6, 6.9 Hz, 2H), 2.40 (dd, *J* = 8.5, 6.9 Hz, 2H); ^{13}C NMR (DMSO-d_6, 100 MHz): δ 174.73, 157.00, 156.23, 130.41, 117.79, 106.33, 102.84, 34.63, 25.37. Given NMR spectra complies with known spectra of 3-(2,4-dihydroxyphenyl) propionic acid standard (^{1}H NMR (DMSO-d_6, 400 MHz): δ 11.98 (s, 1H), 9.14 (s, 1H), 8.96 (s, 1H), 6.80 (d, *J* = 8.1 Hz, 1H), 6.26 (d, *J* = 2.4 Hz, 1H), 6.11 (dd, *J* = 8.1, 2.4 Hz, 1H), 2.63 (dd, *J* = 8.5, 6.9 Hz, 2H), 2.40 (dd, *J* = 8.5, 6.9 Hz, 2H); ^{13}C NMR (DMSO-d_6, 100 MHz): δ 174.73, 157.00, 156.23, 130.41, 117.79, 106.33, 102.83, 34.63, 25.36). The yield of 3-(2,4-dihydroxyphenyl) propionic acid from 59 mg of starting material was 50 mg (75.7 % of the theoretical yield).

2.3.13. Biosynthesis of 3-(2,3-dihydroxyphenyl) propionic acid

E. coli BL21 (DE3) bacteria, containing p5Pmo plasmid, were grown in 200 mL of LB medium at 30 °C and 180 rpm aeration in conical flask (500 mL volume) overnight. High density (15–20 OD) bacterial culture was centrifuged and resuspended in 200 mL of minimal C-750501 medium, in which synthesis of proteins was induced with 1 mM of IPTG at 20 °C and 180 rpm [118]. After 24 h of induction cells were centrifuged (3,220 × *g*, 20 °C) and resuspended in 200 mL of potassium phosphate buffer (pH 7.2). 3-(2-Hydroxyphenyl) propionic acid was added to the final concentration of 2 mM. Bioconversion mixture was incubated for another 12 hours at 30 °C with shaking (180 rpm). Cells were removed by centrifugation for 30 min at 3,220 × *g* (20 °C) and the supernatant were immediately used.

2.4. Molecular biology methods

2.4.1. Purification of genomic DNA

Pseudomonas mandelii 7HK4 bacteria were grown overnight in 20 mL of LB medium containing 1 % of glycerol. Cells were centrifuged for 10 min at

3,220 x *g* (20 °C) and washed with 3 ml of 50 mM citrate buffer (pH 8.2). Cells were divided into 6 parts, each of them was resuspended in 600 µL of lysis buffer (50 mM Tris-HCl (pH 8.0), 50 mM EDTA, 3 % SDS, 1 % mercaptoethanol, 0.2 M NaCl) [119], also 15 µL of 20 mg/mL Proteinase K was added, and incubated for 2 hours at 65 °C. Then lysates were centrifuged for 15 min at 16,100 × *g* (20 °C) and 300 µL of 7.5 M ammonium acetate (pH 6.0) was added to the supernatant, followed by mixing by inversion several times and centrifugation for 20 min at 16,100 × *g* (20 °C). DNA was precipitated with 2 volumes of ethanol overnight at –20 °C, followed by centrifugation. DNA precipitates were resuspended and combined in 60 µL of 20 mM Tris-HCl buffer (pH 8.0) and incubated with 10 µg RNase A. Genomic DNA was purified using Rapid Clean protein removal resin.

2.4.2. Purification of plasmid DNA

Plasmid DNA from *E. coli* was isolated by standard alkaline lysis [119]. *E. coli* bacteria were grown overnight in 20 mL of LB medium. Cells were centrifuged for 10 minutes at 3,220 x *g* (20 °C) and resuspended in 1 volume of lysis solution I (50 mM glucose, 10 mM EDTA, 25 mM Tris-HCl (pH 8.0)). After addition of 2 volumes of freshly made lysis solution II (0.2 N NaOH, 1 % SDS) samples were gently mixed by inverting and incubated for up to 5 min on ice. Later, 1.5 volume of ice-cold 7.5 M ammonium acetate was added to the lysate followed by repeated gentle inversion and incubated for up to 3 min on ice. Lysates were centrifuged for 5 min at 16,100 × *g* (20 °C) and 2 volumes of ice-cold ethanol was added to the supernatants, followed by thorough mixing. pDNA was precipitated after 2 hours or overnight at –20 °C, followed by centrifugation (16,100 × *g*, 20 °C). pDNA precipitates were resuspended in 35 µL of water.

2.4.3. DNA amplification

Multiplication of genes was conducted by PCR using Phusion High-Fidelity PCR Master Mix with HF Buffer, following the user manuals provided by manufacturer of reagents. Amplification conditions:

For *hcdA* gene: initial denaturation for 1 min at 98 °C, then 40 cycles of denaturation for 10 s at 98 °C, annealing for 20 s at 69 °C, and extention for 50 s at 72 °C, final extension for 5 min at 72 °C;

For *hcdB* and *hcdC* genes: initial denaturation for 1 min at 98 °C, then 40 cycles of denaturation for 10 s at 98 °C, annealing for 15 s at 60 °C, and extention for 30 s at 72 °C, final extension for 5 min at 72 °C;

For *XenA38, XenA45* and *XenA205* genes: initial denaturation for 1 min at 98 °C, then 30 cycles of denaturation for 10 s at 98 °C, annealing for 15 s at 68.5 °C, and extention for 60 s at 72 °C, final extension for 5 min at 72 °C;

For 3kb region of *hcdDEFG* genes: initial denaturation for 1 min at 98 °C, then 35 cycles of denaturation for 20 s at 98 °C, annealing and extention for 8 min at 72 °C, final extension for 7 min at 72 °C.

For *hcdE* gene: initial denaturation for 30 s at 98 °C, then 35 cycles of denaturation for 10 s at 98 °C, annealing for 10 s at 65 °C, and extention for 45 s at 72 °C, final extension for 3 min at 72 °C

All PCR primers used during this study are listed in Table 3.

Table 3. The list of primers used in this study.

Primers	Primer sequence, 5'-3'	Features, target	Source
hcdA_F	gtaattccatatggactacgatgtcatcat	*Nde*I restriction site, *hcdA* gene	This study
hcdA_R1	aaaccaagcttctggcttagtccctg	*Hind*III restriction site, *hcdA* gene	This study
hcdA_R2	aaaattctcgagttactggcttagtcccctg	*Xho*I restriction site, STOP codon, *hcdA* gene	This study
hcdB_F	catgccatgggtatgcccgcattaccgactat	*Nco*I restriction site, *hcdB* gene	This study
hcdB_R	aacccaagcttcagccgattcgaaccccg	*Hind*III restriction site, STOP codon, *hcdB* gene	This study
hcdC_F	gtaattccatatgaagcttatttcgtaccg	*Nde*I restriction site, *hcdC* gene	This study
hcdC_R	aaaattctcgagttaggcttcgtcaataacgc	*Xho*I restriction site, STOP codon, *hcdC* gene	This study
Woo1	agagtttgatcmtggctc	16S rRNR gene	[120]
Woo2	gntaccttgttacgactt	16S rRNR gene	[120]
4XenA38 Nde_F	gtaattccatatgagtctgctgcttgaacc	*Nde*I restriction site, *XenA38* gene	This study
4XenA38 tXho_R	aaattctcgagtcaatcacgcaaatccgactc	*Xho*I restriction site, STOP codon, *XenA38* gene	This study
4XenA45 Nde_F	gtaattccatatggagcgtcccatgcccgt	*Nde*I restriction site, *XenA45* gene	This study

4XenA45 tXho_R	aaattctcgagttaaaccagggtcat caacgcct	*Xho*I restriction site, STOP codon, *XenA45* gene	This study
4XenA20 5Nde_F	gtaattccatatggagttaccgatgg ccgc	*Nde*I restriction site, *XenA205* gene	This study
4XenA20 5tXho_R	aaattctcgagttacaactcagcagc caaccg	*Xho*I restriction site, STOP codon, *XenA205* gene	This study
4hp4-16Nde_F	gtaattccatatgatgtcgcttgtgat ggtt	*Nde*I restriction site, *hcdD* gene	This study
4hp7-16Nde_F	gtaattccatatgttggagaacatcat gac	*Nde*I restriction site, *hcdE* gene	This study
4hp7-16Xho_R	aaattctcgagtcaaggacagatga cgtagtt	*Xho*I restriction site, STOP codon, *hcdE* gene	This study
4hp10-16Xho_R	aaattctcgagttaagccaagcgcct gattt	*Xho*I restriction site, STOP codon, *hcdG* gene	This study
4XenA38 qPCR_F	taaacatggcagcgtcaaac	*XenA38* gene, primer for qPCR	This study
4XenA38 qPCR_R	gtttagccgaagcgacaaag	*XenA38* gene, primer for qPCR	This study
4XenA45 qPCR_F	cccagcaagatatccaggac	*XenA45* gene, primer for qPCR	This study
4XenA45 qPCR_R	ctgccttcccagaagaactg	*XenA45* gene, primer for qPCR	This study
4XenA20 5qPCR_ F	aagcagatcagcgatttcgt	*XenA205* gene, primer for qPCR	This study
4XenA20 5qPCR_ R	ggcgaggaactggttaatga	*XenA205* gene, primer for qPCR	This study
4hcdAqP CR_F	ggttttatcggtcgattcca	*hcdA* gene, primer for qPCR	This study
4hcdAqP CR_R	ctccatcttcaagcccagtc	*hcdA* gene, primer for qPCR	This study
4hcdBqP CR_F	aagtcatccagcgagtccag	*hcdB* gene, primer for qPCR	This study

4hcdBqPCR_R	atcggctgtttttcatgacc	*hcdB* gene, primer for qPCR	This study
4hcdCqPCR_F	cgtcgttgaagcaggtgtaa	*hcdC* gene, primer for qPCR	This study
4hcdCqPCR_R	aggcctcaggtatcagagca	*hcdC* gene, primer for qPCR	This study
4hcdRqPCR_F	gaagtcgcgttgaccaagat	*hcdR* gene, primer for qPCR	This study
4hcdRqPCR_R	caaccctgaacccttttgttg	*hcdR* gene, primer for qPCR	This study
4hp1-16qPCR_F	atgccaaggattcaggacag	*Hp4* gene, primer for qPCR	This study
4hp1-16qPCR_R	ttgacgtcctcgggataaac	*Hp4* gene, primer for qPCR	This study
4hp4-16qPCR_F	actggacgtcgaggaagtgt	*hcdD* gene, primer for qPCR	This study
4hp4-16qPCR_R	gcccctaaccctctcagttc	*hcdD* gene, primer for qPCR	This study
4hp7-16qPCR_F	tctgggtaccgcctacaaag	*hcdE* gene, primer for qPCR	This study
4hp7-16qPCR_R	gccaggtctttcaccttctg	*hcdE* gene, primer for qPCR	This study

2.4.4. DNA digestion and ligation

DNA was digested with an appropriate DNA restriction endonuclease according to the recommendations of manufacturer. All ligations were performed using the T4 DNA ligase overnight at 8 °C. The ligase was inactivated by heating the ligation mixture for 10 min at 65 °C.

2.4.5. Preparation of electrocompetent cells and electroporation

E. coli competent cells were prepared by the method described by Sharma and Schimke [121]. Briefly, DNA was mixed with 100 µL of ice-cold competent cells. Later, transferred to the electroporation cuvette (capacity of 100 µL) and

subjected to 20 kV/cm electric pulse using the Eppendorf electroporator. Cells were immediately diluted with 1 mL of LB medium and incubated for 30–60 min at 37 °C with shaking. After the recovery, cells were spread on the plates containing an appropriate antibiotic or substrate.

2.4.6. DNA electrophoresis in agarose gel

Horizontal DNA electrophoresis was performed using 0.8–1.2 % agarose gels in TAE buffer as described by Sambrook et al [119]. Gels were stained with ethidium bromide and analysed under UV using Transilluminator UVT-28ME, Herolab.

2.4.7. Purification of total RNA

Pseudomonas mandelii 7HK4 was cultivated overnight in mineral medium containing 0.05 % of glucose as the sole carbon source. Then cells were sedimented by centrifugation (3,220 × *g*, 10 min, 20 °C) and resuspended in 50 mM potassium phosphate buffer, pH 7.2. *Pseudomonas mandelii* 7HK4 cells were supplemented with 1 mM of various coumarin derivatives and incubated for additional 3 h at 30 °C with shaking. Total RNA was isolated using a RiboPure™ Bacteria RNA Purification Kit according to the recommendations of manufacturer.

2.4.8. Quantitative RT-PCR

cDNA synthesis was performed using a High-Capacity cDNA Reverse Transcription Kit from 340 ng input of total RNA per sample. Quantitative-PCR (qPCR) amplification was performed using a Fast SYBR™ Green Master Mix according to the recommendations of manufacturer on 7500 Fast RealTime PCR system (Thermo Fisher Scientific). qPCR was conducted in 20 µL of reaction mixture containing 10 µL of Fast SYBR™ Green Master Mix, 500 nM of each primer (see Table 3), and 2 µL of the cDNA sample. For quantitative analysis, fluorescence data were recorded after the annealing step. All experiments were carried out in triplicate. To verify the absence of DNA in the total RNA samples, the qPCR was performed directly for RNA samples. The threshold cycle (CT) (threshold value, 5 % of amplification curve plateau) values were obtained using 7500 Fast RealTime PCR Software v2.0 (Thermo Fisher Scientific).

2.5. Analytical methods

2.5.1. High-performance liquid chromatography and mass spectrometry

For the HPLC-MS analysis, most of the analytes were dissolved in acetonitrile, otherwise the aqueous samples were mixed with an equal part of acetonitrile and centrifuged before the analysis. High-performance liquid chromatography and mass spectrometry (HPLC-MS) was carried out using the system, consisting of the CBM-20 control unit, two LC-2020AD pumps, SIL-30AC auto sampler and CTO-20AC column thermostat, using the SPD-M20A detector and LCMS-2020 mass spectrometer with ESI source (Shimadzu, Japan).

Chromatographic fractionation was conducted using YMC-Pack Pro C_{18} column, 150×3 mm (YMC, Japan) at 40 °C, with 0.1 % formic acid solution in water and acetonitrile gradient from 5 % to 95 % for acidic compounds and with water and acetonitrile gradient from 5 % to 95 % for lactones.

Mass spectra were recorded from *m/z* 10 up to 500 *m/z* at 350 °C and ± 4500 V using N_2. Mass spectrometry analysis was carried out using both the positive and negative ionization modes. The data were analysed using LabSolutions LC/MS software (Shimadzu, Japan).

2.5.2. Nuclear magnetic resonance spectroscopy

^{1}H NMR and ^{13}C NMR spectra were recorded in DMSO-d_6 on Avance III 400 NMR spectrometer, at 400 MHz for ^{1}H and 100 MHz for ^{13}C, chemical shifts are reported in ppm relative to solvent resonance signal as an internal standard (^{1}H NMR: δ (DMSO-d_6) = 2.50 ppm; ^{13}C NMR: δ (DMSO-d_6) = 39.52 ppm).

2.5.3. Protein MS-MS analysis

Peptides were subjected to *de novo* sequencing based on matrix-assisted laser desorption ionization time of flight (MALDI-TOF/TOF) mass spectrometry (MS) and subsequent computational analysis at the Proteomics Centre of the Institute of Biochemistry, Life Sciences Center, Vilnius University (Vilnius, Lithuania). The sample was purified as described previously. 0.5 µl of tryptic digests were transferred on 384-well MALDI plate with 0.5 µl 4 mg/ml *α*-cyano-4-hydroxycinnamic acid (CHCA) matrix in 50 % acetonitrile with 0.1 % trifluoroacetic acid and analysed with an Applied Biosystems/MDS SCIEX 4800 MALDI TOF/TOF™ mass spectrometer. Spectra were acquired in the positive reflector mode between 800 and 4000 *m/z* with fixed laser intensity at 3700 (Laser shots: 400; Mass accuracy: ±50

ppm). The most intense peaks of each survey scan (MS) were fragmented for sequence analysis (Collision energy: 1 keV; CID: no CID or medium air pressure CID used; Laser intensity: 4200–4400; Laser shots: 500–1000; Fragment mass accuracy: ±0.1 Da). Sequence analysis and peak lists were generated using GPS Explorer™ De Novo Explorer.

2.5.4. Whole-genome sequencing

The sequencing and subsequent assembly of the *Pseudomonas mandelii* 7HK4 genome was performed by BaseClear (Leiden, The Netherlands). The quality-filtered Illumina FASTQ sequence reads were assembled into a number of contig sequences. The analysis was performed using ABySS version 1.5.1. The contigs were linked and placed into scaffolds based on the alignment, which was performed with BLASR.

2.5.5. Nucleotide sequence determination

Plasmid DNA was purified using the ZYMO Plasmid PREP kit. Concentration of DNA was determined by electrophoresis in agarose gel using the Mass Ruler DNA Ladder (High Range). The nucleotide sequences were determined at the Macrogen (South Korea).

2.6. Analysis of DNA and protein sequences

DNA and protein sequences were analysed using VectorNTI Advance 11.0 [122] and MEGA 5.0 [123,124], respectively. The search of homologues was conducted against NCBI database using BLAST [125]. Phylogenetic trees were constructed by MEGA version 5.0 application tool [123,124], using the Neighbour-joining method (N-J) [126] in accordance with the Maximum Composite Likelihood model for nucleotides or Poisson model for amino acids [127].

2.7. GenBank accession numbers

The accession number for partial 16S ribosomal RNA nucleotide sequence of *Pseudomonas mandelii* 7HK4 is MH346031. Accession numbers for the sequences of *hcdA*, *hcdB* and *hcdC* genes are MH346032, MH346033, MH346034, respectively. Accession numbers for the sequences of *hcdE*, *xenA38* and *xenA45* genes are MW310254, MW310255, MW310256, respectively. The whole fragment of *Pseudomonas mandelii* 7HK4 genome containing *hcd* genes could be found by the accession number MW310253.

3. RESULTS

3.1. Screening and identification of 7-hydroxycoumarin-degrading microorganisms

By the means of enrichment culture using various coumarin derivatives, an aerobic strain 7HK4 degrading 7-hydroxycoumarin was isolated from the garden soil in Lithuania in previous study [54]. This bacterium was tested for its ability to grow on several coumarin derivatives, such as coumarin, 3-hydroxycoumarin, 4-hydroxycoumarin, 6-hydroxycoumarin, 6-methylcoumarin, 6,7-dihydroxycoumarin, and 7-methylcoumarin, as the sole carbon and energy source in a minimal salt medium. However, of all the aforementioned compounds, the strain 7HK4 was able to utilize 7-hydroxycoumarin only. The strain utilized glucose, which was used as a control substrate in whole-cell reactions.

The API 50 CH test was used to study the growth of 7HK4 strain on different carbohydrates. When a carbon source is metabolized, the medium would acidify, however biochemical analysis of this strain showed that acid is not produced from glycerol, erythritol, D-arabinose, L-arabinose, ribose, D-xylose, L-xylose, adonitol, methyl-xyloside, mannitol, galactose, D-glucose, D-fructose, D-mannose, L-sorbose, dulcitol, rhamnose, inositol, sorbitol, α-methyl-D-mannoside, α-methyl-D-glucoside, *N*-acetyl-glucosamine, amygdalin, arbutin, esculin, salicin, cellobiose, maltose, lactose, melibiose, saccharose, trehalose, inulin, melezitose, D-raffinose, amidon, glycogen, xylitol, gentiobiose, D-turanose, D-lyxose, D-tagatose, D-fucose, L-fucose, L-arabitol, D-arabitol, gluconate, 2-keto-gluconate, 5-keto-gluconate. Also, activities for esterase lipase (C8), β-galactosidase, β-glucosidase, esterase (C4), α-galactosidase, lipase (C4), cystine arylamidase, α-chymotrypsin, β-glucuronidase, α-mannosidase, α-fucosidase, alkaline phosphatase, leucinearylamidase, valnearylamidase, trypsin, acid phosphatase, α-glucosidase, *N*-acetyl-β-glucosaminidase were absent. However, activity for naphthol-AS-BI-phosphohydrolase was present.

The nucleotide sequence of 16S rRNA gene was determined by sequencing of the cloned DNA fragment, which was obtained by PCR amplification. The strain 7HK4 showed the highest 16S rDNA sequence similarity to that form *Pseudomonas* genus and was similar to 16S rDNA from *Pseudomonas mandelii* species (identity of 99 %) according to the phylogenetic analysis (Fig. 16).

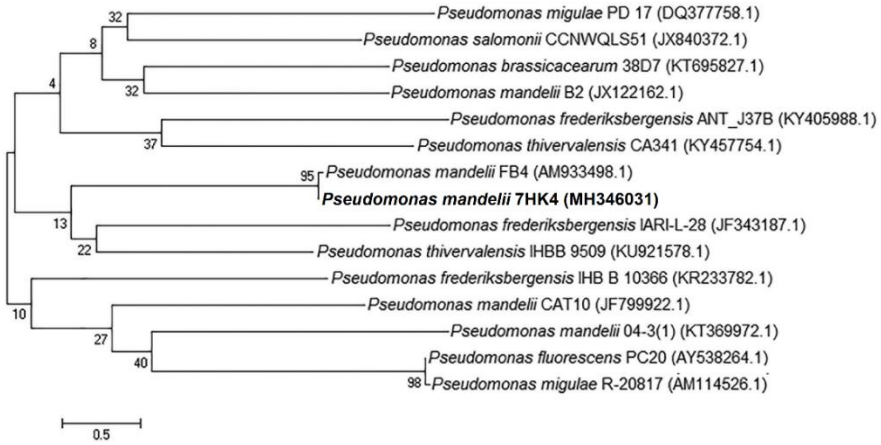

Figure 16. Phylogenetic tree of *Pseudomonas mandelii* 7HK4 bacteria based on partial 16S rDNA sequences. The numbers on the nodes indicate how often (no. of times, %) the species to the right grouped together in 1000 bootstrap samples. Bars represent the number of base substitutions per site. Accession numbers are given in parentheses.

3.2. Bioconversion experiments by using whole cells of *Pseudomonas mandelii* 7HK4

Time-course experiments using whole cells of *Pseudomonas mandelii* 7HK4 pre-grown in the presence of 7-hydroxycoumarin showed that the cells converted coumarin, 6-hydroxycoumarin and 6,7-dihydroxycoumarin in addition to 7-hydroxycoumarin, according to the changes in the UV-VIS spectra (Fig. 17, A–D). UV absorption maxima were dropping down over time, although the biotransformation rates of 6-hydroxycoumarin, 6,7-dihydroxycoumarin and coumarin were approximately 5-fold to 10-fold lower, respectively. After the completion of bioconversions, there were no visible spectra observed for the residual aromatic compound in the reaction mixtures with 7-hydroxycoumarin, except for the reactions with 6-hydroxycoumarin, 6,7-dihydroxycoumarin and coumarin, which had non-disappearing UV absorption maxima at 260–270 nm wavelengths. These spectra are similar to that of 3-phenylpropionic acid (data not shown), suggesting that 7-hydroxycoumarin-induced 7HK4 strain can only catalyze the hydrolysis and reduction of lactone moiety of coumarin, 6-hydroxycoumarin, and 6,7-dihydroxycoumarin producing 3-(2-hydroxyphenyl) propionic, 3-(2,5-dihydroxyphenyl) propionic, and 3-(2,4,5-trihydroxyphenyl) propionic acids, respectively, comparable to similar biotransformations in other microorganisms [9–11,14,16].

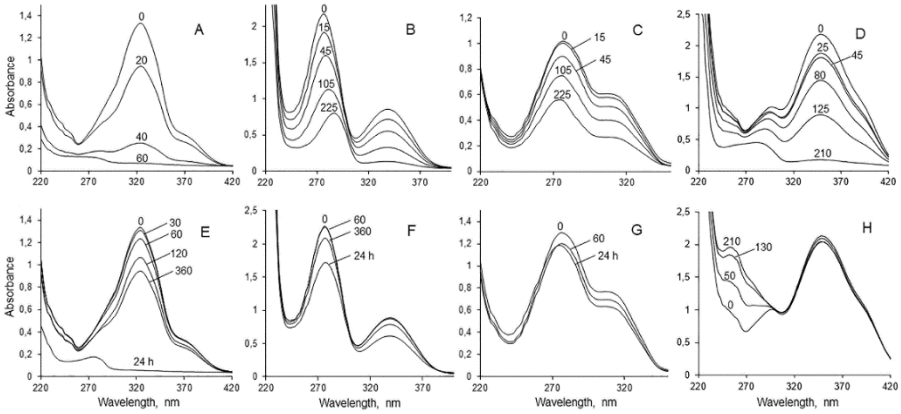

Figure 17. Biotransformation of 7-hydroxycoumarin (A, E), 6-hydroxy-coumarin (B, F), coumarin (C, G) and 6,7-dihydroxycoumarin (D, H) by whole cells of *Pseudomonas mandelii* 7HK4. Cells were pre-grown with 7-hydroxycoumarin (A–D) and glucose (E–H). Biotransformations were carried out with bacterial culture (OD_{600} ~2) in 50 mM potassium phosphate buffer (pH 7.2) at 30 °C with 0.5 mM of substrate. Incubation time is shown in min. 24 h – incubation for 24 hours.

In addition, uninduced *Pseudomonas mandelii* 7HK4 cells grown in the presence of glucose showed delayed and slower conversion of 7-hydroxycoumarin (Fig. 17, E). The bioconversion process only started 0.5 h after the addition of substrate, suggesting that 7-hydroxycoumarin induced its own metabolism. In addition, uninduced cells did not catalyze any conversion or showed delayed and much slower biotransformations for coumarin, 6,7-dihydroxycoumarin and 6-hydroxycoumarin, respectively (Fig. 17, F–H). This demonstrates that in *Pseudomonas mandelii* 7HK4 bacteria, the metabolism of 7- hydroxycoumarin is an inducible process.

It has been shown previously that 3-(2-hydroxyphenyl)-2-propenoic and 3-(2-hydroxyphenyl) propionic acids are the intermediates in a known coumarin metabolic pathway in several microorganisms [9–11,14,16]. By analogy, it was suggested that 3-(2,4-dihydroxyphenyl) propionic acid may be an intermediate metabolite in 7-hydroxycoumarin catabolism. The cells of 7HK4 strain pre-cultivated in the presence of 7-hydroxycoumarin catalysed no conversion of 3-(2-hydroxyphenyl)-2-propenoic or 3-(2-hydroxyphenyl) propionic acid, however 3-(2,4-dihydroxyphenyl) propionic acid was straightforwardly consumed. The HPLC-MS analysis of the bioconversion mixtures showed that *Pseudomonas mandelii* 7HK4 cells cultivated in the presence of 7-hydroxycoumarin produce 3-(2,4-dihydroxyphenyl) propionic acid as an

intermediate metabolite (Fig. 18). In 7HK4 bacteria grown on glucose, the aforementioned compound was not observed suggesting that 3-(2,4-dihydroxyphenyl) propionic acid is an intermediate metabolite during 7-hydroxycoumarin degradation.

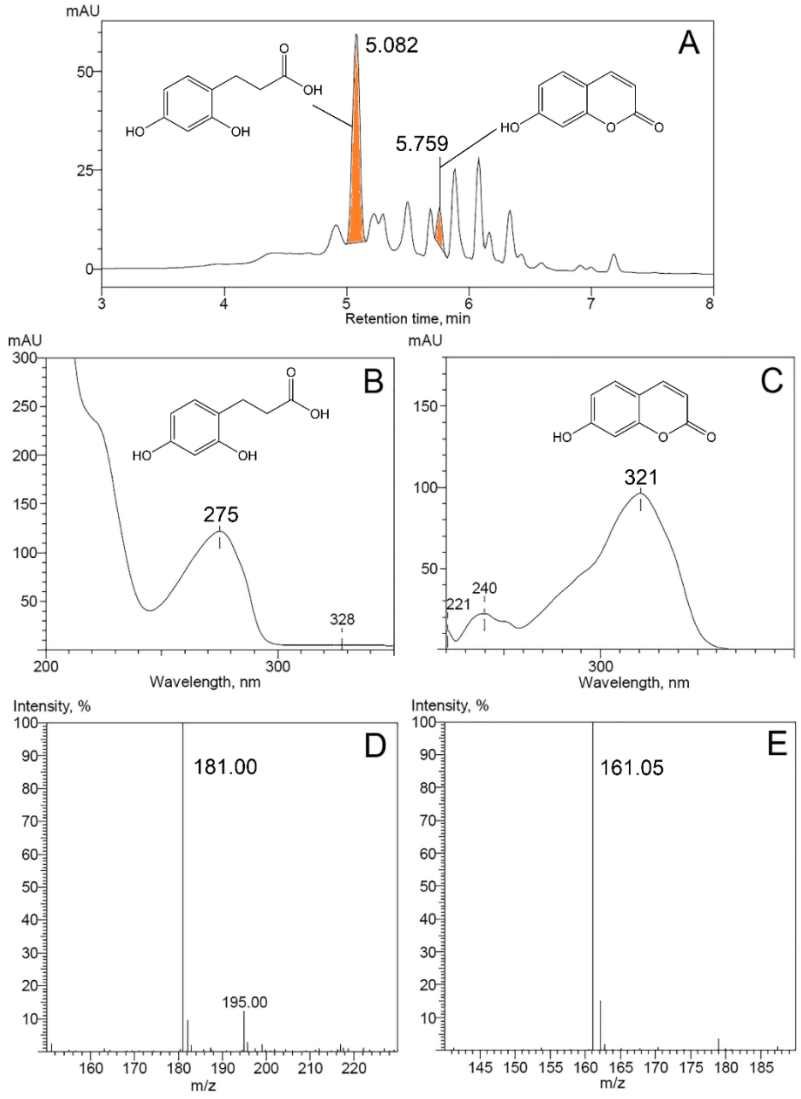

Figure 18. *Pseudomonas mandelii* 7HK4 bacteria were grown in the presence of 7-hydroxycoumarin, and produced metabolites were analysed by HPLC-MS. UV 254 nm trace of metabolites (a). UV and MS spectra of peaks with retention times 5.082 min (b and d) and 5.759 min (c and e). The negative ions $[M\text{-}H]^-$ generated are at m/z 181 (3-(2,4-dihydroxyphenyl) propionic acid) and 161 (7-hydroxycoumarin).

3.3. Screening for XenA reductase homologues in the genome of *Pseudomonas mandelli* 7HK4

Reduction of activated coumarin C=C-bond could be catalysed by ERs [63]. It was reported that as a member of OYE family Xenobiotic Reductase A (XenA) from *Pseudomonas putida* 86 has the ability to reduce the C-3/C-4 double bond of 8-hydroxycoumarin forming from a cleavage of the *N*-heterocyclic ring of quinoline [128]. Therefore, to find out whether *Pseudomonas mandelii* 7HK4 cells utilized the ERs for the catabolism of 7-hydroxycoumarin, we used the amino acid sequence of the known XenA protein to search for the homologues encoded in the partially sequenced genome of *Pseudomonas mandelii* 7HK4 [129]. In this way, three genes denoted as *xenA38*, *xenA45* and *xenA205* encoding putative reductases with close similarity to the known XenA proteins were discovered. The products of the *xenA38*, *xenA45* and *xenA205* genes belonged to the mycofactocin system FadH/OYE oxidoreductase family. The first two proteins had the most resemblance to a putative NADH oxidoreductase from *Pseudomonas fluorescens* SBW25 and 2,4-dienoyl-CoA reductase from *Pseudomonas fluorescens* F113, respectively (Fig. 19, a and b). XenA205 protein was similar to 2,4-dienoyl-CoA reductase from *Pseudomonas* sp. ok602 (Fig. 19, c). All three genes were scattered throughout the genome of *Pseudomonas mandelli* 7HK4 and were unlikely belonging to any putative gene clusters.

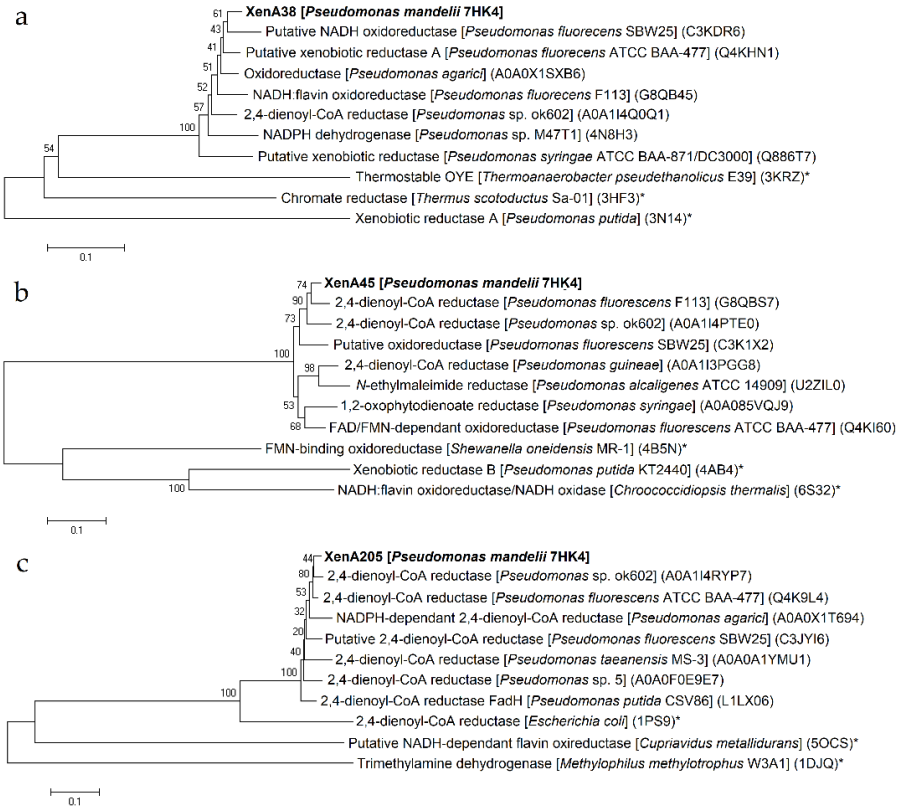

Figure 19. Phylogenetic trees of XenA38 (a), XenA45 (b) and XenA205 (c) proteins. Neighbour joining analyses were performed on the closest homologues with or without known structures and/or function. The numbers on the nodes indicate how often (no. of times, %) the species to the right grouped together in 1000 bootstrap samples. Bars represent the number of amino acid substitutions per site. UniProt/PDB accession numbers are given in parentheses. Proteins with known structure and/or function are marked with an asterix (*).

3.3.1. Characterization of putative xenobiotic reductases

E. coli BL21 cells transformed with the pET21b plasmid harbouring *xenA38*, *xenA45* or *xenA205* gene were used for the assay of the activity of the appropriate enzyme by time course experiments. *E. coli* BL21 containing *xenA38* gene showed bioconversion of coumarin, 6-hydroxycoumarin, 6-methylcoumarin, 7-hydroxycoumarin, 7-methylcoumarin and 6,7-dihydroxycoumarin according to the changes in the UV-VIS spectra (Fig. 20, a–f). Whole cells of *E. coli* BL21 containing XenA45 reductase showed similar activities against these substrates except for the reaction with 6,7-

dihydroxycoumarin of which UV-VIS spectra did not change over time (Fig. 20, g–l). No activities were observed with *o*-coumaric acid and 2,4-dihydroxycinnamic acid. The *E. coli* cells with *xenA205* gene or without any of these genes showed no activity towards those compounds. These findings revealed that *Pseudomonas mandelii* 7HK4 encode two putative xenobiotic reductases, which could utilize a number of differently substituted coumarins.

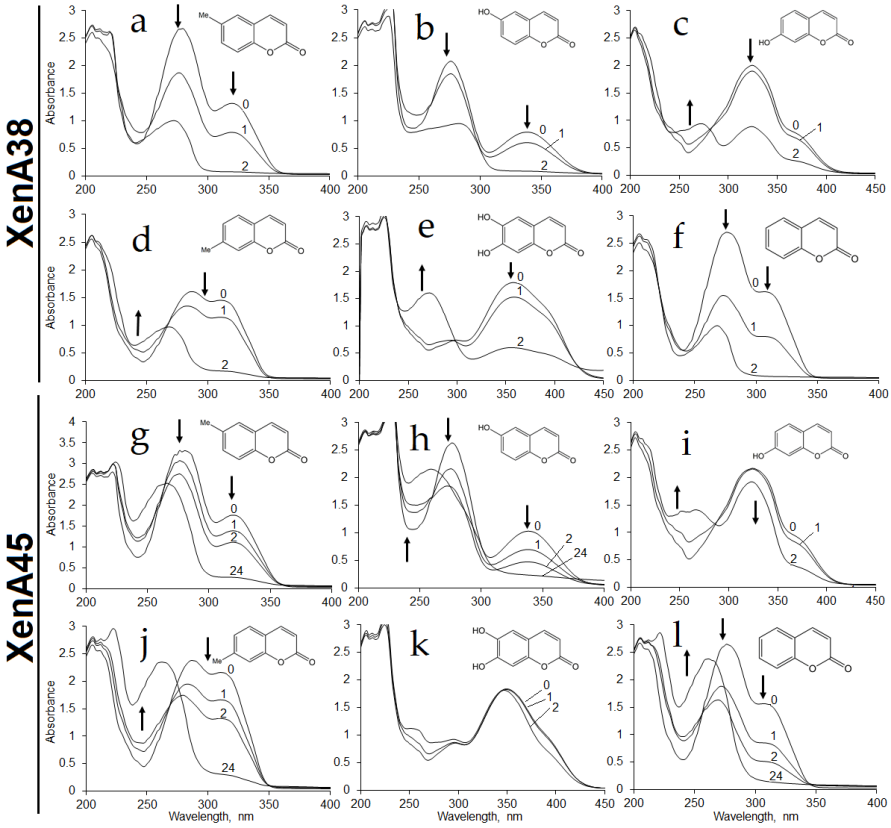

Figure 20. Biotransformation of 6-methylcoumarin (a and g), 6-hydroxycoumarin (b and h), 7-hydroxycoumarin (c and i), 7-methylcoumarin (d and j), 6,7-dihydroxycoumarin (e and k) and coumarin (f and l) by whole cells of *E. coli* BL21 containing *xenA38* (a–f) or *xenA45* (g–l) gene. Biotransformation was carried out in 50 mM potassium phosphate buffer pH 7.2 at 30 °C with 0.5 mM of substrate. Arrows indicate changes of absorbance. Incubation time is shown in hours. 24 h – incubation for 24 hours.

For further characterization the C-terminal His_6-tagged XenA38 and XenA45 proteins were produced in *E. coli* BL21, and purified by affinity chromatography. Both purified enzymes migrated as ~40 kDa bands in SDS-

PAGE, the solution of XenA45 enzyme was colourless contrary to the XenA38 protein that had a bright yellow colour inferring that the protein contained a tightly bound flavin [130,131]. However, all attempts to measure enzymatic activity under aerobic conditions gave no results.

3.4. Identification of 7-hydroxycoumarin-inducible proteins

To elucidate which enzymes are involved in 7-hydroxycoumarin metabolism, *Pseudomonas mandelii* 7HK4 cells were cultivated in a mineral medium supplemented with 7-hydroxycoumarin (0.3 mM) or glucose (0.3 mM) as the sole carbon and energy source. Several 7-hydroxycoumarin-inducible proteins of different molecular mass were observed by using SDS-PAGE analysis of cell-free extracts from *Pseudomonas mandelii* 7HK4 (Fig. 21, A).

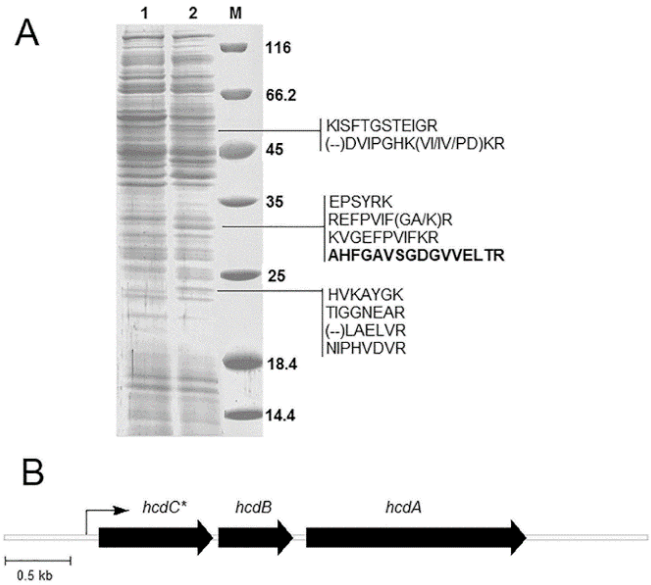

Figure 21. (A) SDS-PAGE analysis of cell-free extracts of *Pseudomonas* sp. 7HK4. Bacteria were cultivated in the presence of GLC (lane 1) or 7HK (lane 2). M – molecular mass ladder (kDa). The arrows indicate inducible 23, 32 and 50 kDa proteins. The peptide sequences determined by MS-MS are given on the right. The sequence in bold was identified after the peptide sequences obtained by MS-MS were compared with the partially sequenced genome of *Pseudomonas mandelii* 7HK4. (B) Organization of *hcd* genes in *Pseudomonas* sp. 7HK4 bacteria. The arrows indicate ORFs encoding HcdA, HcdB and HcdC. The gene for the 7-hydroxycoumarin-inducible protein of 31.2 kDa is marked by an asterix.

Three bands corresponding to the inducible proteins of 23, 32 and 50 kDa (Fig. 21, A) were excised from the SDS-PAGE gel and analysed by MS-MS sequencing. For the identification of corresponding genes of inducible proteins, the sequences of the identified peptides were searched against the partial 7HK4 genome sequence. Thus, the genome fragment (Fig. 21, B) was discovered, encoding a 31.2 kDa protein containing 16 aa-long sequence (Fig. 21, A – bolded sequence) identical to that found in 7-hydroxycoumarin-inducible ~32 kDa protein.

Adjacent to the 31.2 kDa protein-encoding gene, two open reading frames (ORFs) were identified. All three genes are arranged on the same DNA strand, and are separated by short intergenic regions, suggesting that these genes are organized into an operon (Fig. 21, B). The putative operon was designated *hcdABC* (**h**ydroxy**c**oumarin **d**egrading operon), where *hcdC* encodes the 31.2 kDa protein.

3.5. Quantitative RT-PCR analysis of the *Pseudomonas mandelii* 7HK4 transcripts induced by coumarins

To investigate whether the expression of the *hcdABC* gene cluster and putative reductase genes were dependent on 7-hydroxycoumarin, quantitative PCR analysis was performed. *Pseudomonas mandelii* 7HK4 cells were induced with various coumarin derivatives and total RNA was isolated as described in Materials and Methods. Results revealed that the expression of each of the *xenA38* and *xenA45* genes were not induced when *Pseudomonas mandelii* 7HK4 was cultivated in the presence of either 7-hydroxycoumarin, or the other coumarin derivatives (Fig. 22, a). Moreover, *xenA45* gene was not expressed under any tested condition, although the expression levels of the *xenA38* gene were significantly higher than its counterpart. Hence, *xenA38* mRNA synthesis levels of hydroxycoumarin-induced 7HK4 strain cells were compared to glucose-grown (non-induced) cells, which showed that the transcription of *xenA38* gene was increased two-fold in the presence of 6-hydroxycoumarin and three-fold in the presence of 7-hydroxycoumarin. Expression of *xenA38* gene was compared to expression levels of *hcdABC* genes. It was found that the levels of mRNA synthesis of *hcdABC* genes were increased 1000-fold in the presence of 7-hydroxycoumarin or 3-(2,4-dihydroxyphenyl) propionic acid (Fig. 22, b). Therefore, we concluded that the *hcdABC* gene cluster was dependent on 7-hydroxycoumarin, however *xenA38* mRNA levels are too low to be induced by coumarin derivatives and XenA38 could be more as a constitutive enzyme that shares a broad reducing activity in the *Pseudomonas mandelii* 7HK4 cells.

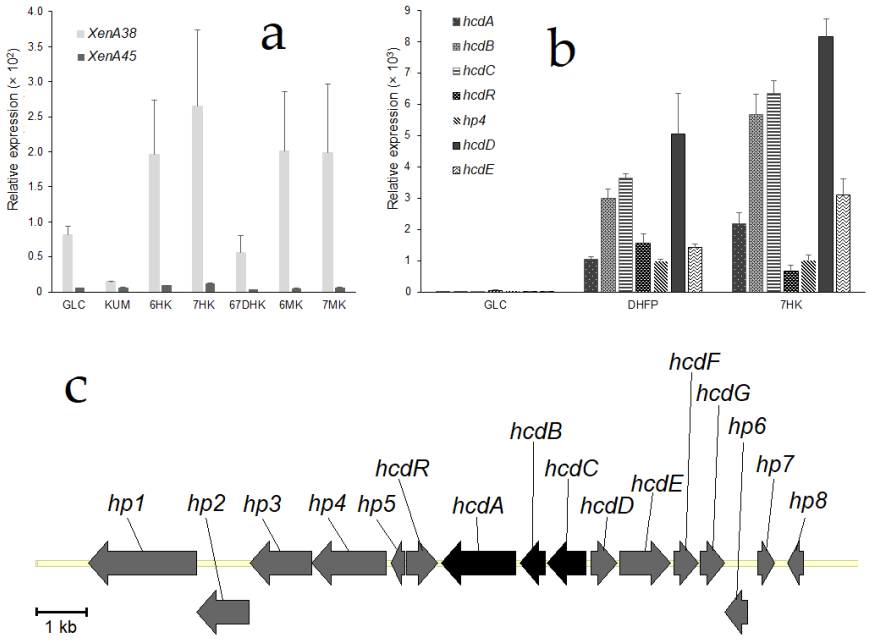

Figure 22. Quantitative RT-PCR analysis of *Pseudomonas mandelii* 7HK4 transcripts. Strain 7HK4 was cultivated in minimal medium supplemented with either 1 mM coumarin derivative (induced conditions) or glucose (non-induced condition) as a single source of carbon. (a) qPCR analysis of the transcription of *xenA38* and *xenA45* genes. (b) qPCR analysis of the transcription of *hcdABCRDE* and *hp4* genes. Primers were designed to amplify the regions of corresponding genes. The data are presented as relative RNA amounts calculated from the threshold cycles using the threshold cycle of 16S RNA as a reference. The averages of three independent runs are presented. GLC – glucose; KUM – coumarin; 6HK – 6-hydroxycoumarin; 7HK – 7-hydroxycoumarin; 6MK – 6-methylcoumarin; 7MK – 7-methylcoumarin; 67DHK – 6,7-dihydroxycoumarin; DHFP – 3-(2,4-dihydroxyphenyl) propionic acid. (c) Organization of *hcdABCDEFG* genes in *Pseudomonas mandelii* 7HK4 bacteria. The black arrows indicate in previous paragraph described ORFs encoding putative HcdA, HcdB, HcdC proteins and grey arrows indicate *hcdDEFG* genes and ORFs encoding hypothetical proteins (hp).

For further investigation, we conducted a quantitative PCR analysis of genes that are adjacent to *hcdABC* gene cluster (Fig. 22, c). The results revealed that randomly chosen putative *hp4*, *hcdR*, *hcdD* and *hcdE* genes were also induced in *Pseudomonas mandelii* 7HK4 cells (Fig. 22, b). Expression

levels of *hcdR*, *hp4*, *hcdD* and *hcdE* genes were increased approximately 1000-fold, and were similar to expression levels of the *hcdABC* genes under the same conditions. Each of *hcdABCR*, *hp4*, *hcdD* and *hcdE* gene was specifically induced when *Pseudomonas mandelii* 7HK4 was cultivated in the presence of either 3-(2,4-dihydroxyphenyl) propionic acid or 7-hydroxycoumarin. In addition, a 100-fold increase of mRNA synthesis of these genes was also observed in *Pseudomonas mandelii* 7HK4 cells pre-cultivated with 7-methylcoumarin. No expression of the analysed genes was observed in *Pseudomonas mandelii* 7HK4 cells pre-cultivated with coumarin, 6-hydroxycoumarin, 6-methylcoumarin, 6,7-dihydroxycoumarin, *o*-coumaric acid, *p*-coumaric acid, 2,4-dihydroxycinnamic acid, quinoline and isoquinoline.

3.6. Analysis of the genome locus encoding the 7-hydroxycoumarin-inducible protein

Analysis of *Pseudomonas mandelii* 7HK4 genome sequences showed that the inducible 31.2 kDa protein (HcdC) belongs to the fumarylacetoacetate (FAA) hydrolase family, which includes such enzymes as 2-keto-4-pentenoate hydratase, 2-oxohepta-3-ene-1,7-dioic acid hydratase, 2-hydroxy-6-oxo-6-phenylhexa-2,4-dienoate hydrolase or bifunctional isomerases/decarboxylases (catechol pathway) (see Figure S2 in the Supplementary Material). The FAA family proteins are usually involved in the last stages of bacterial metabolism of aromatic compounds [132–134], suggesting that 31.2 kDa protein from *Pseudomonas mandelii* 7HK4 participates in the final steps of 7-hydroxycoumarin metabolism, after oxidative cleavage of the aromatic ring.

A BLAST analysis of *hcdA* and *hcdB* sequences revealed that these genes encode the putative FAD-binding hydroxylase and ring-cleavage dioxygenase, respectively. HcdA protein was not assigned to any family, but it showed similarity to a putative 2-polyprenyl-6-methoxyphenol hydroxylase (see Figure S2 in the Supplementary Material). This type of enzymes belongs to class A of FAD-binding monooxygenases, which are involved in bacterial degradation of aromatic compounds [87,88,135,136]. The product of the *hcdB* gene belongs to the cl14632 superfamily that combines a variety of structurally related metalloproteins, including the type I extradiol dioxygenases (see Figure S2 in the Supplementary Material). The type I extradiol dioxygenases catalyze the incorporation of both atoms of molecular oxygen into aromatic substrates that results in the cleavage of the aromatic rings [137,138].

3.6.1. Production and substrate specificity of HcdA hydroxylase

For further characterization of HcdA hydroxylase, the *hcdA* gene was amplified by PCR and cloned into the pET21b expression vector. The sequence was confirmed by Sanger sequencing. The recombinant C-terminally His_6-tagged soluble protein was produced in *Escherichia coli* BL21, and purified by affinity chromatography. The purified enzyme migrated as a ~62 kDa band on SDS-PAGE (Fig. 23, a), and had a bright yellow colour with absorbance maxima at 380 and 450 nm wavelengths (Fig. 23, b), suggesting that the protein contains a tightly bound flavin [79,130,131]. The gel-filtration showed that the purified HcdA protein is a monomer (Fig. 23, c).

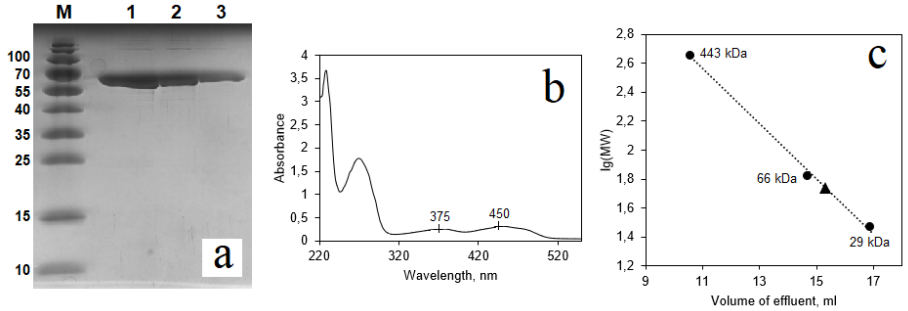

Figure 23. (a) SDS-PAGE of His_6-tagged HcdA protein purified by affinity chromatography. Lanes 1–3 – various amounts of eluted protein. M – molecular mass ladder (kDa). (b) UV/Vis's spectrum of HcdA protein purified by affinity chromatography. (c) Analytical gel filtration chromatography of HcdA protein. The calibration curve used to estimate the native molecular weight based on the elution position during analytical gel filtration is indicated. Filled circles – carbonic anhydrase (MW = 29 kDa), albumin (MW = 66 kDa) and apoferritin (MW = 443 kDa); filled triangle – native HcdA protein.

The specificity for both flavin and nicotinamide cofactors was investigated (Fig. 24). The HcdA hydroxylase was able to utilize either NADH or NADPH, although the oxidation rates of NADPH were almost two-fold lower. The addition of FAD or FMN to the reaction mixtures showed no significant changes in NADPH oxidation, however additional FAD and FMN increased the oxidation rates of NADH by 6 to 12 %, respectively (Fig. 24). The optimum reaction conditions for the HcdA activity were found to be a low ionic strength 25 mM tricine buffer, pH 7.8–8.0 and 18–25 ºC temperature (Fig. 25 and 26).

The NADH oxidation assay was used to determine the kinetic parameters of HcdA. The K_M value for NADH calculated from the initial velocity analysis was 50.10 ± 3.50 µM in the presence of 500 µM 3-(2,4-dihydroxyphenyl) propionic acid (Fig. 27), and the apparent K_M for 3-(2,4-dihydroxyphenyl) propionic acid was 13.00 ± 1.20 µM in the presence of 300 µM NADH (Figure 28), with k_{cat} of 7.91 ± 0.17 s^{-1}. Besides, the initial velocities were measured for HcdA with an excess of FMN varying both NADH and 3-(2,4-dihydroxyphenyl) propionic acid concentrations using steady state kinetics and the NADH oxidation assay. The derived velocities were plotted using the double reciprocal plots, which indicated the formation of a ternary complex since lines were not parallel but intersected in the upper left quadrant (Fig. 29) [139].

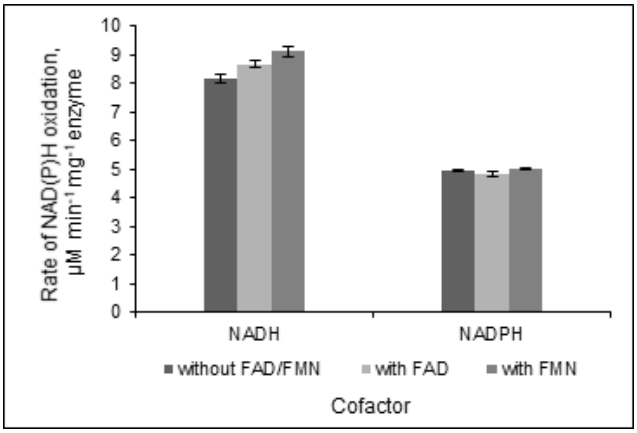

Figure 24. Specificity of HcdA protein to flavin and nicotinamide cofactors. Enzymatic assays were carried out in 50 mM tricine buffer (pH 7.8) with 40 nM HcdA enzyme and 50 µM of 3-(2,4-dihydroxyphenyl) propionic acid, in presence of 75 µM NAD(P)H with/without 30 µM FAD/FMN at 22 ºC. Rates of NAD(P)H oxidation were observed at 340 nm wavelength. Experiment was performed in triplicate and error bars indicate standard deviation.

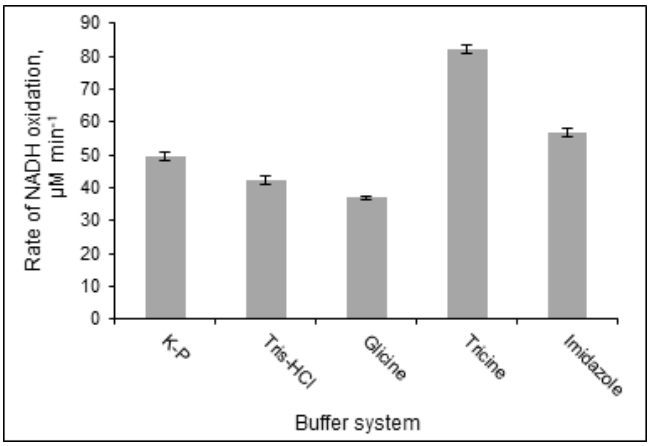

Figure 25. Activity of HcdA protein in different buffer systems. Enzymatic assays were carried out in 50 mM potassium phosphate (K-P), Tris-HCl, glycine, tricine or imidazole buffers (pH 8.0) with excess of HcdA enzyme and 150 µM of 3-(2,4-dihydroxyphenyl) propionic acid, in presence of 100 µM NADH at 22 ºC. Rates of NADH oxidation were observed at 340 nm wavelength. Experiment was performed in triplicate and error bars indicate standard deviation.

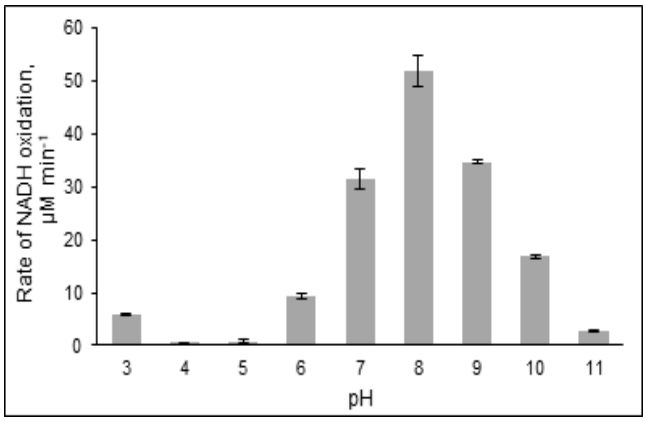

Figure 26. Activity of HcdA protein in different pH. Enzymatic assays were carried out in 50 mM potassium phosphate (K-P) buffer with excess of HcdA enzyme and 150 µM of 3-(2,4-dihydroxyphenyl) propionic acid, in presence of 100 µM NADH at 22 ºC. Rates of NADH oxidation were observed at 340 nm wavelength. Experiment was performed in triplicate and error bars indicate standard deviation.

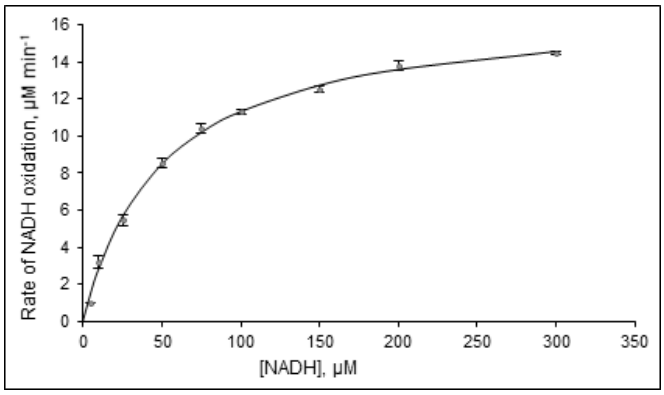

Figure 27. Kinetic analysis of HcdA as determined by NADH oxidation. Initial velocities were measured in the presence of 25 mM tricine buffer (pH 7.8) with 35.8 nM HcdA enzyme, 500 µM of 3-(2,4-dihydroxyphenyl) propionic acid, 30 µM FMN and 5–300 µM NADH at 22 ºC. The curve for the NADH oxidation assay was fit to the standard equation for Michaelis-Menten reactions. Rates of NADH oxidation were observed at 340 nm wavelength. Experiment was performed in triplicate and error bars indicate standard deviation.

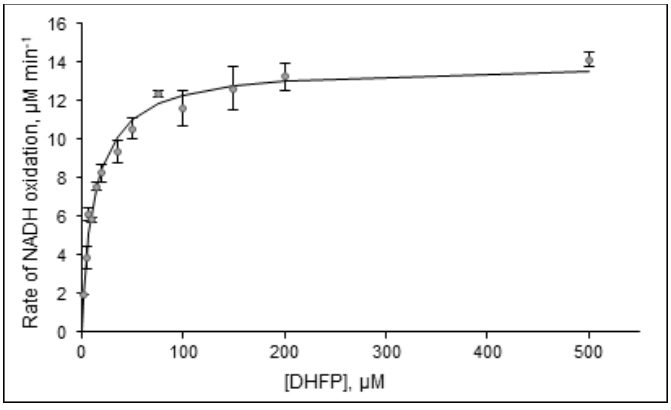

Figure 28. Kinetic analysis of HcdA as determined by NADH oxidation. Initial velocities were measured in the presence of 25 mM tricine buffer (pH 7.8) with 35.8 nM HcdA enzyme, 300 µM of NADH, 30 µM FMN and 2–500 µM 3-(2,4-dihydroxyphenyl) propionic acid (DHFP) at 22 ºC. The curve for the NADH oxidation assay was fit to the standard equation for Michaelis-Menten reactions. Rates of NADH oxidation were observed at 340 nm wavelength. Experiment was performed in triplicate and error bars indicate standard deviation.

The activity of the HcdA enzyme was assayed in the presence of NADH cofactor against various substrates. The highest rate of oxidation of NADH was recorded in the presence of 3-(2,4-dihydroxyphenyl) propionic acid. A 40-fold lower rate was observed when *trans*-2,4-dihydroxycinnamic acid was used as the substrate. The HcdA was not active towards *trans*-cinnamic, *cis*-2,4-dihydroxycinnamic, 3-(2-hydroxyphenyl) propionic, 3-(2-hydroxyphenyl)-2-propenoic, 3-(4-hydroxyphenyl)-2-propenoic, 3-(3-hydroxyphenyl)-2-propenoic, 3-(2-bromophenyl) propionic, 3-(2-nitrophenyl) propionic and 3-phenylpropionic acids, cinnamyl alcohol, pyrocatechol, 3-methylcatechol, 4-methylcatechol, 2-propylphenol, 2-propenylphenol, 2-ethylphenol, *o*-cresol, *o*-tyrosine, resorcinol, 2,3-dihydroxypyridine, 2-hydroxy-4-aminopyridine, *N*-methyl-2-pyridone, *N*-ethyl-2-pyridone, *N*-propyl-2-pyridone, *N*-butyl-2-pyridone, indoline and indole. These data demonstrate that the HcdA is a highly specific monooxygenase, which shows a strong preference to 3-(2,4-dihydroxyphenyl) propionic acid. The addition of His_6-tag did not affect the enzymatic activity of the HcdA protein.

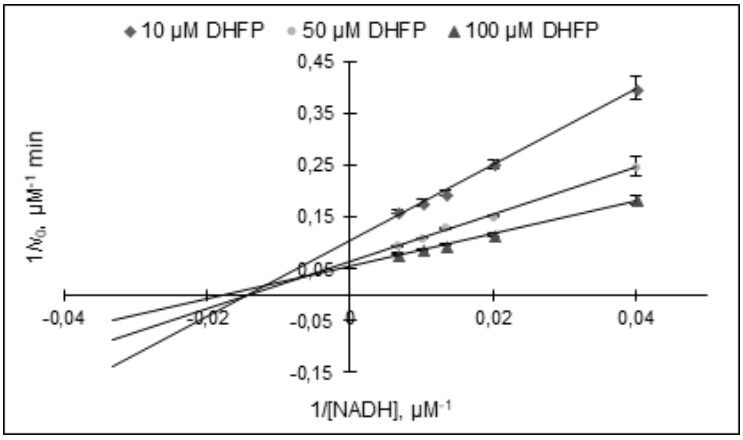

Figure 29. Double reciprocal plot of NADH oxidation as a function of NADH concentration. Ternary complex formation of FMN loaded HcdA with NADH and 3-(2,4-dihydroxyphenyl) propionic acid. 3-(2,4-Dihydroxyphenyl) propionic acid concentrations used were 10 µM (filled diamonds), 50 µM (filled circles), and 100 µM (filled triangles). Rates of NADH oxidation were observed at 340 nm wavelength. Experiment was performed in triplicate and error bars indicate standard deviation.

The product of the reaction catalysed by the HcdA hydroxylase was analysed by UV-VIS absorption spectroscopy and HPLC-MS. A new UV absorption maximum was observed at 340 and 490 nm upon addition of 3-

(2,4-dihydroxyphenyl) propionic acid to the reaction mixture. The consequent red colouring was observed, which indicated the presence of *para*- or *ortho*-quinone [140], a presumed product of the autooxidation of the corresponding hydroquinone. The same coloration was also observed *in vivo* when *Pseudomonas mandelii* 7HK4 cells were grown in an excess of 7-hydroxycoumarin and when *Escherichia coli* BL21 cells harbouring the p4pmPmo plasmid were cultured in the presence of 3-(2,4-dihydroxyphenyl) propionic acid. HPLC-MS analysis of the reaction mixtures of both *in vitro* and *in vivo* bioconversions confirmed the formation of 3-(trihydroxyphenyl) propionic acid and quinone, found $[M-H]^-$ masses were 197 (traces seen only *in vivo*) and 195, respectively (Fig. 30).

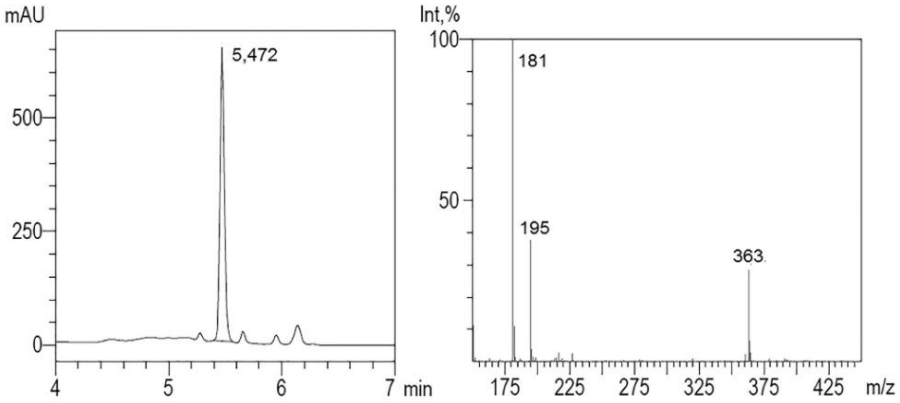

Figure 30. HPLC-MS analysis of 3-(2,4-dihydroxyphenyl) propionic acid bioconversion mixture *in vitro*. UV 254 nm trace of 3-(2,4-dihydroxyphenyl) propionic acid and its hydroxylated product under the same peak with retention time 5.472 min (on the left), and MS spectrum of the dominant peak (on the right). The negative ions $[M-H]^-$ generated are at m/z 181 (3-(2,4-dihydroxyphenyl) propionic acid), 195 (product of 3-(trihydroxyphenyl) propionic acid autooxidation).

However, the structure of the product was not confirmed at this stage by chemical analysis since it was not possible to chromatographically separate the product from the reaction mixture. The substrate and product have similar structures and chemical properties; therefore, both were detected under the same HPLC-MS chromatogram peak with retention time of ~5.5 min.

3.6.2. Synthesis and substrate specificity of HcdB dioxygenase

HcdB dioxygenase was synthesized from the plasmid pET28b having *hcdB* gene in *E. coli* BL21. All attempts to purify HcdB aerobically resulted in the loss of the enzymatic activity, even in the presence of organic stabilizers, such as glycerol, ethanol, and acetone, that were known as stabilizers for similar enzymes [141–143]. The addition of dithiothreitol and ferrous sulphate to the aerobically purified protein did not restore its activity, although it had been shown to activate and/or stabilize other extradiol dioxygenases [141–145].

Therefore, due to the highly unstable nature of the HcdB enzyme, all the activity measurements were carried out *in vivo* using the whole cells of *E. coli* BL21 transformed with the pTHPPDO plasmid. The bioconversion of pyrocatechol, 3-methylcatechol, 3-methoxycatechol, 4-methylcatechol, 3-(2,3-dihydroxyphenyl) propionic and caffeic acids in each case produced yellow products with the absorbance maxima expected for the proximal *meta*-cleavage products of these catechols (Fig. 31, solid line) [56,146,147].

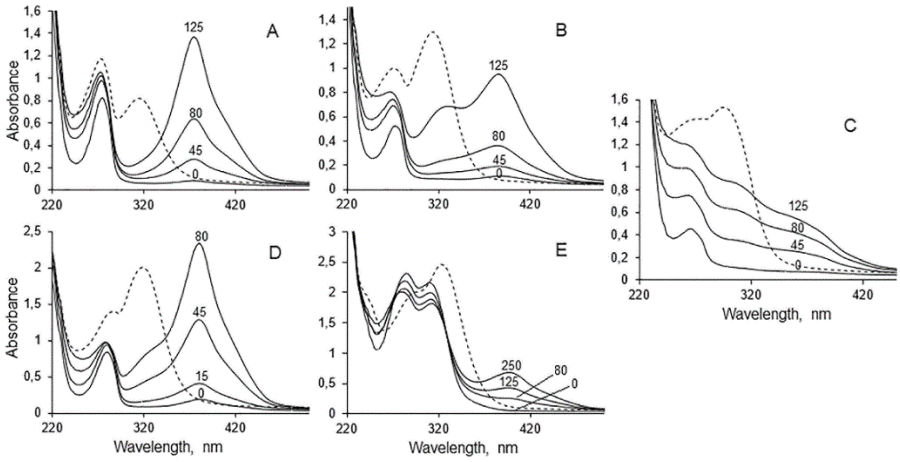

Figure 31. Biotransformations of pyrocatechol (A), 3-methylcatechol (B), 3-methoxycatechol (C), 4-methylcatechol (D) and caffeic acid (E) by whole cells of *E. coli* BL21 containing *hcdB* gene. Biotransformations were carried out in 50 mM potassium phosphate buffer pH 7.5 (solid line) at 30 °C with 0.5–1 mM of substrate. Incubation time is shown in min. Dashed lines indicate peak shifts to a shorter wavelength after acidification of reaction mixtures.

No changes in colour took place, but the absorbance maxima shifts were observed during reactions with pyrogallol, gallacetophenone, 2',3'-dihydroxy-4'-methoxyaceto-phenone hydrate, 3,4-dihydroxybenzoic acid, 2,3,4-trihydroxybenzoic acid and 2,3,4-trihydroxy-benzophenone (Fig. 32). No

activity was observed with 1,2,4-benzenetriol and 6,7-dihydroxycoumarin. The *E. coli* cells without the *hcdB* gene showed no activity towards the aforementioned compounds. The expected shift of peaks of the UV-VIS spectra of the reaction products to a shorter wavelength were observed after acidification of the reaction mixtures containing pyrocatechol, 3-methylcatechol, 3-methoxycatechol, 4-methylcatechol and caffeic acid (Fig. 31, dashed line) [116,148]. These findings revealed that *hcdB* encodes an extradiol dioxygenase, which can utilize a number of differently substituted catechols.

Furthermore, the HcdB dioxygenase was co-produced with the HcdA hydroxylase in *E. coli* BL21 cells. The activity of those cells towards 3-(2,4-dihydroxyphenyl) propionic acid was analysed. No coloration occurred during the incubation of over 72 h, compared to the formation of a reddish bioconversion product by *E. coli* cells containing the *hcdA* gene only. Products of 3-(2,4-dihydroxyphenyl) propionic acid conversion by HcdA and HcdB were analysed by HPLC-MS. Ions with masses 181, 195 and 197 ($[M-H]^-$) were not detected showing a complete conversion of substrate and its hydroxylated forms. Also, none of the expected ions ($[M-H]^-$ 229 or $[M+H]^+$ 231) were observed for a presumed product of the oxidative cleavage of 3-(trihydroxyphenyl) propionic acid.

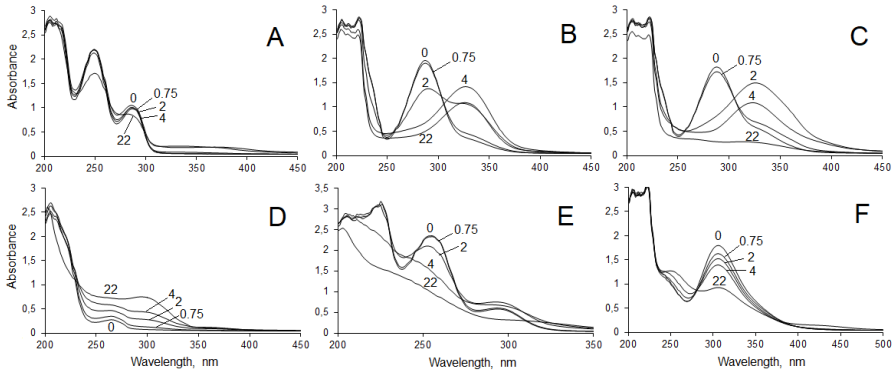

Figure 32. Biotransformations of 3,4-dihydroxybenzoic acid (A), 2',3'-dihydroxy-4'-methoxyaceto-phenone hydrate (B), gallacetophenone (C), pyrogallol (D), 2,3,4-trihydroxybenzoic acid (E) and 2,3,4-trihydroxy-benzophenone (F) by whole cells of *E. coli* BL21 containing *hcdB* gene. Biotransformations were carried out in 50 mM potassium phosphate buffer pH 7.5 at 30 °C with 0.5–1 mM of substrate. Incubation time is shown in hours.

3.6.3. Isolation and identification of 3-(2,4-dihydroxyphenyl) propionic acid bioconversion product

Due to difficulties in detecting colourless *meta*-cleavage product of catechol derivative, and since no reasonable mass spectra could be registered, we decided to transform a cleavage product into the derivative of picolinic acid by incubation with NH_4Cl as described in Materials and Methods. The formation of a picolinic acid derivative was proven by HPLC-MS analysis, which showed the formation of $[M-H]^-$ ion 210 mass (Fig. 33), corresponding to the addition of NH_3 to the *meta*-cleavage product and the loss of two H_2O molecules [149].

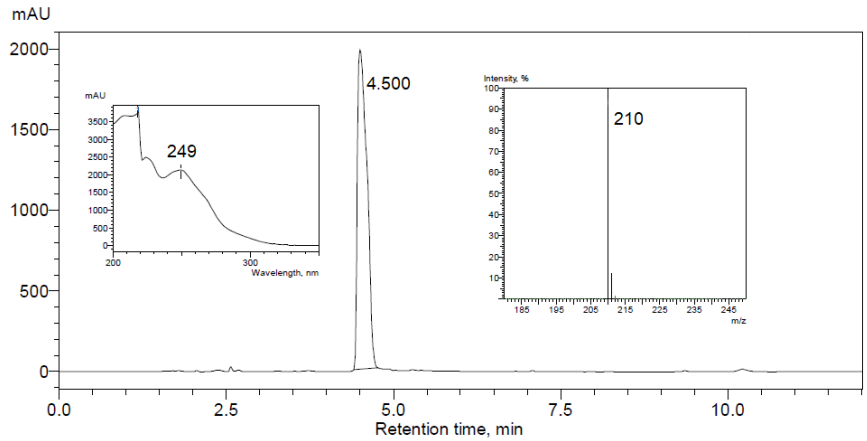

Figure 33. HPLC-MS analysis of 3-(2,4-dihydroxyphenyl) propionic acid bioconversion mixture *in vivo*. UV 254 nm trace of picolinic acid derivative with retention time of 4.500 min, UV spectrum and MS spectrum of the dominant peak. The negative ion $[M-H]^-$ generated are at m/z 210.

The ^1H NMR spectrum of this derivative [δ 7.73 (s, 1H), 6.89 (s, 1H), 2.65 (t, J = 7.4 Hz, 2H), 2.38 (t, J = 7.4 Hz, 2H)] showed a set of two aryl protons that, from the coupling pattern (singlet + singlet), were in *meta*- or *para*-positions to each other on the aromatic ring [150] (Fig. 34). The appearance in the spectrum of two triplets with chemical shifts of 2.38 and 2.65 ppm indicated the presence of four methylene protons [150].

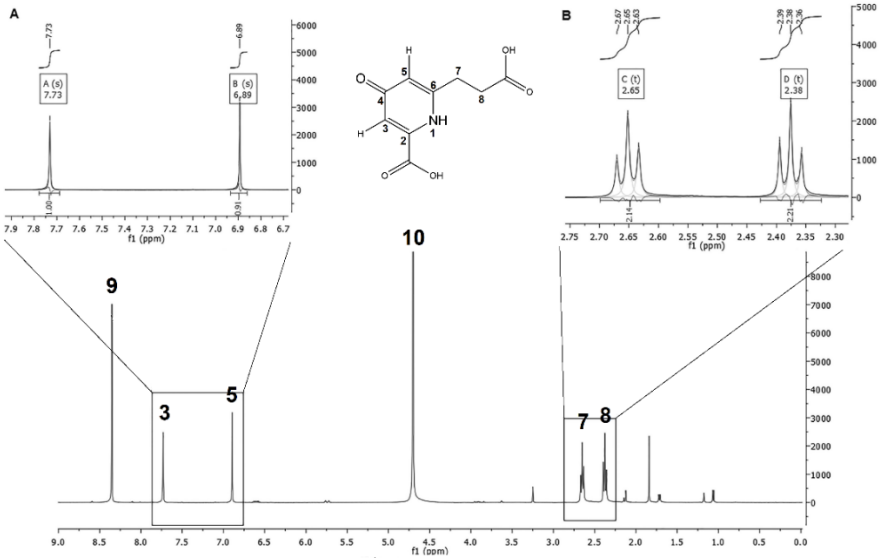

Figure 34. [1]H NMR spectrum (400 MHz, Deuterium Oxide) of 6-(2-carboxyethyl)-4-oxo-1,4-dihydropyridine-2-carboxylic acid. Identification of aryl (A) and methylene (B) protons. 9 – trace impurities of formic acid; 10 – solvent residual peak.

The [13]C NMR spectrum [δ 181.51, 179.99, 171.01, 143.14, 136.74, 130.11, 115.22, 35.50, 24.00] showed two sp^3 carbons with chemical shifts of 24.00 and 35.50 ppm, and three sp^2 carbons of carbonyl groups with chemical shifts of 171.01, 179.99 and 181.51 ppm, respectively (Fig. 35). The carbonyl carbon atoms were the most strongly deshielded and their resonances formed a separate region at the highest frequency. Another four sp^2 carbon signals were in the aromatic carbon region [150,151]. The presence of the third carbonyl group indicated the formation of *oxo*-pyridine, for which six possible theoretical structures of *oxo*-picolinic acid derivative were presumed (Fig. 36).

Since the [1]H NMR spectrum showed a set of two singlet aryl protons in *meta*- or *para*-positions to each other, only structures 7 and 9 (Fig. 36) were further analysed. Besides, pyridine aromatic carbons are usually differentiated into two resonances at higher field (C-3/5, *meta* position) and three at lower field (C-2/6, *ortho* position; C-4, *para* position), where the electron-withdrawing effect of nitrogen is effective [150,151].

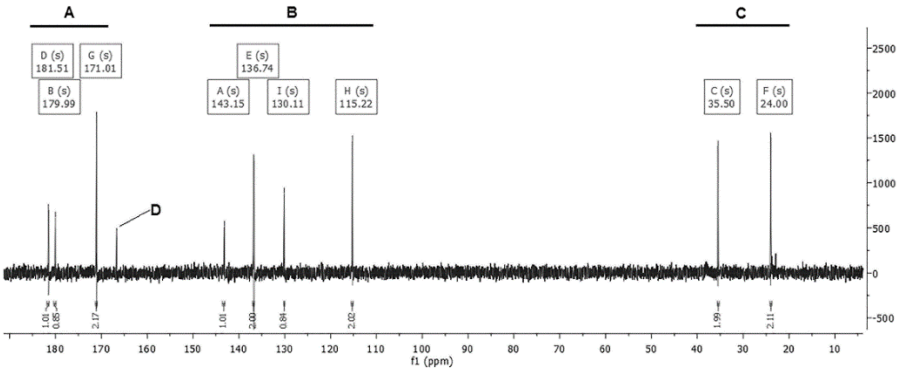

Figure 35. ^{13}C NMR spectrum (101 MHz, Deuterium oxide) of 6-(2-carboxyethyl)-4-oxo-1,4-dihydropyridine-2-carboxylic acid. Identification of carbonyl (A), aryl (B) and methylene (C) carbons. D – trace impurities of formic acid.

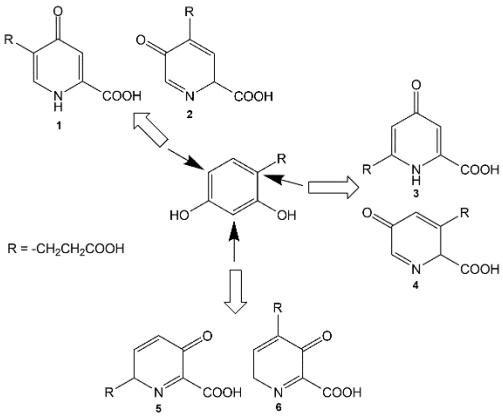

Figure 36. Suggested structures of *oxo*-picolinic acid derivative, formed during oxidative ring cleavage of 3-(2,4-dihydroxyphenyl) propionic acid and conversion of the ring fission product. Solid lines indicate possible positions of hydroxylation by HcdA enzyme; hollow arrays indicate the probable *oxo*-picolinic acid derivatives forming after hydroxylation at each position.

The chemical shift of 115.22 ppm showed that the analysed compound had relatively strongly shielded unsubstituted aromatic carbon, which should be in *meta*-position from nitrogen, in *ortho*-position from the carbonyl group, and in *meta*- or *para*-position from the carboxyl group (Fig. 37, C5 atom) [152,153]. This led to the conclusion that structure 3 (Fig. 36), 6-(2-carboxyethyl)-4-oxo-1,4-dihydropyridine-2-carboxylic acid, was formed during incubation of *meta*-cleavage product of catechol with NH_4Cl, as depicted in Fig. 38.

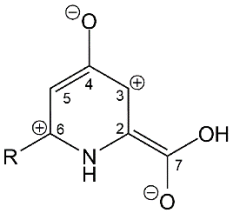

Figure 37. Resonance structure of oxo-picolinic acid derivative showing electron densities on aromatic carbons.

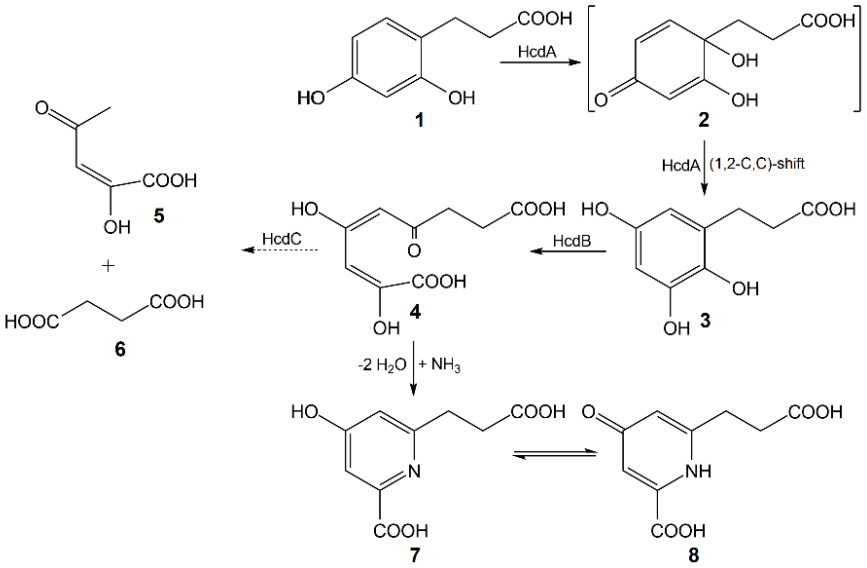

Figure 38. The proposed metabolic pathway of 3-(2,4-dihydroxyphenyl) propionic acid in *Pseudomonas mandelii* 7HK4 cells. Incubation of the compound **4** with NH_4Cl gives picolinic acid derivative. **1** – 3-(2,4-dihydroxyphenyl) propionic acid; **2** – 3-(1,2-dihydroxy-4-oxocyclohexa-2,5-dienyl)-propanoic acid; **3** – 3-(2,3,5-trihydroxyphenyl) propionic acid; **4** – (*2E*,*4E*)-2,4-dihydroxy-6-oxonona-2,4-dienedioic acid; **5** – (*E*)-2-hydroxy-4-oxopent-2-enoic acid; **6** – succinic acid; **7** – 6-(2-carboxyethyl)-4-hydroxypicolinic acid; **8** – 6-(2-carboxyethyl)-4-oxo-1,4-dihydropyridine-2-carboxylic acid; HcdA – 3-(2,4-dihydroxyphenyl) propionic acid 1-monooxygenase; HcdB – 3-(2,3,5-trihydroxyphenyl) propionic acid 1,2-dioxygenase; HcdC – putative (*2E*,*4E*)-2,4-dihydroxy-6-oxonona-2,4-dienedioic acid hydrolase. The dashed arrow indicates a hypothetical reaction.

These data allowed the reconstruction of the consecutive oxidation of 3-(2,4-dihydroxyphenyl) propionic acid catalysed by the HcdA and HcdB enzymes. Hence, 3-(2,3,5-trihydroxyphenyl) propionic acid was the product of oxidation of 3-(2,4-dihydroxyphenyl) propionic acid by the HcdA hydroxylase. The molecular mass of 198 of 3-(2,3,5-trihydroxyphenyl) propionic acid and capability to form *para*-quinone agreed with the UV-VIS and HPLC-MS data on the bioconversion of 3-(2,4-dihydroxyphenyl) propionic by the HcdA hydroxylase. The formation of 3-(2,3,5-trihydroxyphenyl) propionic acid from 3-(2,4-dihydroxyphenyl) propionic acid was possible only through oxidative *ipso*-rearrangement, a unique reaction where *ipso*-hydroxylation of the 3-(2,4-dihydroxyphenyl) propionic acid takes place with a simultaneous shift of the propionic acid group to the vicinal position (Fig. 38) [89,103,105,154]. During the second step, 3-(2,3,5-trihydroxyphenyl) propionic acid was cleaved by HcdB extradiol dioxygenase at the *meta*-position leading to the formation of (*2E,4E*)-2,4-dihydroxy-6-oxonona-2,4-dienedioic acid. The further imine formation and tautomerization in the presence of ammonium ions [115,116] led to 6-(2-carboxyethyl)-4-oxo-1,4-dihydropyridine-2-carboxylic acid (Fig. 38).

3.6.4. Production of the HcdC protein

HcdC gene was expressed from the plasmid p2K4PH in *E. coli* BL21. The addition of *E. coli* extracts containing the HcdC protein did not cause decolorization of the *meta*-cleavage products of 3-(2,3-dihydroxyphenyl) propionic acid, pyrocatechol, 3-methylcatechol or 4-methylcatechol formed in the presence of the HcdB extradiol dioxygenase. Also, the addition of $NAD(P)^+$ to these reaction mixtures did not induce decolorization of the *meta*-cleavage products [155]. To confirm the function of HcdC, *E. coli* BL21 cells were transformed with plasmids bearing *hcdA, hcdB* and *hcdC* genes. The expression of all three genes in *E. coli* cells was confirmed by SDS-PAGE, the enzymes migrated as 62, 31 and 20 kDa bands, respectively (see Figure S3 in the Supplementary Material).

The bioconversion of 3-(2,4-dihydroxyphenyl) propionic acid was conducted in *E. coli* cells containing all three recombinant proteins. Later, the reaction mixture was incubated with NH_4Cl, and the reaction products were analysed by HPLC-MS. The ions $[M-H]^-$ and $[M+H]^+$ with masses of 210 and 212, respectively, were not detected, compared to the bioconversion mixture with *E. coli* cells containing *hcdAB* genes only. This showed a complete conversion of *meta*-cleavage product of the catechol derivative, therefore no picolinic acid derivative could be obtained. No reaction products of (*2E,4E*)-

2,4-dihydroxy-6-oxonona-2,4-dienedioic acid hydrolysis by the HcdC protein were identified. We suggest that the later compound was converted to succinic acid, which entered the Krebs cycle, and (*E*)-2-hydroxy-4-oxopent-2-enoic acid, which could be further converted by *E. coli* cells, thus complicating the extraction of these reaction products. Nevertheless, it may be concluded that all three enzymes encoded by the *hcdABC* operon are responsible for the catabolism of 3-(2,4-dihydroxyphenyl) propionic acid in *Pseudomonas mandelii* 7HK4 bacteria.

3.7. Analysis of the genome locus adjacent to 7-hydroxycoumarin-inducible *hcdABC* gene cluster

Further, a genomic region approximately 3 kb upstream of the *hcdABC* gene cluster containing *hcdD, hcdE, hcdF* and *hcdG* genes was amplified by PCR and cloned into the pACYCDuet-1 expression vector. The recombinant HcdD, HcdE, HcdF and HcdG proteins were produced together in *E. coli* BL21 strain, and the expression was confirmed by SDS-PAGE. The whole cells of *E. coli* BL21 transformed with the pHP4-10 plasmid were used for the bioconversion of coumarin, 6-hydroxycoumarin, 6-methylcoumarin, 7-hydroxycoumarin, 7-methylcoumarin, 7-methoxycoumarin, 4-methyl-7-hydroxycoumarin and 6,7-dihydroxycoumarin. Time course experiments revealed the reduction of UV absorption maxima of these substrates over time. After the completion of bioconversions, there was a non-disappearing UV absorption maximum at 260–280 nm wavelengths similar to that of 3-(2,4-dihydroxyphenyl) propionic acid (see Figure S4 in the Supplementary Material). This suggest that *E. coli* BL21 cells transformed with the pHP4-10 plasmid can catalyze the reduction and/or hydrolysis of lactone moiety of coumarin derivatives. When activity rates were compared conversion of the 7-hydroxycoumarin was the fastest, and conversions of all methyl-, methoxy-substituted coumarins were the lowest. In addition, no activity was observed with 3-hydroxycoumarin, 4-hydroxycoumarin, 7-ethoxycoumarin, *o*-coumaric acid, 2,4-dihydroxycinnamic acid, 7-hydroxyquinoline-(1H)-2-one, 3,4-dihydroquinoline-(1H)-2-one, 2-hydroxy-quinoline or 3,4-dihydro-7-hydroxyquinoline-(1H)-2-one, which implied that one or all together studied hypothetical proteins were specific for coumarin derivatives with unsubstituted and non-hydrolysed lactone moiety. The *E. coli* cells without the *hcdD, hcdE, hcdF* and *hcdG* genes showed no activity towards the aforementioned compounds.

Furthermore, the recombinant HcdD, HcdE, HcdF and HcdG proteins were co-produced with the HcdA hydroxylase and HcdB dioxygenase in *E. coli*

BL21 cells, which were used for bioconversion of 7-hydroxycoumarin. Conversion products were analysed by HPLC-MS. Ions with $[M-H]^-$ masses 161 (for 7-hydroxycoumarin) and 163 (for 7-hydroxy-3,4-dihydrocoumarin) were not detected showing a complete conversion of substrate and its reduced form, respectively. However, ions with $[M-H]^-$ mass 181 (for 3-(2,4-dihydroxyphenyl) propionic acid) and with $[M+H]^+$ mass 212 (for 6-(2-carboxyethyl)-4-oxo-1,4-dihydropyridine-2-carboxylic acid) were observable showing the accumulation of reduced and hydrolysed form of substrate that was further converted to (2*E*,4*E*)-2,4-dihydroxy-6-oxonona-2,4-dienedioic acid by HcdA and HcdB enzymes. Some part of produced (2*E*,4*E*)-2,4-dihydroxy-6-oxonona-2,4-dienedioic acid reacted with ammonium anions that were in bioconversion broth resulting in formation of picolinic acid (Fig. 39). These results were compared to the bioconversion of 7-hydroxycoumarin by *E. coli* cells containing *hcdD, hcdE, hcdF* and *hcdG* genes only, which showed the accumulation of only one reaction product with ion $[M-H]^-$ mass 181. This led to the conclusion that hypothetical HcdD, HcdE, HcdF and HcdG proteins may be used in the early stages of 7-hydroxycoumarin metabolism by *Pseudomonas mandelii* 7HK4 bacteria, producing 3-(2,4-dihydroxyphenyl) propionic acid which later could be as a substrate for proteins coded by *hcdABC* gene cluster.

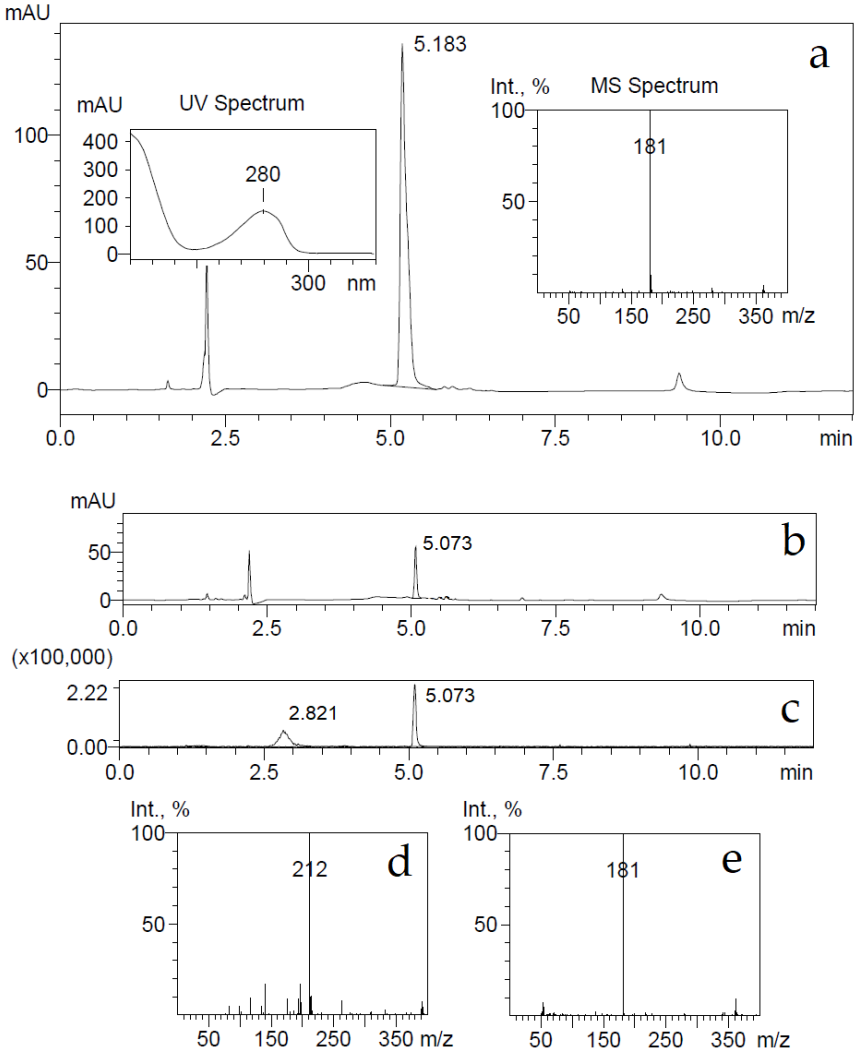

Figure 39. (a) Bioconversion of 7-hydroxycoumarin by *E. coli* BL21 bacteria harbouring pHP4-10 plasmid. Produced metabolites were analysed by HPLC-MS. UV 280 nm trace, UV and MS spectra of metabolite with retention time 5.183 min. The negative ion $[M\text{-}H]^-$ generated are at m/z 181 (3-(2,4-dihydroxyphenyl) propionic acid). (b) HPLC chromatogram of 7-hydroxycoumarin bioconversion by *E. coli* BL21 bacteria harbouring pHP4-10, p4pmPmo and pTHPPDO plasmids. MS chromatogram (c) and MS spectra of metabolites with retention times 2.821 min (d) and 5.073 min (e). The negative ion $[M\text{-}H]^-$ generated are at m/z 181 (3-(2,4-dihydroxyphenyl) propionic acid) and the positive ion $[M+H]^+$ generated are at m/z 212 (6-(2-carboxyethyl)-4-oxo-1,4-dihydropyridine-2-carboxylic acid).

A BLAST analysis of *hcdE* and *hcdG* sequences revealed that these genes encode the putative zinc-dependent alcohol dehydrogenase (Fig. 40) and NAD(P)H-dependent FMN reductase proteins, respectively. However, two other HcdD and HcdF proteins belong to less characterized groups of proteins, with similarities to *Bacillus chorismate* mutase-like (BCM-like) or cupin-like protein families, respectively.

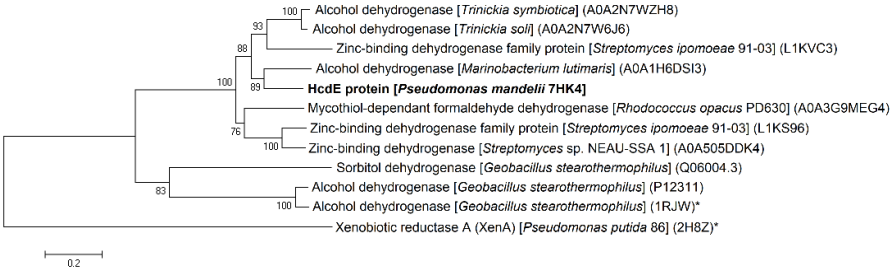

Figure 40. Phylogenetic tree of HcdE protein from *Pseudomonas mandelii* 7HK4 bacteria. Neighbour joining analyses were performed on the closest homologues with or without known structures and/or function. The numbers on the nodes indicate how often (no. of times, %) the species to the right grouped together in 1000 bootstrap samples. Bars represent the number of amino acid substitutions per site. UniProt/PDB accession numbers are given in parentheses. Proteins with known structure and/or function are marked with an asterix (*).

3.7.1. Isolation and identification of 7-hydroxycoumarin bioconversion product

Previously was shown that *Pseudomonas* sp. 30-1 and *Aspergillus niger* ATCC 11394 utilize a putative zinc-binding and NADH-dependent oxidoreductases to reduce coumarin generating dihydrocoumarin [10,14]. Therefore, we decided further analyse HcdE protein that has the most resemblance to alcohol dehydrogenases (Fig. 40).

E. coli BL21 cells harbouring the pHP7 plasmid were used for the conversion of 7-hydroxycoumarin as described in Materials and Methods. The consumption of substrate was monitored by UV-VIS absorption spectroscopy and HPLC-MS. The UV absorption maximum changed from 340 nm to 270 nm, also HPLC-MS analysis after conversion showed the accumulation of reaction products with ion $[M-H]^-$ masses 163, 181 and some substrate retains with ion $[M-H]^-$ mass 161 (Fig. 41). Detected ion $[M-H]^-$ mases 181 and 161 implied that bioconversion reaction was incomplete due to substrate inhibition and presumed reaction product 7-hydroxy-3,4-dihydrocoumarin may have

proceeded through hydrolysis forming 3-(2,4-dihydroxyphenyl) propionic acid.

Conversion product was purified yielding 3-(2,4-dihydroxyphenyl) propionic acid only as it was proven by HPLC-MS, ^{1}H and ^{13}C NMR analysis. To check weather supposed reaction product 7-hydroxy-3,4-dihydrocoumarin could have been advanced through hydrolysis during the conversion reaction, 7-hydroxy-3,4-dihydrocoumarin was chemically synthesized as described in Materials and Methods, and investigated imitating the bioconversion conditions. Small amounts (2 mM) of either 7-hydroxy-3,4-dihydrocoumarin, or 3-(2,4-dihydroxyphenyl) propionic acid were dissolved in 50 mM potassium phosphate buffer (pH 7.2) and incubated for several hours. Later, these compounds were extracted from aqueous solution with either dichloromethane, or ethyl acetate, then removing the solvent and dissolving precipitates in acetonitrile. Analysis of these samples by HPLC-MS showed that dichloromethane solvent can extract 7-hydroxy-3,4-dihydrocoumarin only, on the other hand extraction by ethyl acetate works equally for both analytes. Both ion $[M-H]^-$ masses 163 and 181 were detected in 7-hydroxy-3,4-dihydrocoumarin samples after extraction by ethyl acetate from aqueous solution (Fig. 42).

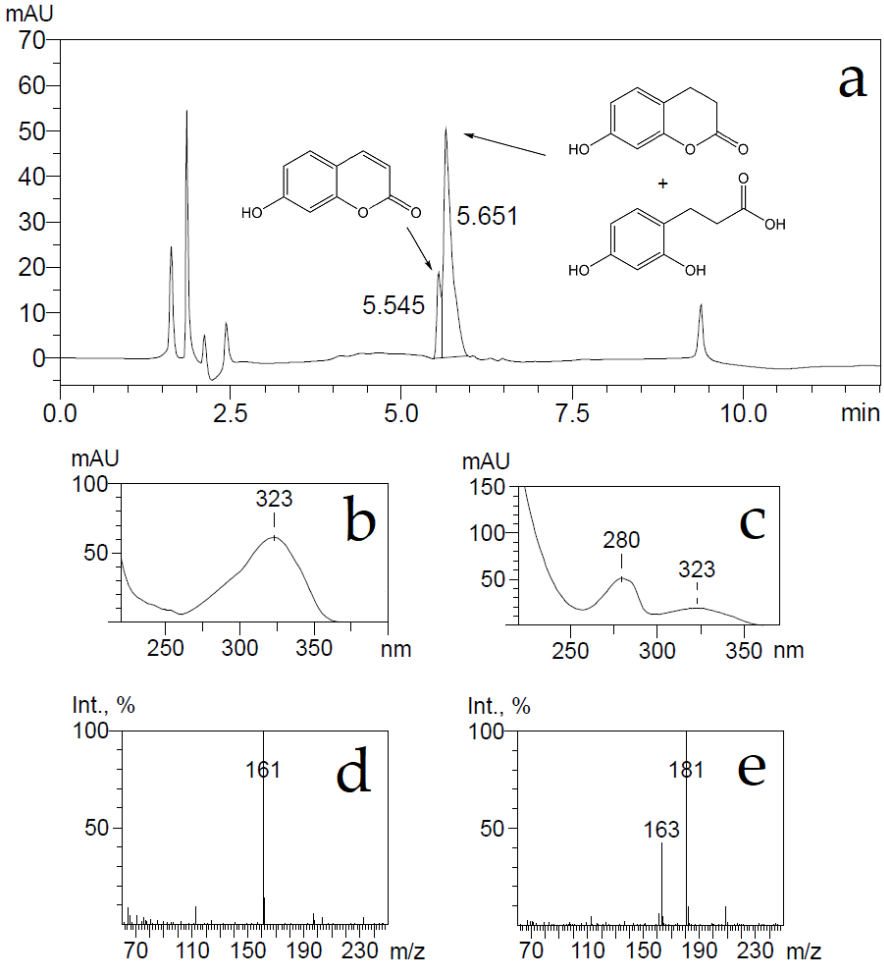

Figure 41. Bioconversion of 7-hydroxycoumarin by *E. coli* BL21 bacteria containing the induced *hcdE* gene. Produced metabolites were analysed by HPLC-MS. UV 280 nm trace of metabolites (a). UV and MS spectra of peaks with retention times 5.545 min (b and d) and 5.651 min (c and e). The negative ions $[M\text{-}H]^-$ generated are at m/z 181 (3-(2,4-dihydroxyphenyl) propionic acid), 161 (7-hydroxycoumarin) and 163 (7-hydroxy-3,4-dihydrocoumarin).

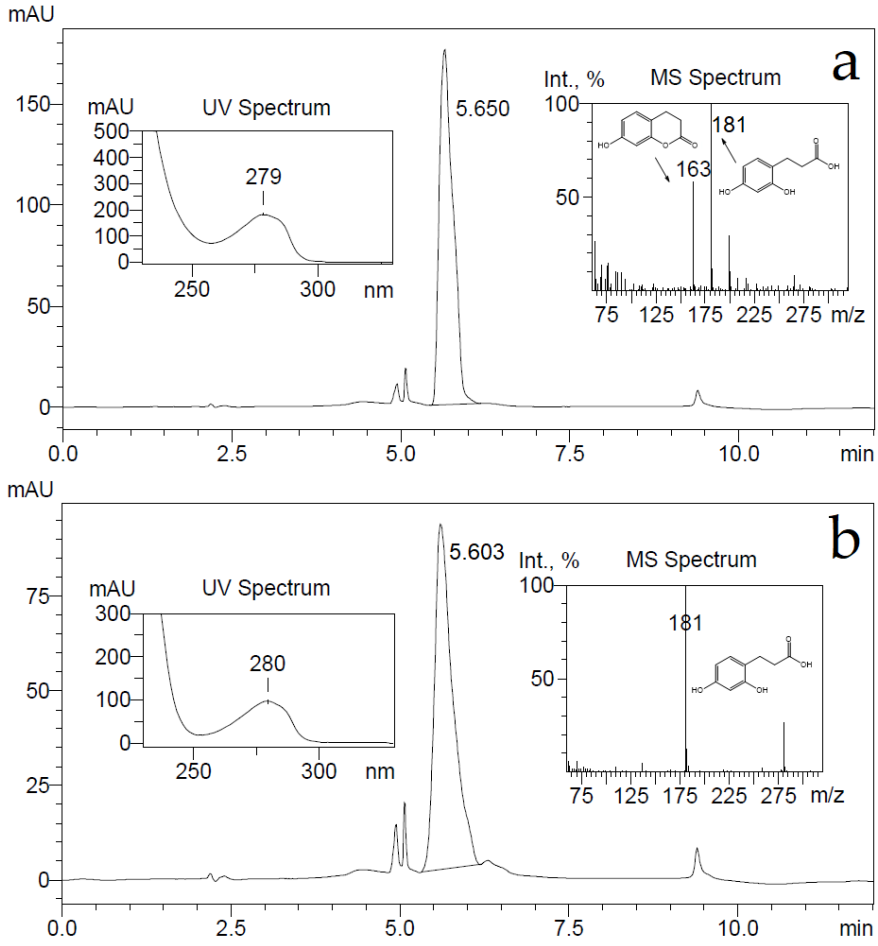

Figure 42. HPLC chromatograms of 7-hydroxy-3,4-dihydrocoumarin (a) and 3-(2,4-dihydroxyphenyl) propionic acid (b) at 280 nm wavelength. 2 mM of compounds were incubated in 50 mM potassium phosphate buffer (pH 7.2) for several hours and extracted by ethyl acetate. Corresponding UV and MS spectra of the main peaks were presented. The negative ions $[M-H]^-$ generated are at m/z 181 (3-(2,4-dihydroxyphenyl) propionic acid) and 163 (7-hydroxy-3,4-dihydrocoumarin).

Further, the elution time of 7-hydroxy-3,4-dihydrocoumarin sample was the same as of 3-(2,4-dihydroxyphenyl) propionic acid sample. Longer than 24-hour incubations of 7-hydroxy-3,4-dihydrocoumarin in aqueous buffer solutions lead to disappearance of ion $[M-H]^-$ mass 163 in HPLC-MS analysis. This experiment confirmed that 7-hydroxy-3,4-dihydrocoumarin

proceeds through hydrolysis during the incubation in aqueous solution and extraction by organic solvents.

It was concluded that 7-hydroxycoumarin is reduced by HcdE enzyme resulting in formation of 7-hydroxy-3,4-dihydrocoumarin. However due to possible strong inhibition of HcdE enzyme by its substrate the conversion rates are low enough that prolonged conversion time would affect the reaction product 7-hydroxy-3,4-dihydrocoumarin, which tends to undergo hydrolysis in aqueous solutions.

3.7.2. Characterization of HcdE protein

The *hcdE* gene was expressed and the recombinant C-terminally His_6-tagged protein was produced in *E. coli* BL21 bacteria. Soluble and colourless HcdE protein was purified by affinity chromatography and analysed by SDS-PAGE, enzyme migrated as a ~40 kDa band (see Figure S5 in the Supplementary Material). Enzyme specificity for several cofactors was investigated. The HcdE enzyme was able to utilize NADPH only. The addition of FAD or FMN to the reaction mixtures showed no changes in either NADH or NADPH oxidation. The optimum reaction conditions for the HcdE activity were found to be a low ionic strength 50 mM phosphate-citrate buffer of pH 7.0 at 22 ºC (Fig. 43 and 44).

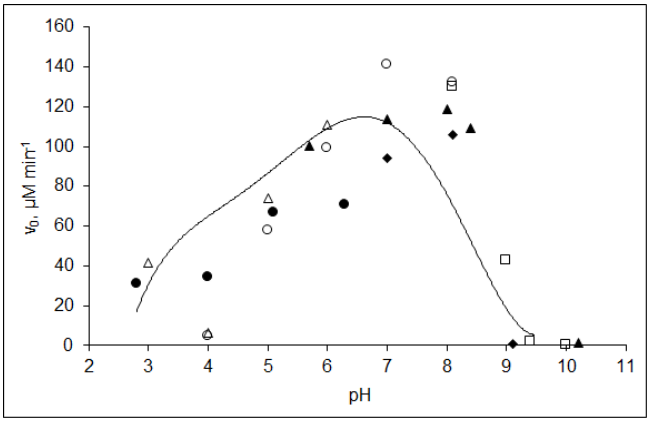

Figure 43. Activity of hp7 protein in different pH. Enzymatic assays were carried out in 50 mM of potassium phosphate (filled triangles), sodium acetate (filled circles), Tris-HCl (filled diamonds), tricine-sodium (empty squares), sodium phosphate and sodium citrate (empty circles) or sodium citrate (empty triangles) buffers with 5 µg of hp7 enzyme and 60 µM of 7-hydroxycoumarin, in presence of 160 µM NADPH at 22 ºC. Rates of bimolecular reaction were observed at 340 nm wavelength.

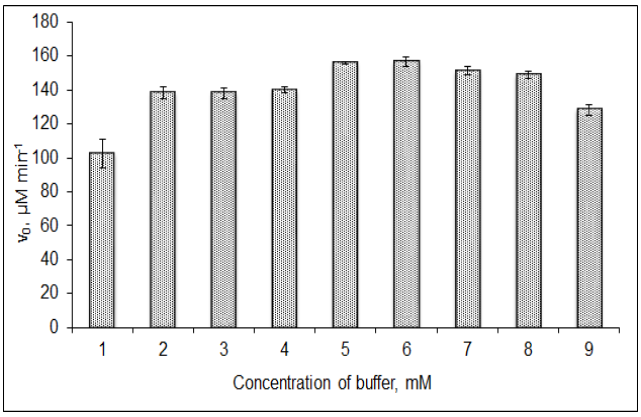

Figure 44. Activity of hp7 protein in buffers of different ionic strength. Enzymatic assays were carried out in 10–150 mM sodium phosphate (Na-P)/sodium citrate (Na-Citr) buffers (pH 7.0) with 5 µg of hp7 enzyme and 60 µM of 7-hydroxycoumarin, in presence of 160 µM NADPH at 22 ºC. Rates of bimolecular reaction were observed at 340 nm wavelength. Experiment was performed in triplicate and error bars indicate standard deviation. 1 – 5 mM Na-P and 5 mM Na-Citr; 2 – 10 mM Na-P and 10 mM Na-Citr; 3 – 10 mM Na-P, 10 mM Na-Citr and 10 mM of NaCl; 4 – 25 mM Na-P and 25 mM Na-Citr; 5 – 15 mM Na-P and 35 mM Na-Citr; 6 – 35 mM Na-P and 15 mM Na-Citr; 7 – 25 mM Na-P, 25 mM Na-Citr and 25 mM of NaCl; 8 – 50 mM Na-P and 50 mM Na-Citr; 9 – 25 mM Na-P, 25 mM Na-Citr and 100 mM of NaCl.

The activity of the HcdE enzyme was assayed in the presence of NADPH cofactor against various coumarin substrates. The highest enzymatic activity was recorded in the presence of 7-hydroxycoumarin. A 1.6-, 2-, 3.4- and 17-fold lower rates were observed when 6,7-dihydroxycoumarin, 6-hydroxycoumarin, 6-methylcoumarin and coumarin were used as the substrates, respectively. The HcdE enzyme was not active towards 7-methylcoumarin, 7-methoxycoumarin, 7-ethoxycoumarin, 4-methyl-7-hydroxycoumarin, 3-hydroxycoumarin, 4-hydroxycoumarin, *trans*-cinnamic, *trans*-2,4-dihydroxycinnamic, *o*-coumaric, *m*-coumaric, *p*-coumaric and caffeic acids, cinnamyl alcohol, 7-hydroxyquinoline-(1*H*)-2-one, 3,4-dihydroquinoline-(1*H*)-2-one, 2-hydroxyquinoline, 3,4-dihydro-7-hydroxyquinoline-(1*H*)-2-one and indole. Activity of HcdE enzyme *in vitro* contradicts the results given by *E. coli* BL21 cells harbouring the pHP7 plasmid which actually showed some activities towards 7-methylcoumarin, 7-methoxycoumarin and even 4-methyl-7-hydroxycoumarin (Fig. 45).

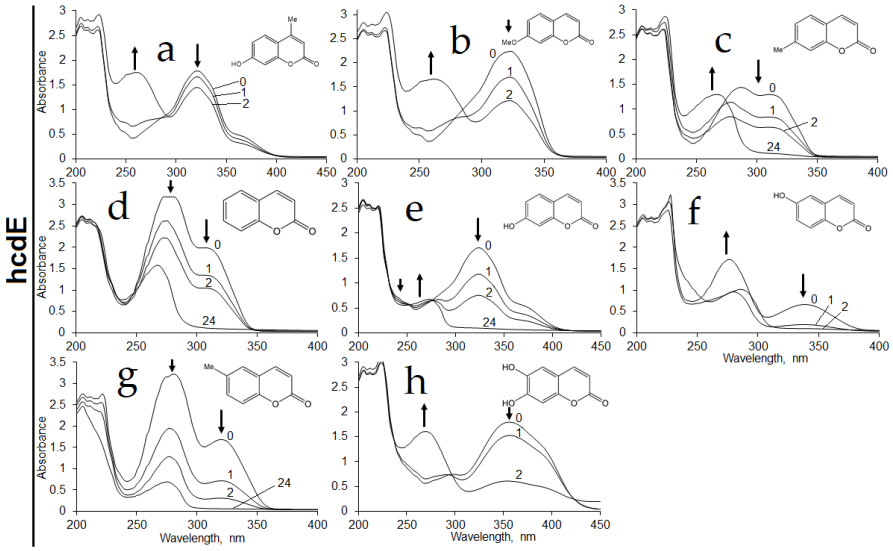

Figure 45. Biotransformation of 4-methyl-7-hydroxycoumarin (a), 7-methoxycoumarin (b), 7-methylcoumarin (c), coumarin (d), 7-hydroxycoumarin (e), 6-hydroxycoumarin (f), 6-methylcoumarin (g) and 6,7-dihydroxycoumarin (h) by whole cells of *E. coli* BL21 containing *hcdE* gene. Biotransformation was carried out in 50 mM potassium phosphate buffer pH 7.2 at 30 °C with 0.5 mM of substrate. Arrows indicate changes of absorbance. Incubation time is shown in min. 24 h – incubation for 24 hours.

This implied that these substrates have strong enzyme inhibiting properties which could be bypassed within *E. coli* BL21 cells by limiting substrate transportation through the cell membrane, thus maintaining a low concentration of substrate within cells.

The initial velocities were measured for HcdE protein with varying both NADPH and 7-hydroxycoumarin concentrations to determine kinetic properties of HcdE enzyme. The estimation of the kinetic parameters was performed by fitting the data to the Michaelis-Menten expression of the bimolecular reaction rate (Equation 1):

$$v = \frac{[E_0]k_{bim}k_{NADPH}[NADPH][7HK]}{k_{NADPH}[NADPH]+k_{bim}[7HK]\left(K_M^{NADPH}+[NADPH]+K_i[NADPH][7HK]\right)} \quad (1)$$

where [NADPH] is the concentration of NADPH; [7HK] is the concentration of 7-hydroxycoumarin; v is the observed rate; k_{bim} is the bimolecular rate constant of 7-hydroxycoumarin reduction, expressed as k_{7HK}/K_M^{7HK} (where $K_M^{7HK} = (k_{m2} + k_{7HK})/k_2$); k_{NADPH} is the rate constant of NADPH oxidation;

K_M^{NADPH} is the K_M for NADPH at saturating 7-hydroxycoumarin levels (where $K_M^{NADPH} = (k_{m1} + k_{NADPH})/k_1$); and K_i is the inhibition constant of 7-hydroxycoumarin. The action of 7-hydroxycoumarin reduction and NADPH oxidation is represented by the proposed reaction scheme (Fig. 46).

$$E_0 + NADPH \underset{k_{m1}}{\overset{k_1}{\rightleftharpoons}} E_1 \xrightarrow{k_{NADPH}} E_2 \quad (2)$$

$$E_2 + 7HK \underset{k_{m2}}{\overset{k_2}{\rightleftharpoons}} E_3 \xrightarrow{k_{7HK}} E_0 + NADP^+ + 7HKH_2 \quad (3)$$

$$E_1 + 7HK \underset{k_d}{\overset{k_a}{\rightleftharpoons}} E_i \quad (4)$$

Figure 46. A proposed reaction scheme of HcdE.

The reductive half-reaction sequence was modelled as shown in Equation 2, where E_0 is oxidized hcdE enzyme form, E_1 is the $hcdE_{ox}$-NADPH charge-transfer complex, and E_2 is reduced hcdE enzyme form and bound $NADP^+$. The oxidative half-reaction sequence was modelled as shown in the Equation 3, where 7HK is 7-hydroxycoumarin, E_3 is $hcdE_{red}$-7HK charge-transfer complex and bound $NADP^+$, and $7HKH_2$ is 7-hydroxy-3,4-dihydrocoumarin.

It has been also showed that 7-hydroxycoumarin acts as a strong inhibitor of hcdE enzyme at higher concentrations (Fig. 47). Based on the equation of bimolecular reaction rate (Equation 1) we propose that inhibition occurs when 7-hydroxycoumarin bounds to the $hcdE_{ox}$-NADPH charge-transfer complex (E_1) rather than oxidized HcdE enzyme form (E_0) (Equation 4). Therefore, 7-hydroxycoumarin is likely pseudo-competitive inhibitor characterized by the inhibition constant K_i (expressed as k_d/k_a) that is equal to 22 mM for 7-hydroxycoumarin. The determined k_{bim} value of reduction of 7-hydroxycoumarin by HcdE was equal to 1490 $mM^{-1}s^{-1}$. Additionally, a rate constant (k_{cat}) of 27 s^{-1} and a K_M^{NADPH} of 20 μM have been determined for NADPH.

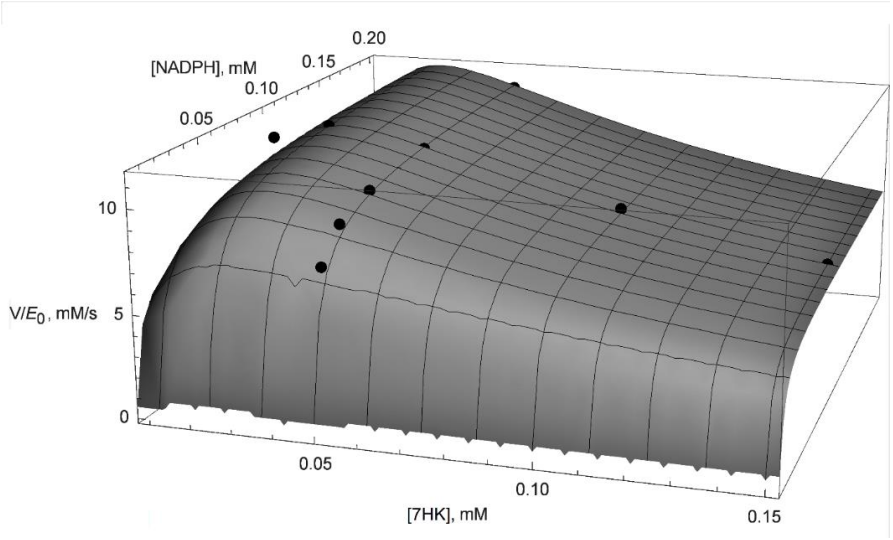

Figure 47. 3D plot of HcdE enzyme kinetic titration data their fit. Enzymatic assays were carried out in 50 mM potassium phosphate (K-P) buffer (pH 7.0) with 5–200 µM NADPH and 5–150 µM 7-hydroxycoumarin at 22 ºC. HcdE concentration was kept constant at 99 nM. Rates of bimolecular reaction were observed at 365 nm wavelength. Black spheres represent the mean values of three replicates of the initial enzyme rates. The wire frame surface represents the fitted function.

DISCUSSION

Although coumarins are widely abundant in nature and are intensively used in biotechnology as precursory compounds [156], the metabolic pathways in microorganisms are still not known in sufficient detail. In this study, *Pseudomonas mandelii* 7HK4 strain was isolated from soil and it was shown that these bacteria can utilize 7-hydroxycoumarin as a sole source of carbon and energy. Several other coumarin derivatives were also tested, but none of those substrates support the growth of *Pseudomonas mandelii* 7HK4. However, the experiments with the 7-hydroxycoumarin-induced whole cells show that *Pseudomonas mandelii* 7HK4 has the enzymes that are able to transform coumarin, 6-hydroxycoumarin and 6,7-dihydroxycoumarin. The products of these biotransformations give UV spectra similar to the UV spectrum of 3-(2,4-dihydroxyphenyl) propionic acid, suggesting that *Pseudomonas mandelii* 7HK4 bacteria can catalyze hydrolysis and reduction of lactone moiety of these substrates. Later, 3-(2,4-dihydroxyphenyl) propionic acid has been identified as an intermediate metabolite during biotransformations of 7-hydroxycoumarin. This finding agrees with the data published for the conversion of coumarin by *Pseudomonas* spp., *Arthrobacter* spp., and *Aspergillus* spp., which all catalyze the hydrolysis and reduction of coumarin producing 3-(2-hydroxyphenyl) propionic acid as the main intermediate [9–11,14]. However, compared with *Pseudomonas mandelii* 7HK described in this study, little is known about the bioconversion of other coumarin derivatives as well as further conversions of 3-(2-hydroxyphenyl) propionic acid in bacteria listed above.

The analysis of the 7-hydroxycoumarin-inducible proteins lead to the identification of the genomic locus *hcd* encoding the enzymes required for 7-hydroxycoumarin degradation. A BLAST search uncovered that *hcdA*, *hcdB*, *hcdC* and *hcdE* encode an aromatic flavin-binding hydroxylase, a ring-cleavage dioxygenase, a hydroxymuconic semialdehyde hydrolase and an alcohol dehydrogenase, respectively.

Thus far, only a few studies have been published discussing the reduction of coumarins in microorganisms [10,14]. To date, it was known that coumarin could be reduced at the double bond in the α-pyrone ring by coumarin reductase and NADH as the first step resulting in dihydrocoumarin, followed by hydrolysis between the oxygen and carbonyl carbon atoms of the ring [10,14]. On the other hand, the initial attack on coumarin could also be hydrolysis to *o*-coumaric acid, only then followed by reduction to melilotic acid [16]. Some enzymes having coumarin reducing activity have been biochemically characterized [10], however barely genetic data or enzyme mechanisms have

been presented. In the present study, we discovered a HcdE protein that is produced in *Pseudomonas mandelii* 7HK4 when grown with 7-hydroxycoumarin as a sole source of carbon and energy, and it catalyses the NADPH-dependent reduction of several coumarin derivatives including coumarin itself, 6-methylcoumarin, 6-hydroxycoumarin, 7-hydroxycoumarin and 6,7-dihydroxycoumarin. HcdE appears to have a high specificity for coumarin derivatives with unsubstituted and non-hydrolysed lactone moiety, thus other structurally related substrates, such as quinolin-2(1*H*)-one or 7-hydroxyquinolin-2(1*H*)-one are not used by the HcdE enzyme. Also, there is one discrepancy between conversions with whole cells and pure enzyme in this research. Whole cells of *E. coli* BL21 harbouring *hcdE* gene are able to reduce low levels of 7-methylcoumarin, 7-methoxycoumarin and 4-methyl-7-hydroxycoumarin, while the purified HcdE enzyme alone is not. Although the results are not conclusive, we propose that the whole cells limit substrate transportation through the cell membrane maintaining a non-inhibitive concentration of substrate within cells. We showed that HcdE dehydrogenase is inhibited by its substrate 7-hydroxycoumarin at higher concentrations with the inhibition constant K_i that is equal to 22 mM for 7-hydroxycoumarin. The inhibition occurs when 7-hydroxycoumarin bounds to the $HcdE_{ox}$-NADPH charge-transfer complex (E_1), thus reducing the NADPH oxidation rate.

HcdE dehydrogenase is, to our best knowledge, the first ene-reductase of MDR family involved in the *in vivo* degradation of coumarin compounds. And only one functionally related enzyme, such as XenA reductase from *Pseudomonas putida* 86 is known [62]. XenA reductase has well-described primary and secondary structures, yet it belongs to another family of ERs – OYEs, catalysing FMN and NAD(P)H dependent reduction of coumarin and 8-hydroxycoumarin. The determined k_{bim} value of reduction of 7-hydroxycoumarin by HcdE dehydrogenase was equal to 1490 $mM^{-1}s^{-1}$. Additionally, a rate constant (k_{cat}) of 27 s^{-1} have been determined for NADPH oxidation by hcdE dehydrogenase, which is almost 10-fold lower compared to rate constant of 215 s^{-1} for NADPH oxidation by XenA reductase from *Pseudomonas putida* 86 [66,157]. The difference in NADPH oxidation between two functionally similar hcdE and XenA reductases could be due to observable competitive inhibition of HcdE enzyme by its substrate while XenA reductase is not inhibited.

The bioconversion of 7-hydroxycoumarin was completed *in vivo*, and the reduced product of the hcdE protein was confirmed by HPLC-MS and NMR analysis, also comparing to chemically synthesized 7-hydroxy-3,4-dihydrocoumarin. It was shown that 7-hydroxycoumarin is reduced at the C-3/C-4 double bond of its lactone moiety forming 7-hydroxy-3,4-

dihydrocoumarin. However due to strong inhibition of HcdE enzyme by its substrate the conversion rates are low enough that prolonged conversion time would affect the reaction product 7-hydroxy-3,4-dihydrocoumarin. Later compound is a lactone - cyclic ester that is much more reactive than its acyclic analogues. Additionally, it has a phenyl ring attached and the fact that it is a phenolic ester, 7-hydroxy-3,4-dihydrocoumarin is significantly more reactive against hydroxyl anions proceeding through hydrolysis in aqueous solutions resulting in formation of 3-(2,4-dihydroxyphenyl) propionic acid.

Further, biochemical analysis of the HcdA protein confirmed its similarity to class A FAD-binding enzymes (FMOs) [79,87,88,130,135,136]. HcdA is functionally related to previously well-described hydroxylases, such as OhpB monooxygenase from *Rhodococcus* sp. V49 [53], MhpA monooxygenase from *E. coli* K-12 [158] and *Comamonas testosteroni* TA441 [159], HppA monooxygenase from *Rhodococcus globerulus* PWD1 [142], and also *para*-hydroxybenzoate hydroxylase (PHBH) from *P. Fluorescens* [160]. HcdA appears to have a high specificity for 3-(2,4-dihydroxyphenyl) propionic acid, converting it to 3-(2,3,5-trihydroxyphenyl) propionic acid, and a 40-fold lower activity towards trans-2,4-dihydroxycinnamic acid. Other structurally related substrates are not used by HcdA. Unlike HcdA, other related FMOs have a broader specificity for substrates. For example, OhpB monooxygenase is capable to oxidize 2-hydroxy-, 3-hydroxyphenylpropionic and cinnamic acids [53]. The HppA enzyme is more specific to 3-hydroxyphenylpropionic, but 4-chlorophenoxyacetic as well as 4-methyl-2-chlorophenoxyacetic acids are also oxidized [142]. On the other hand, all described FMOs including HcdA are NAD(P)H dependent, which reduces flavin for the hydroxylation of substrates [87,88,135,136]. The narrow specificity of HcdA to its natural substrate is typical for class A flavoproteins and shows the importance of HcdA enzyme in metabolism of 7-hydroxycoumarin. The kinetic analysis of HcdA yields K_M values of 50.10 ± 3.50 μM and 13.00 ± 1.20 μM for NADH and 3-(2,4-dihydroxyphenyl) propionic acid, respectively. However, no kinetic parameters have been reported for OhpB, MhpA and HppA hydroxylases for comparison, though PHBH has been shown to have a kcat of 22.83 s^{-1} [161], which is 3-fold higher than a turnover number for the HcdA enzyme.

The hydroxylated product of the HcdA protein was analysed by oxidizing it with the HcdB dioxygenase, followed by a chemical modification to the corresponding derivative of picolinic acid. The structure of the later compound was confirmed by ^{1}H NMR and ^{13}C NMR spectra. This allowed the reconstruction of the reaction products of both HcdA and HcdB enzymes. It was shown that a hydroxylation of 3-(2,4-dihydroxyphenyl) propionic acid occurs at *ipso*-position of phenolic ring followed by an internal rearrangement

and involving (1,2-C,C)-shift (NIH shift) of propionic acid moiety, hence forming 3-(2,3,5-trihydroxyphenyl) propionic acid (Fig. 38). This would explain both the high specificity of HcdA enzyme for substrates with para-substituted phenol and inability of *Pseudomonas mandelii* 7HK4 bacteria to utilize coumarin derivatives other than 7-hydroxycoumarin as the sole source of carbon and energy. Only a few classes of enzymes are able to catalyze *ipso*-reactions: laccases, peroxidases, dioxygenases, glutathione S-transferases (GST), cytochrome P450-dependent monooxygenases (CYP) and flavin-dependent monooxygenases. Among the known examples of *ipso*-enzymes, there are dioxygenases from *Comamonas testosteroni* T2 and *Sphingomonas* sp. strain RW1, which are involved in the desulfonation of 4-sulfobenzoate by *ipso*-substitution [97,98]. A rat liver CYP system is able to convert *p*-chloro, *p*-bromo, *p*-nitro, *p*-cyano, *p*-hydroxymethyl, *p*-formyl and *p*-acetyl phenols to hydroquinone by *ipso*-hydroxylation [100]. GST is capable of catalysing desulfonylation of sulfonylfuropyridine compounds by nucleophilic attack of the glutathione sulphur atom at *ipso*-position [162]. These are the examples of electrophilic or nucleophilic *ipso*-substitution reactions, however in some cases, a primary *ipso*-group is not eliminated, instead it is shifted to *meta*-position. NIH shift restabilizes cyclohexadienone intermediate, because it leads to a rearomatization [89,103,105,154]. We showed that, similarly to flavin-dependent monooxygenases from *Sphingomonas* sp. TTNP3 and *Sphingobium xenophagum* strains, which are responsible for the degradation of alkylphenols, such as bisphenol A, octylphenol, *t*-butylphenol, *n*-octyloxyphenol and *t*-butoxyphenol, HcdA-catalysed reaction involves a NIH shift. Usually, NIH shift products are formed during the side reactions, and these internal rearrangements of an alkyl group upon the *ipso*-hydroxylation are spontaneous and non-enzymatic in *Sphingomonas* sp. strains [103,163]. An interesting novelty is that HcdA hydroxylase produces only one product, which has the *ipso*-group shifted to the *meta*-position. Therefore, we propose that in the case of HcdA, NIH shift occurs enzymatically, but not spontaneously or by a dienone-phenol rearrangement mechanism [164], since all bioconversions were performed under neutral or basic conditions. Although a further investigation is needed to determine the exact mechanism of the HcdA enzyme activity.

The analysis of the extradiol dioxygenase HcdB shows that this enzyme has a lower specificity for substrates. It catalyses a conversion of the hydroxylated product of the HcdA enzyme to (*2E,4E*)-2,4-dihydroxy-6-oxonona-2,4-dienedioic acid (Fig. 38). Also, HcdB is capable oxidizing pyrocatechol, 3-methylcatechol, 3-methoxycatechol, 4-methylcatechol, 3-(2,3-dihydroxyphenyl) propionic and caffeic acids using a *meta*-cleavage

mechanism forming yellow products. HcdB belongs to type I, class II extradiol dioxygenases [137,138], and is functionally related to OhpD catechol 2,3-dioxygenase from *Rhodococcus* sp. V49 [53], MhpB extradiol dioxygenase from *E. coli* K-12 [158,165], MpcI extradiol dioxygenase from *Alcaligenes eutrophus* [165], HppB extradiol dioxygenase from *Rhodococcus globerulus* PWD1 [142], and DbfB 2,2',3-trihydroxybiphenyl dioxygenase from *Sphingomonas* sp. RW1 [141].

Finally, we demonstrate that (2*E*,4*E*)-2,4-dihydroxy-6-oxonona-2,4-dienedioic acid, the ring cleavage product of HcdB protein, is subsequently hydrolysed by the putative HcdC hydroxymuconic semialdehyde hydrolase. This enzyme has a low sequence homology to any of the previously characterized enzymes from *Rhodococcus* sp. V49 [53], *E. coli* K-12 [158], *Comamonas testosteroni* TA441 [159] or *Rhodococcus globerulus* PWD1 [142], therefore further investigation is needed to elucidate the exact mechanism of the hydrolysis and the specificity of the HcdC enzyme for substrates.

Additionally, during the analysis of the *Pseudomonas mandelii* 7HK4 genome sequences adjacent to the *hcdE* gene it was also expected to detect genes encoding hydrolase-like enzymes that could be harnessed by 7HK4 strain for hydrolysis of 7-hydroxy-3,4-dihydrocoumarin. Transcriptional analysis revealed that like *hcdE, hcdD* gene was also induced in *Pseudomonas mandelii* 7HK4 cells pre-grown with 7-hydroxycoumarin. *HcdD* and *hcdE* together with *hcdF* and *hcdG* genes are arranged on the same DNA strand, and are separated by short intergenic regions, suggesting that these genes are organized into an operon. HcdD protein is similar to *Bacillus* chorismate mutase-like (BCM-like) family proteins, and is in agreement with the first representatives of Pfam family (formerly DUF1185) [166]. We propose that this protein could be stimulating 7-hydroxy-3,4-dihydrocoumarin formation similarly to homologues protein TgnF which stimulates TgnE-dependent succinic acid semialdehyde oxidation in *Acinetobacter baylyi* ADP1 bacteria [167]. Further, HcdF is a cupin-like protein which could be classified as member of RmlC-like Cupins superfamily. It comprises of families with members displaying diverse functions ranging from enzymatic activities like dioxygenases, hydrolases and epimerases to non-enzymatic functions [168–170]. We believe that HcdF could act as a 7-hydroxy-3,4-dihydrocoumarin hydrolase, however further investigation is needed to elucidate its exact function in *Pseudomonas mandelii* 7HK4 strain. And the last HcdG protein from *hcdDEFG* gene cluster belongs to NAD(P)H-dependent FMN reductase superfamily. Flavodoxins are widely involved in the electron-transfer reactions required for the metabolism of pyruvate, nitrogen and pyridine nucleotides in bacteria [171–173].

Also, *in silico* analysis of the *Pseudomonas mandelii* 7HK4 genome provided evidence that 7HK4 strain has even more ER enzymes capable of utilizing various coumarin derivatives. Two putative xenobiotic reductases XenA38 and XenA45 from 7HK4 strain were produced in *E. coli* bacteria, and their activities were determined *in vivo*. We demonstrated that coumarin, 6-hydroxycoumarin, 6-methylcoumarin, 7-hydroxycoumarin, 7-methylcoumarin and 6,7-dihydroxycoumarin are reduced by the putative XenA38 and XenA45 reductases. Analysis of mRNA synthesis levels showed that production of XenA38 and XenA45 proteins are not induced by any coumarin in *Pseudomonas mandelii* 7HK4 cells, although XenA38 enzyme has higher expression levels in 7HK4 strain grown in the absence of coumarins. Such enzymes as XenA38 with the constitutive expression and the broad substrate specificity explain the wide variety of aromatic substances that can be degraded by bacteria like *Pseudomonas* genus.

In summary, here we report a 7-hydroxycoumarin catabolic pathway in *Pseudomonas mandelii* 7HK4 bacteria. New metabolites and genes responsible for the degradation of 7-hydroxycoumarin have been isolated and identified. Our results show that the degradation of 7-hydroxycoumarin in *Pseudomonas mandelii* 7HK4 involves a distinct metabolic pathway, compared to the previously characterized coumarin catabolic routes in *Pseudomonas*, *Arthrobacter* and *Aspergillus* species [9–15]. New gene responsible for the reduction of 7-hydroxycoumarin has been isolated and identified. Our results show that the reduction of 7-hydroxycoumarin in *Pseudomonas mandelii* 7HK4 involves a similar approach like in the previously characterized coumarin catabolic routes in *Pseudomonas* sp. 30-1 and *Aspergillus niger* ATCC 11394 [10,14]. *Pseudomonas mandelii* 7HK4 bacteria employ unique NADPH-dependent alcohol dehydrogenase family protein HcdE for the reduction of the C-3/C-4 double bond of 7-hydroxycoumarin lactone moiety forming 7-hydroxy-3,4-dihydrocoumarin. HcdE dehydrogenase described in this work has a significantly distant sequence homology from the previously characterized enzyme implicated in the degradation of structurally similar substrate, such as 8-hydroxycoumarin in *Pseudomonas putida* 86 [62]. Further, it has been shown that *Pseudomonas mandelii* 7HK4 bacteria employ a unique flavin binding *ipso*-hydroxylase for the oxidation of the aromatic ring of 3-(2,4-dihydroxyphenyl) propionic acid.

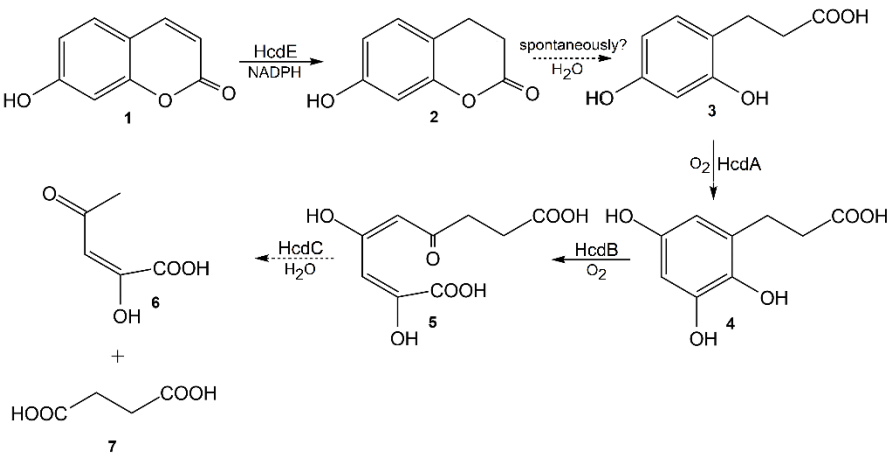

Figure 48. The proposed catabolic pathway of 7-hydroxycoumarin in *Pseudomonas mandelii* 7HK4 bacteria. 1 – 7-hydroxycoumarin; 2 – 7-hydroxy-3,4-dihydrocoumarin; 3 – 3-(2,4-dihydroxyphenyl) propionic acid; 4 – 3-(2,3,5-trihydroxyphenyl) propionic acid; 5 – (2*E*,4*E*)-2,4-dihydroxy-6-oxonona-2,4-dienedioic acid; 6 – (*E*)-2-hydroxy-4-oxopent-2-enoic acid; 7 – succinic acid; HcdA – 3-(2,4-dihydroxyphenyl) propionic acid 1-monooxygenase; HcdB – 3-(2,3,5-trihydroxyphenyl) propionic acid 1,2-dioxygenase; HcdC – putative (2*E*,4*E*)-2,4-dihydroxy-6-oxonona-2,4-dienedioic acid hydrolase; HcdE – 7-hydroxycoumarin reductase. The dashed arrows indicate a hypothetical reaction.

None of the proteins described in this study have substantial sequence homology to the previously characterized enzymes implicated in the degradation of structurally similar substrates, such as 3-(2-hydroxyphenyl) propionic acid in *Rhodococcus* sp. V49 [53], 3-(3-hydroxyphenyl) propionic acid and 3-hydroxycinnamic acid in *E. coli* K-12 [158], *Comamonas testosteroni* TA441 [159], *Rhodococcus globerulus* PWD1 [142], or even 4-hydroxyphenylacetate in *Escherichia coli* W [174]. Thus, our results provide a fundamentally new insight into the degradation of hydroxycoumarins by the soil microorganisms. In addition, the discovered new bacteria and enzymes can be further employed for the development of novel biocatalytic processes useful for industry.

CONCLUSIONS

1. A *hcd* gene cluster of *Pseudomonas mandelii* 7HK4 bacteria encodes enzymes required for the degradation of 7-hydroxycoumarin.
2. NADPH-dependent alcohol dehydrogenase HcdE reduces 7-hydroxycoumarin to 7-hydroxy-3,4-dihydrocoumarin.
3. *Ipso*-monooxygenase HcdA oxidizes 3-(2,4-dihydroxyphenyl) propionic acid to 3-(2,3,5-trihydroxyphenyl) propionic acid.
4. HcdB extradiol dioxygenase oxidizes 3-(2,3,5-trihydroxyphenyl) propionic acid to (2*E*,4*E*)-2,4-dihydroxy-6-oxonona-2,4-dienedioic acid.
5. Putative hydroxymuconic semialdehyde hydrolase HcdC hydrolyses (2*E*,4*E*)-2,4-dihydroxy-6-oxonona-2,4-dienedioic acid.

REFERENCES

(1) Sarker SD, Nahar L. Progress in the Chemistry of Naturally Occurring Coumarins. 2017, pp 241–304.

(2) Bourgaud F, Hehn A, Larbat R, Doerper S, Gontier E, Kellner S, Matern U. Biosynthesis of Coumarins in Plants: A Major Pathway Still to Be Unravelled for Cytochrome P450 Enzymes. Phytochemistry Reviews, 2006, pp 293–308.

(3) Murray RDH, Méndez J, Brown SA. The natural coumarins: occurrence, chemistry, and biochemistry. Chichester, New York, Wiley, 1982.

(4) Mazid, Ta K, Mohammad F. Role of Secondary Metabolites in Defense Mechanisms of Plants. 2011, Vol. 3.

(5) Kayser O, Kolodziej H. Antibacterial Activity of Simple Coumarins: Structural Requirements for Biological Activity. Zeitschrift fur Naturforschung - Section C Journal of Biosciences, 1999, 54(3–4), pp 169–174.

(6) de Souza SM, Delle Monache F, Smâ A. Antibacterial Activity of Coumarins. 2005, Vol. 60.

(7) Yang L, Ding W, Xu Y, Wu D, Li S, Chen J, Guo B. New Insights into the Antibacterial Activity of Hydroxycoumarins against *Ralstonia Solanacearum*. Molecules, 2016, 21(4).

(8) Serghini K, Pérez de Luque A, Castejón-Muñoz M, García-Torres L, Jorrín JV. Sunflower (Helianthus Annuus L.) Response to Broomrape (Orobanche Cernua Loefl.) Parasitism: Induced Synthesis and Excretion of 7-Hydroxylated Simple Coumarins. Journal of experimental botany, 2001, 52(364).

(9) Shieh HS, Blackwood AC. Use of Coumarin by Soil Fungi. Canadian Journal of Microbiology, 1969, 15, pp 647–648.

(10) Nakayama Y, Nonomura S, Tatsumi C. The Metabolism of Coumarin by a Strain of *Pseudomonas*. Agricultural and Biological Chemistry, 1973, 37(6), pp 1423–1437.

(11) Levy CC, Weinstein GD. The Metabolism of Coumarin by a Microorganism. II. The Reduction of *o*-Coumaric Acid to Melilotic Acid. Biochemistry, 1964, 3(12), pp 1944–1947.

(12) Bellis DM. Metabolism of Coumarin and Related Compounds in Cultures of *Penicillium* Species. Nature, 1958, 182(4638), pp 806–807.

(13) Bocks SM. Fungal Metabolism-I. The Transformations of Coumarin, *o*-Coumaric Acid and *Trans*-Cinnamic Acid by *Aspergillus Niger*. Phytochemistry, 1967, 6(1), pp 127–130.

(14) Aguirre-Pranzoni C, Orden AA, Bisogno FR, Ardanaz CE, Tonn CE, Kurina-Sanz M. Coumarin Metabolic Routes in *Aspergillus* Spp. Fungal Biology, 2011, 115(3), pp 245–252.
(15) Marumoto S, Miyazawa M. Microbial Reduction of Coumarin, Psoralen, and Xanthyletin by *Glomerella Cingulata*. Tetrahedron, 2011, 67(2), pp 495–500.
(16) Levy CC, Frost P. The metabolism of coumarin by a microorganism. Melilotate hydroxylase. Journal of Biological Chemistry, 1966, 241, pp 997–1003.
(17) Vogel A. Darstellung von Benzoesäure Aus Der Tonka-Bohne Und Aus Den Meliloten - Oder Steinklee - Blumen. Annalen der Physik und der physikalischen Chemie, 1820, 64(2), pp 161–166.
(18) Elis GP, West GB. Progress in Medicinal Chemistry 10; North-holland publishing company: Amsterdam, 1974.
(19) Walton NJ, Brown DE, Harborne JB. Classes and functions of secondary products from plants. In Chemicals from Plants; World scientific/Imperial college press, 1999, pp 1–25.
(20) Carlton BD. Coumarins. Encyclopedia of Toxicology, 2005.
(21) Bourgaud F, Hehn A, Larbat R, Doerper S, Gontier E, Kellner S, Matern U. Biosynthesis of Coumarins in Plants: A Major Pathway Still to Be Unravelled for Cytochrome P450 Enzymes. Phytochemistry Reviews, 2006, pp 293–308.
(22) Repčák M, Imrich J, Franeková M. Umbelliferone, a Stress Metabolite of *Chamomilla Recutita* (L.) Rauschert. Journal of Plant Physiology, 2001, 158(8), pp 1085–1087.
(23) Pastírová A, Repčák M, Eliašová A. Salicylic Acid Induces Changes of Coumarin Metabolites in *Matricaria Chamomilla* L. Plant Science, 2004, 167(4), pp 819–824.
(24) Chong J, Baltz R, Schmitt C, Beffa R, Fritig B, Saindrenan P. Downregulation of a Pathogen-Responsive Tobacco UDP-Glc Phenylpropanoid Glucosyl-transferase Reduces Scopoletin Glucoside Accumulation, Enhances Oxidative Stress, and Weakens Virus Resistance. Plant Cell, 2002, 14(5), pp 1093–1107.
(25) Yang E, Zhao YN, Zhang K, MacK P. Daphnetin, One of Coumarin Derivatives, Is a Protein Kinase Inhibitor. Biochemical and Biophysical Research Communications, 1999, 260(3), pp 682–685.
(26) NDong C, Anzellotti D, Ibrahim RK, Huner NPA, Sarhan F. Daphnetin Methylation by a Novel *O*-Methyltransferase Is Associated with Cold Acclimation and Photosystem II Excitation Pressure in Rye. Journal of Biological Chemistry, 2003, 278(9), pp 6854–6861.

(27) George HL, VanEtten HD. Characterization of Pisatin-Inducible Cytochrome P450s in Fungal Pathogens of Pea That Detoxify the Pea Phytoalexin Pisatin. Fungal Genetics and Biology, 2001, 33(1), pp 37–48.
(28) Lacy A. Studies on Coumarins and Coumarin-Related Compounds to Determine Their Therapeutic Role in the Treatment of Cancer. Current Pharmaceutical Design, 2005, 10(30), pp 3797–3811.
(29) Dall'Acqua F, Vedaldi D, Recher M. The photoreaction between furocoumarins and various DNA with different base compositions. Photochemistry and Photobiology, 1978, 27(1), pp 33–36.
(30) Četkauskaitė A, Zimkus A. Ekologinė Biochemija. Vilnius University: Vilnius, 2008.
(31) Kataranovski M, Vlaski M, Kataranovski D, Tosić N, Mandić-Radić S, Todorović V. Immunotoxicity of epicutaneously applied anticoagulant rodenticide warfarin: evaluation by contact hypersensitivity to DNCB in rats. Toxicology, 2003, 188(1), pp 83–100.
(32) Mazimba O. Umbelliferone: Sources, Chemistry and Bioactivities Review. Bulletin of Faculty of Pharmacy, Cairo University, 2017, 55(2), pp 223–232.
(33) Murray R, Mendez J, Wiley SBJ. Coumarin Activity in Plants and Bioorganism Aspects. 1982.
(34) Lee JH, Bang HB, Han SY, Jun JG. A Convenient Total Synthesis of (+)-Decursinol from Resorcinol. Bulletin of the Korean Chemical Society, 2006, 27(12), pp 2104–2106.
(35) Singh R, Singh B, Singh S, Kumar N, Kumar S, Arora S. Umbelliferone - An Antioxidant Isolated from Acacia Nilotica (L.) Willd. Ex. Del. Food Chemistry, 2010, 120(3), pp 825–830.
(36) Mazimba O, Majinda RRT, Modibedi C, Masesane IB, Cencič A, Chingwaru W. Tylosema Esculentum Extractives and Their Bioactivity. Bioorganic and Medicinal Chemistry, 2011, 19(17), pp 5225–5230.
(37) Kanimozhi G, Prasad NR, Ramachandran S, Pugalendi KV. Umbelliferone Modulates Gamma-Radiation Induced Reactive Oxygen Species Generation and Subsequent Oxidative Damage in Human Blood Lymphocytes. European Journal of Pharmacology, 2011, 672(1–3), pp 20–29.
(38) Kassim NK, Rahmani M, Ismail A, Sukari MA, Ee GCL, Nasir NM, Awang K. Antioxidant Activity-Guided Separation of Coumarins and Lignan from *Melicope Glabra* (Rutaceae). Food Chemistry, 2013, 139(1–4), pp 87–92.

(39) Ramu R, Shirahatti PS, Zameer F, Ranganatha L, Nagendra Prasad MN. Inhibitory Effect of Banana (*Musa* Sp. Var. Nanjangud Rasa Bale) Flower Extract and Its Constituents Umbelliferone and Lupeol on α-Glucosidase, Aldose Reductase and Glycation at Multiple Stages. South African Journal of Botany, 2014, 95, pp 54–63.

(40) Muthu R, Thangavel P, Selvaraj N, Ramalingam R, Vaiyapuri M. Synergistic and Individual Effects of Umbelliferone with 5-Flurouracil on the Status of Lipid Peroxidation and Antioxidant Defense against 1,2-Dimethylhydrazine Induced Rat Colon Carcinogenesis. Biomedicine and Preventive Nutrition, 2013, 3(1), pp 74–82.

(41) Kiełbus M, Skalicka-Woźniak K, Grabarska A, Jeleniewicz W, Dmoszyńska-Graniczka M, Marston A, Polberg K, Gawda P, Klatka J, Stepulak A. 7-Substituted Coumarins Inhibit Proliferation and Migration of Laryngeal Cancer Cells in Vitro. Anticancer Research, 2013, 33(10), pp 4347–4356.

(42) Du L, Li M, Zheng S, Wang B. Rational Design of a Fluorescent Hydrogen Peroxide Probe Based on the Umbelliferone Fluorophore. Tetrahedron Letters, 2008, 49(19), pp 3045–3048.

(43) Brown SA, Towers GH, Wright D. Biosynthesis of the Coumarins.Tracer Studies on Coumarin Formation in Hierochloe Odorata and Melilotus Officinalis. Canadian Journal of Biochemistry and Physiology, 1960, 38(2), pp 143–156.

(44) Ellis BE, Amrhein N. The "NIH-Shift" during Aromatic *Ortho*-Hydroxylation in Higher Plants. Phytochemistry, 1971, 10(12), pp 3069–3072.

(45) Teutsch HG, Hasenfratz MP, Lesot A, Stoltz C, Garnier JM, Jeltsch JM, Durst F, Werck-Reichhart D. Isolation and Sequence of a CDNA Encoding the Jerusalem Artichoke Cinnamate 4-Hydroxylase, a Major Plant Cytochrome P450 Involved in the General Phenylpropanoid Pathway. Proceedings of the National Academy of Sciences of the United States of America, 1993, 90(9), pp 4102–4106.

(46) Kindl H. *Ortho*-Hydroxylation of Aromatic Carboxylic Acids in Higher Plants. Hoppe-Seyler's Zeitschrift fur Physiologische Chemie, 1971, 352(1), pp 78–84.

(47) Brown SA. Biosynthesis of 6,7-Dihydroxycoumarin in *Cichorium Intybus*. Canadian Journal of Biochemistry and Cell Biology, 1985, 63(4), pp 292–295.

(48) Floss HG, Mother U. On the biochemistry of furocumatin in *Pimpinella magna*. Zeitschrift fur Naturforschung - Section B Journal of Chemical Sciences, 1964, pp 770–771.

(49) Lake BG. Coumarin Metabolism, Toxicity and Carcinogenicity: Relevance for Human Risk Assessment. Food and Chemical Toxicology, 1999, pp 423–453.
(50) Bye A, King AHK. The Biosynthesis of 4-Hydroxycoumarin and Dicoumarol by *Aspergillus Fumigatus*. Fresenius 237, 1970, Vol. 117.
(51) Narasimha G, Kumari K, Ganesh R, Anitha R, Aravind S. Complete Reduction of 2*H*-Pyran-2-One Moiety of Coumarin and 6-Methyl-Coumarin by *Colletotrichum Capsici*. Zeitschrift für Naturforschung C, 2004, 59(5-6), pp 405–407.
(52) Sariaslani FS, Rosazza JP. Novel Biotransformations of 7-Ethoxycoumarin by *Streptomyces Griseus*. Applied and Environmental Microbiology, 1983, 46(2), pp 468–474.
(53) Powell JAC, Archer JAC. Molecular Characterisation of a *Rhodococcus Ohp* Operon. Antonie Van Leeuwenhoek, 1998, 74(1-3), pp 175–188.
(54) Krikštaponis A. Kumarinus skaidančių bakterijų tyrimas. Vilniaus universitetas, Vilnius, 2013.
(55) Dagley S, Chapman PJ, Gibson DT. The Metabolism of *P*-Phenylpropionic Acid by an *Achromobacter*. The biochemical journal, 1965, 97(3), pp 643–650.
(56) Burlingame R, Chapman PJ. Catabolism of Phenylpropionic Acid and Its 3-Hydroxy Derivative by *Escherichia Coli*. Journal of Bacteriology, 1983, 155(1), pp 113–121.
(57) Harwood CS, Parales RE. The β-Ketoadipate Pathway and the Biology of Self-Identity. Annual Review of Microbiology, 1996, pp 553–590.
(58) Khomenkov VG, Shevelev AB, Zhukov VG, Zagustina NA, Bezborodov AM, Popov VO. Organization of Metabolic Pathways and Molecular-Genetic Mechanisms of Xenobiotic Biodegradation in Microorganisms: A Review. Prikladnaia biokhimiia i mikrobiologiia, 2008, pp 133–152.
(59) Sahoo NK, Ramesh A, Pakshirajan K. Bacterial Degradation of Aromatic Xenobiotic Compounds: An Overview on Metabolic Pathways and Molecular Approaches. In Microorganisms in Environmental Management: Microbes and Environment. Springer Netherlands, 2013, pp 201–220.
(60) Harayama S, Timmis K. Metal Ions in Biological Systems. 1992.
(61) Gibson JS, Harwood C. Metabolic Diversity in Aromatic Compound Utilization by Anaerobic Microbes. Annual Review of Microbiology, 2002, 56 (1), pp 345–369.
(62) Griese JJ, P. Jakob R, Schwarzinger S, Dobbek H. Xenobiotic Reductase A in the Degradation of Quinoline by *Pseudomonas Putida* 86: Physiological Function, Structure and Mechanism of 8-

Hydroxycoumarin Reduction. Journal of Molecular Biology, 2006, 361 (1), pp 140–152.
(63) Stuermer R, Hauer B, Hall M, Faber K. Asymmetric Bioreduction of Activated C=C Bonds Using Enoate Reductases from the Old Yellow Enzyme Family. Current Opinion in Chemical Biology, 2007, pp 203–213.
(64) Toogood HS, Scrutton NS. Discovery, Characterization, Engineering, and Applications of Ene-Reductases for Industrial Biocatalysis. American Chemical Society, 2018, pp 3532–3549.
(65) Scholtissek A, Tischler D, Westphal A, van Berkel W, Paul C. Old Yellow Enzyme-Catalysed Asymmetric Hydrogenation: Linking Family Roots with Improved Catalysis. Catalysts, 2017, 7 (12), pp 130.
(66) Toogood HS, Gardiner JM, Scrutton NS. Biocatalytic Reductions and Chemical Versatility of the Old Yellow Enzyme Family of Flavoprotein Oxidoreductases. ChemCatChem, 2010, pp 892–914.
(67) Winkler CK, Faber K, Hall M. Biocatalytic Reduction of Activated C=C-Bonds and beyond: Emerging Trends. Current Opinion in Chemical Biology, 2018, pp 97–105.
(68) Pesic M, Fernández-Fueyo E, Hollmann F. Characterization of the Old Yellow Enzyme Homolog from *Bacillus Subtilis* (YqjM). ChemistrySelect, 2017, 2 (13), pp 3866–3871.
(69) Rohdich F, Wiese A, Feicht R, Simon H, Bacher A. Enoate Reductases of Clostridia. Cloning, Sequencing, and Expression. Journal of Biological Chemistry, 2001, 276 (8), pp 5779–5787.
(70) Nordling E, Jörnvall H, Persson B. Medium-Chain Dehydrogenases/Reductases (MDR): Family Characterizations Including Genome Comparisons and Active Site Modelling. European Journal of Biochemistry, 2002, 269 (17), pp 4267–4276.
(71) Moummou H, Kallberg Y, Tonfack LB, Persson B, van der Rest B. The Plant Short-Chain Dehydrogenase (SDR) Superfamily: Genome-Wide Inventory and Diversification Patterns. BMC Plant Biology, 2012, 12.
(72) Lygidakis A, Karuppiah V, Hoeven R, Ní Cheallaigh A, Leys D, Gardiner JM, Toogood HS, Scrutton NS. Pinpointing a Mechanistic Switch Between Ketoreduction and "Ene" Reduction in Short-Chain Dehydrogenases/ Reductases. Angewandte Chemie, 2016, 128 (33), pp 9748–9752.
(73) Magallanes-Noguera C, Cecati FM, Mascotti ML, Reta GF, Agostini E, Orden AA, Kurina-Sanz M. Plant Tissue Cultures as Sources of New Ene- and Ketoreductase Activities. Journal of Biotechnology, 2017, 251, pp 14–20.

(74) Yanto Y, Yu HH, Hall M, Bommarius AS. Characterization of Xenobiotic Reductase A (XenA): Study of Active Site Residues, Substrate Spectrum and Stability. Chemical Communications, 2010, 46 (46), pp 8809–8811.
(75) Kataoka M, Honda K, Shimizu S. 3,4-Dihydrocoumarin Hydrolase with Haloperoxidase Activity from *Acinetobacter Calcoaceticus* F46. European Journal of Biochemistry, 2000, 267(1), pp 3–10.
(76) Honda K, Kataoka M, Sakuradani E, Shimizu S. Role of *Acinetobacter Calcoaceticus* 3,4-Dihydrocoumarin Hydrolase in Oxidative Stress Defence against Peroxoacids. European Journal of Biochemistry, 2003, 270 (3), pp 486–494.
(77) Schink B, Philipp B, Müller J. Anaerobic Degradation of Phenolic Compounds. Naturwissenschaften, 2000, pp 12–23.
(78) Al-Khalid T, El-Naas MH. Aerobic Biodegradation of Phenols: A Comprehensive Review. Critical Reviews in Environmental Science and Technology, 2012, pp 1631–1690.
(79) van Berkel WJH, Kamerbeek NM, Fraaije MW. Flavoprotein Monooxygenases, a Diverse Class of Oxidative Biocatalysts. Journal of Biotechnology, 2006, pp 670–689.
(80) Artimo P, Jonnalagedda M, Arnold K, Baratin D, Csardi G, de Castro E, Duvaud S, Flegel V, Fortier A, Gasteiger E, Grosdidier A, Hernandez C, Ioannidis V, Kuznetsov D, Liechti R, Moretti S, Mostaguir K, Redaschi N, Rossier G, Xenarios I, Stockinger H. ExPASy: SIB Bioinformatics Resource Portal. Nucleic Acids Research, 2012, 40 (W1).
(81) Bugg TDH. Introduction to Enzyme and Coenzyme Chemistry: Third Edition; John Wiley and Sons, 2012.
(82) Riebel A, de Gonzalo G, Fraaije MW. Expanding the Biocatalytic Toolbox of Flavoprotein Monooxygenases from *Rhodococcus Jostii* RHA1. Journal of Molecular Catalysis B: Enzymatic, 2013, 88, pp 20–25.
(83) Massey V. Activation of Molecular Oxygen by Flavins and Flavoproteins. Journal of Biological Chemistry, 1994, pp 22459–22462.
(84) Ghisla S, Massey V. Mechanisms of Flavoprotein-catalyzed Reactions. European Journal of Biochemistry, 1989, 181 (1), pp 1–17.
(85) Entsch B, van Berkel WJH. Structure and Mechanism of Para-hydroxybenzoate Hydroxylase. The FASEB Journal, 1995, 9 (7), pp 476–483.
(86) Massey V. The Chemical and Biological Versatility of Riboflavin. Biochemical Society Transactions, 2000, 28 (4), pp 283.

(87) Chaiyen P. Flavoenzymes Catalyzing Oxidative Aromatic Ring-Cleavage Reactions. Archives of Biochemistry and Biophysics, 2010, pp 62–70.
(88) Crozier-Reabe K, Moran GR. Form Follows Function: Structural and Catalytic Variation in the Class a Flavoprotein Monooxygenases. International Journal of Molecular Sciences, 2012, pp 15601–15639.
(89) Ricken B, Kolvenbach BA, Corvini PF. Ipso-Substitution-the Hidden Gate to Xenobiotic Degradation Pathways. Current Opinion in Biotechnology, 2015, pp 220–227.
(90) Ohe T, Mashino T, Hirobe M. Novel Metabolic Pathway of Arylethers by Cytochrome P450: Cleavage of the Oxygen-Aromatic Ring Bond Accompanying Ipso-Substitution by the Oxygen-Atom of the Active Species in Cytochrome P450 Models and Cytochrome P450. Archives of Biochemistry and Biophysics, 1994, 310 (2), pp 402–409.
(91) Ohe T, Mashino T, Hirobe M. Substituent Elimination Fromp-Substituted Phenols by Cytochrome P450. Drug Metabolism and Disposition, 1997, 25 (1).
(92) Chivukula M, Renganathan V. Phenolic Azo Dye Oxidation by Laccase from *Pyricularia Oryzae*. Applied and Environmental Microbiology, 1995, 61 (12).
(93) Kunamneni A, Ballesteros A, Plou FJ, Alcalde M. Fungal Laccase - a Versatile Enzyme for Biotechnological Applications. Recent Advancement in White Biotechnology Through Fungi, 2019, pp 429–457.
(94) Leonowicz A, Cho N, Luterek J, Wilkolazka A, Wojtas-Wasilewska M, Matuszewska A, Hofrichter M, Wesenberg D, Rogalski J. Fungal Laccase: Properties and Activity on Lignin. Journal of Basic Microbiology, 2001, pp 185–227.
(95) Iimura Y, Hartikainen P, Tatsumi K. Dechlorination of Tetrachloroguaiacol by Laccase of White-Rot *Basidiomycete Coriolus Versicolor*. Applied Microbiology and Biotechnology, 1996, 45 (3), pp 434–439.
(96) Wong DWS. Structure and Action Mechanism of Ligninolytic Enzymes. Applied Biochemistry and Biotechnology, 2009, pp 174–209.
(97) Locher HH, Leisinger T, Cook AM. 4-Sulphobenzoate 3,4-Dioxygenase. Purification and Properties of a Desulphonative Two-Component Enzyme System from *Comamonas Testosteroni* T-2. Biochemical Journal, 1991, 274 (3), pp 833–842.
(98) Bunz P, Cook AM. Dibenzofuran 4,4a-Dioxygenase from *Sphingomonas* Sp. Strain RW1: Angular Dioxygenation by a Three-Component Enzyme System. Journal of Bacteriology, 1993, 175 (20), pp 6467–6475.

(99) Lessner DJ, Johnson GR, Parales RE, Spain JC, Gibson DT. Molecular Characterization and Substrate Specificity of Nitrobenzene Dioxygenase from *Comamonas* Sp. Strain JS765. Applied and Environmental Microbiology, 2002, 68 (2), pp 634–641.
(100) Vatsis KP, Coon MJ. Ipso-Substitution by Cytochrome P450 with Conversion of p-Hydroxybenzene Derivatives to Hydroquinone: Evidence for Hydroperoxo-Iron as the Active Oxygen Species. Archives of Biochemistry and Biophysics, 2002, 397 (1), pp 119–129.
(101) Tang H, Yao Y, Zhang D, Meng X, Wang L, Yu H, Ma L, Xu P. A Novel NADH-Dependent and FAD-Containing Hydroxylase Is Crucial for Nicotine Degradation by *Pseudomonas Putida*. Journal of Biological Chemistry, 2011, 286 (45), pp 39179–39187.
(102) Porter AW, Hay AG. Identification of OpdA, a Gene Involved in Biodegradation of the Endocrine Disrupter Octylphenol. Applied and Environmental Microbiology, 2007, 73 (22), pp 7373–7379.
(103) Kolvenbach BA, Corvini PF. The Degradation of Alkylphenols by *Sphingomonas* Sp. Strain TTNP3 - a Review on Seven Years of Research. New Biotechnology, 2012, pp 88–95.
(104) Koerts J, Soffers AEMF, Vervoort J, de Jager A, Rietjens IMCM. Occurrence of the NIH Shift upon the Cytochrome P450-Catalyzed in Vivo and in Vitro Aromatic Ring Hydroxylation of Fluorobenzenes. Chemical Research in Toxicology, 1998, 11 (5), pp 503–512.
(105) Martin G, Dijols S, Capeillere-Blandin C, Artaud I. Hydroxylation Reaction Catalyzed by the *Burkholderia Cepacia* AC1100 Bacterial Strain. Involvement of the Chlorophenol-4-Monooxygenase. European Journal of Biochemistry, 1999, 261 (2), pp 533–539.
(106) Haddock JD. Aerobic Degradation of Aromatic Hydrocarbons: Enzyme Structures and Catalytic Mechanisms. In Handbook of Hydrocarbon and Lipid Microbiology, 2010, pp 1057–1069.
(107) Vaillancourt F, Bolin J, Eltis L. The Ins and Outs of Ring-Cleaving Dioxygenases. Critical Reviews in Biochemistry and Molecular Biology, 2006, pp 241–267.
(108) Krikštaponis A. *Pseudomonas* sp. 7HK4 bakterijose 7-Hidroksikumarino metabolizme dalyvaujančių monooksigenazių tyrimas. Vilniaus universitetas, Vilnius, 2015.
(109) Sivashanmugam A, Murray V, Cui C, Zhang Y, Wang J, Li Q. Practical Protocols for Production of Very High Yields of Recombinant Proteins Using *Escherichia Coli*. Protein Science, 2009, 18 (5), pp 936–948.

(110) Langley WD, Adams R. Condensation of Certain Nitriles and Various Poly-Hydroxyphenols to Form Phenolic Acids. Journal of the American Chemical Society, 1922, 44 (10), pp 2320–2330.
(111) Studier FW. Protein Production by Auto-Induction in High Density Shaking Cultures. Protein expression and purification, 2005, 41 (1), pp 207–234.
(112) Lowry OH, Rosebrough NJ, Farr AL, Randall RJ. Protein Measurement with the Folin Phenol Reagent. The Journal of biological chemistry, 1951, 193 (1), pp 265–275.
(113) Laemmli UK. Cleavage of Structural Proteins during the Assembly of the Head of Bacteriophage T4. Nature, 1970, 227 (5259), pp 680–685.
(114) Gundry RL, White MY, Murray CI, Kane LA, Fu Q, Stanley BA, van Eyk JE. Preparation of Proteins and Peptides for Mass Spectrometry Analysis in a Bottom-up Proteomics Workflow. Current Protocols in Molecular Biology, 2009.
(115) Müller R, Lingens F. Oxidative Ring-Cleavage of Catechol in Meta-Position by Superoxide. Zeitschrift fur Naturforschung - Section C Journal of Biosciences, 1989, 44 (3–4), pp 207–211.
(116) Riegert U, Heiss G, Fischer P, Stolz A. Distal Cleavage of 3-Chlorocatechol by an Extradiol Dioxygenase to 3-Chloro-2-Hydroxymuconic Semialdehyde. Journal of Bacteriology, 1998, 180(11), pp 2849–2853.
(117) Serra S, Castagna A, Valentino M. Biocatalytic Synthesis of Natural Dihydrocoumarin by Microbial Reduction of Coumarin. Catalysts, 2019, 9 (8), pp 665.
(118) Pan YB, Grisham MP, Burner DM. A Polymerase Chain Reaction Protocol for the Detection of *Xanthomonas Albilineans*, the Causal Agent of Sugarcane Leaf Scald Disease. Plant Disease, 1997, 81 (2), pp 189–194.
(119) Sambrook J. Molecular Cloning: A Laboratory Manual, 3rd ed. Cold Spring Harbor Laboratory Press: Cold Spring Harbor, N.Y., 2001.
(120) Godon JJ, Zumstein E, Dabert P, Habouzit F, Moletta R. Molecular Microbial Diversity of an Anaerobic Digestor as Determined by Small-Subunit RDNA Sequence Analysis. Applied and Environmental Microbiology, 1997, 63 (7), pp 2802–2813.
(121) Sharma RC, Schimke RT. Preparation of Electro-Competent *E. Coli* Using Salt-Free Growth Medium. BioTechniques, 1996, 20 (1), pp 42–44.

(122) Gorelenkov V, Antipov A, Lejnine S, Daraselia N, Yuryev A. Set of Novel Tools for PCR Primer Design. BioTechniques, 2001, 31 (6), pp 1326–1330.
(123) Thompson JD, Higgins DG, Gibson TJ. CLUSTAL W: Improving the Sensitivity of Progressive Multiple Sequence Alignment through Sequence Weighting, Position-Specific Gap Penalties and Weight Matrix Choice. Nucleic Acids Research, 1994, 22(22), pp 4673–4680.
(124) Tamura K, Peterson D, Peterson N, Stecher G, Nei M, Kumar S. MEGA5: Molecular Evolutionary Genetics Analysis Using Maximum Likelihood, Evolutionary Distance, and Maximum Parsimony Methods. Molecular biology and evolution, 2011, 28 (10), pp 2731–2739.
(125) Altschul SF, Gish W, Miller W, Myers EW, Lipman DJ. Basic Local Alignment Search Tool. Journal of Molecular Biology, 1990, 215 (3), pp 403–410.
(126) Saitou N, Nei M. The Neighbor-Joining Method: A New Method for Reconstructing Phylogenetic Trees. Molecular Biology and Evolution, 1987, 4 (4), pp 406–425.
(127) Zuckerkandl E, Pauling L. Evolutionary Divergence and Convergence in Proteins. In Evolving Genes and Proteins. Elsevier, 1965, pp 97–166.
(128) Griese JJ, Jakob RP, Schwarzinger S, Dobbek H, Jakob R, Biochemie L. Xenobiotic Reductase A in the Degradation of Quinoline by *Pseudomonas Putida* 86: Physiological Function, Structure and Mechanism of 8-Hydroxycoumarin Reduction. Journal of Molecular Biology, 2006, 361, pp 140–152.
(129) Krikštaponis A, Meškys R. Biodegradation of 7-Hydroxycoumarin in *Pseudomonas Mandelii* 7HK4 via Ipso-Hydroxylation of 3-(2,4-Dihydroxyphenyl)-Propionic Acid. Molecules, 2018, 23 (10).
(130) MacHeroux P, Kappes B, Ealick SE. Flavogenomics - A Genomic and Structural View of Flavin-Dependent Proteins. FEBS Journal, 2011, pp 2625–2634.
(131) Nakamura S, Nakamura T, Ogura Y. Absorption Spectrum of Flavin Mononucleotide Semiquinone. Journal of Biochemistry, 1963, 53, pp 143–146.
(132) Roper DI, Cooper RA. Purification, Nucleotide Sequence and Some Properties of a Bifunctional Isomerase/Decarboxylase from the Homoprotocatechuate Degradative Pathway of *Escherichia Coli* C. European Journal of Biochemistry, 1993, 217 (2), pp 575–580.
(133) Diaz E, Timmis KN. Identification of Functional Residues in a 2-Hydroxymuconic Semialdehyde Hydrolase. A New Member of the α/β

Hydrolase-Fold Family of Enzymes Which Cleaves Carbon-Carbon Bonds. Journal of Biological Chemistry, 1995, 270 (11), pp 6403–6411.
(134) Lim JC, Lee J, Jang JD, Lim JY, Min KR, Kim CK, Kim Y. Characterization of the PcbE Gene Encoding 2-Hydroxypenta-2,4-Dienoate Hydratase in *Pseudomonas* Sp. DJ-12. Archives of pharmacal research, 2000, 23 (2).
(135) Lle M, Moonen JH, Fraaije MW, Rietjens IMCM, Laane C, van Berkel WJH. Flavoenzyme-Catalyzed Oxygenations and Oxidations of Phenolic Compounds. Advanced synthesis and catalysis, 2002, 344 (10), pp 1023–1035.
(136) Romero E, Gómez Castellanos JR, Gadda G, Fraaije MW, Mattevi A. Same Substrate, Many Reactions: Oxygen Activation in Flavoenzymes. Chemical Reviews. American Chemical Society, 2018, pp 1742–1769.
(137) Abu-Omar MM, Loaiza A, Hontzeas N. Reaction Mechanisms of Mononuclear Non-Heme Iron Oxygenases. Chemical Reviews, 2005, pp 2227–2252.
(138) Cho HJ, Kim K, Sohn SY, Cho HY, Kim KJ, Kim MH, Kim D, Kim E, Kang BS. Substrate Binding Mechanism of a Type I Extradiol Dioxygenase. Journal of Biological Chemistry, 2010, 285 (45), pp 34643–34652.
(139) Cornish-Bowden A. Fundamentals of Enzyme Kinetics. Wiley-Blackwell, 2012.
(140) Koptyug A. Atlas of Spectra of Aromatic and Heterocyclic Compounds; Novosibirsk Institute of Organic Chemistry, Siberian Br., Academy of Sci. USSR: Novosibirsk, 1983.
(141) Happe B, Eltis LD, Poth H, Hedderich R, Timmisi KN. Characterization of 2,2',3-Trihydroxybiphenyl Dioxygenase, an Extradiol Dioxygenase from the Dibenzofuran-and Dibenzo-p-Dioxin-Degrading Bacterium *Sphingomonas* Sp. Strain RW1. Journal of Bacteriology, 1993, 175(22), pp 7313-7320.
(142) Barnes MR, Duetz WA, Williams PA. A 3-(3-Hydroxyphenyl) Propionic Acid Catabolic Pathway in *Rhodococcus Globerulus* PWD1: Cloning and Characterization of the Hpp Operon. Journal of Bacteriology, 1997, 179(19), pp 6145-6153.
(143) Vaillancourt FH, Haro MA, Drouin NM, Karim Z, Maaroufi H, Eltis LD. Characterization of Extradiol Dioxygenases from a Polychlorinated Biphenyl-Degrading Strain That Possess Higher Specificities for Chlorinated Metabolites. Journal of Bacteriology, 2003, 185 (4), pp 1253–1260.

(144) Asturiasl JA, Eltiso LD, Prucha M, Timmisn KN. Analysis of Three 2,3-Dihydroxybiphenyl 1,2-Dioxygenases Found in *Rhodococcus Globerulus* P6. Identification of a new family of extradiol dioxygenases. Journal of Biological Chemistry, 1994, 269(10), pp 7807-7815.

(145) Wolgel SA, Dege JE, Perkins-Olson PE, Juarez-Garcia CH, Crawford RL, Munck E, Lipscomb JD. Purification and Characterization of Protocatechuate 2,3-Dioxygenase from *Bacillus Macerans*: A New Extradiol Catecholic Dioxygenase. Journal of Bacteriology, 1993, 175(14), pp 4414-4426.

(146) Bayly RC, Dagley S, Gibson DT. The Metabolism of Cresols by Species of *Pseudomonas*. The Biochemical journal, 1966, 101 (2), pp 293–301.

(147) Duggleby CJ, Williams RA. Purification and Some Properties of the 2-Hydroxy-6-Oxohepta-2,4-Dienoa Te Hydrolase (2-Hydroxymuconic Semialdehyde Hydrolase) Encoded by the TOL Plasmid PWW0 from *Pseudomonus Putida* Mt-2. Microbiology society, 1986, Vol. 132.

(148) Wieser M, Ebersp~icher J, Vogler B, Lingens F. Metabolism of 4-Chlorophenol by *Azotobacter* Sp. GPI: Structure of Cleavage Product of 4-Chlorocatechol the Meta. FEMS Microbiology Letters, 1994, 116(1), pp 73-78.

(149) Smith MB. March's advanced organic chemistry reactions, mechanisms, and structure. 6th edition. John Wiley & Sons, Inc., Hoboken, NJ, 2007.

(150) Gunther H. NMR Spectroscopy: Basic Principles, Concepts and Applications in Chemistry, 3rd Edition.; Wiley-VCH: Weinheim, Germany, 2013.

(151) Simons WW. The Sadtler Guide to Carbon-13 NMR Spectra; Sadtler Research Laboratories: Philadelphia, US, 1983.

(152) Retcofsky HL, Friedel RA. Carbon-13 Nuclear Magnetic Resonance Spectra of Monosubstituted Pyridines. 1969.

(153) Thomas S, Brühl I, Heilmann D, Kleinpeter E. 13C NMR Chemical Shift Calculations for Some Substituted Pyridines: A Comparative Consideration. Journal of Chemical Information and Computer Sciences. American Chemical Society, 1997, pp 726–730.

(154) Gabriel FLP, Heidlberger A, Rentsch D, Giger W, Guenther K, Kohler HPE. A Novel Metabolic Pathway for Degradation of 4-Nonylphenol Environmental Contaminants by Sphingomonas *Xenophaga Bayram*: Ipso-Hydroxylation and Intramolecular Rearrangement. Journal of Biological Chemistry, 2005, 280 (16).

(155) Sala-Trepat JM, Murray K, Williams PA. The Metabolic Divergence in the Meta Cleavage of Catechols by *Pseudomonas Putida* NCIB 100 15

Physiological Significance and Evolutionary Implications, 1972, Vol. 28.

(156) Venugopala KN, Rashmi V, Odhav B. Review on Natural Coumarin Lead Compounds for Their Pharmacological Activity. BioMed Research International, 2013.

(157) Toogood HS, Scrutton NS. New Developments in 'Ene'-Reductase Catalysed Biological Hydrogenations. Current Opinion in Chemical Biology, 2014.

(158) Diaz E, Ferrandez A, Prieto MA, Garcia JL. Biodegradation of Aromatic Compounds by *Escherichia Coli*. Microbiology and Molecular Biology Reviews, 2001, 65 (4), pp 523–569.

(159) Arai H, Yamamoto T, Ohishi T, Shimizu T, Nakata T, Kudo T. Genetic Organization and Characteristics of the 3-(3-Hydroxyphenyl) Propionic Acid Degradation Pathway of *Comamonas Testosteroni* TA441. Microbiology, 1999, 145 (Pt 10), pp 2813-2820.

(160) Muller F, Voordouw G, Berkel WJH, Steennis PJ, Visser S, Rooijen PJ. A Study of P-Hydroxybenzoate Hydroxylase from *Pseudomonas Fluorescens*. Improved Purification, Relative Molecular Mass, and Amino Acid Composition. European Journal of Biochemistry, 1979, 101 (1), pp 235–244.

(161) Shuman B, Dix TA. Cloning, Nucleotide Sequence, and Expression of a p-Hydroxybenzoate Hydroxylase Isozyme Gene from *Pseudomonas Fluorescens*. The Journal of Biological Chemistry, 1993, 268 (23), pp 17057–17062.

(162) Zhao Z, Koeplinger KA, Peterson T, Conradi RA, Burton PS, Suarato A, Heinrikson RL, Tomasselli AG. Mechanism, Structure-Activity Studies, and Potential Applications of Glutathione S-Transferase-Catalyzed Cleavage of Sulfonamides. Drug Metabolism and Disposition, 1999, 27 (9).

(163) Corvini PFX, Meesters RJW, Schäffer A, Schröder HF, Vinken R, Hollender J. Degradation of a Nonylphenol Single Isomer by *Sphingomonas* Sp. Strain TTNP3 Leads to a Hydroxylation-Induced Migration Product. Applied and Environmental Microbiology, 2004, 70 (11), pp 6897–6900.

(164) Arnold RT, Buckley JS, Richter J. The Dienone-Phenol Rearrangement. Journal of the American Chemical Society, 1947, 69 (10), pp 2322–2325.

(165) Spence EL, Kawamukai M, Sanvoisin J, Braven H, Bugg TDH. Catechol Dioxygenases from *Escherichia Coli* (MhpB) and *Alcaligenes Eutrophus* (MpcI): Sequence Analysis and Biochemical Properties of a

Third Family of Extradiol Dioxygenases. Journal of Bacteriology, 1996, 178(17), pp 5249-5256.

(166) Bakolitsa C, Kumar A, Jin KK, McMullan D, Krishna SS, Miller MD, Abdubek P, Acosta C, Astakhova T, Axelrod HL, Burra P, Carlton D, Chen C, Chiu HJ, Clayton T, Das D, Deller MC, Duan L, Elias Y, Ellrott K, Ernst D, Farr CL, Feuerhelm J, Grant JC, Grzechnik A, Grzechnik SK, Han GW, Jaroszewski L, Johnson HA, Klock HE, Knuth MW, Kozbial P, Marciano D, Morse AT, Murphy KD, Nigoghossian E, Nopaku A, Okach L, Paulsen J, Puckett C, Reyes R, Rife CL, Sefcovic N, Tien HJ, Trame CB, Trout C, van den Bedem H, Weekes D, White A, Xu Q, Hodgson KO, Wooley J, Elsliger MA, Deacon AM, Godzik A, Lesley SA, Wilson IA. Structures of the First Representatives of Pfam Family PF06684 (DUF1185) Reveal a Novel Variant of the Bacillus Chorismate Mutase Fold and Suggest a Role in Amino-Acid Metabolism. Acta Crystallographica Section F: Structural Biology and Crystallization Communications, 2010, 66 (10), pp 1182–1189.

(167) Perchat N, Saaidi PL, Darii E, Pellé C, Petit JL, Besnard-Gonnet M, de Berardinis V, Dupont M, Gimbernat A, Salanoubat M, Fischer C, Perret A. Elucidation of the Trigonelline Degradation Pathway Reveals Previously Undescribed Enzymes and Metabolites. Proceedings of the National Academy of Sciences of the United States of America, 2018, 115 (19), pp E4358–E4367.

(168) Dunwell JM, Culham A, Carter CE, Sosa-Aguirre CR, Goodenough PW. Evolution of Functional Diversity in the Cupin Superfamily. Trends in Biochemical Sciences, 2001, pp 740–746.

(169) Agarwal G, Rajavel M, Gopal B, Srinivasan N. Structure-Based Phylogeny as a Diagnostic for Functional Characterization of Proteins with a Cupin Fold. PLoS One, 2009, 4(5), pp 5736.

(170) Dunwell JM, Purvis A, Khuri S. Cupins: The Most Functionally Diverse Protein Superfamily? Phytochemistry, 2004, 65 (1), pp 7–17.

(171) Agarwal R, Bonanno JB, Burley SK, Swaminathan S. Structure Determination of an FMN Reductase from *Pseudomonas Aeruginosa* PA01 Using Sulfur Anomalous Signal. Acta Crystallographica Section D: Biological Crystallography, 2006, 62 (4), pp 383–391.

(172) Liger D, Graille M, Zhou CZ, Leulliot N, Quevillon-Cheruel S, Blondeau K, Janin J, van Tilbeurgh H. Crystal Structure and Functional Characterization of Yeast YLR011wp, an Enzyme with NAD(P)H-FMN and Ferric Iron Reductase Activities. Journal of Biological Chemistry, 2004, 279 (33), pp 34890–34897.

(173) Sancho J. Flavodoxins: Sequence, Folding, Binding, Function and Beyond. Cellular and Molecular Life Sciences, 2006, pp 855–864.
(174) Mari M, Prieto MA, Di´az E, Di´az D, Garci´a JL, Garci´a G. Molecular Characterization of the 4-Hydroxyphenylacetate Catabolic Pathway of *Escherichia Coli* W: Engineering a Mobile Aromatic Degradative Cluster. Journal of Bacteriology, 1996, 178(1), 111-120.
(175) Babiker MEH, Samrein BMA, Mousa AG, Heyam SA. Linking Aromatic Hydroxy Metabolic Functionalization of Drug Molecules to Structure and Pharmacologic Activity. Molecules, 2018, 23(9).

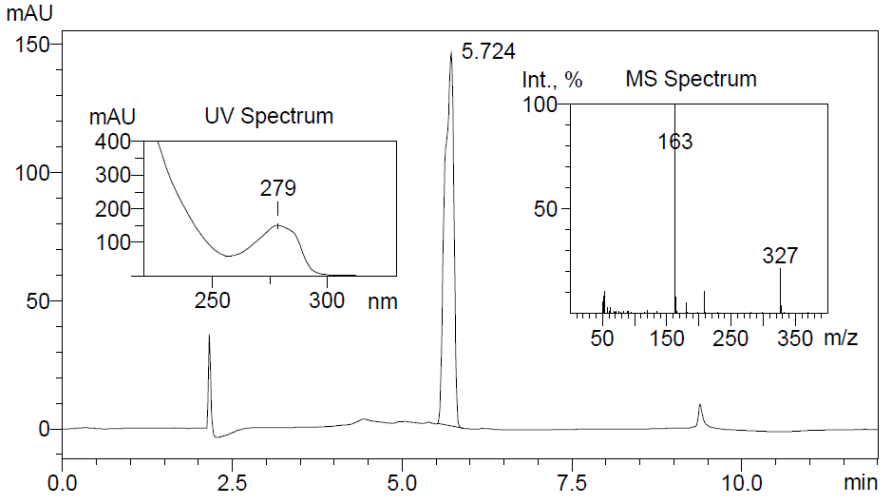

Figure S1. HPLC chromatogram of 7-hydroxy-3,4-dihydrocoumarin at 280 nm wavelength. 1 mM of compound was dissolved in acetonitrile. Corresponding UV and MS spectra of the main peak were presented. The negative ions $[M\text{-}H]^-$ generated are at m/z 163 (7-hydroxy-3,4-dihydrocoumarin) and 327 (dimer of 7-hydroxy-3,4-dihydrocoumarin).

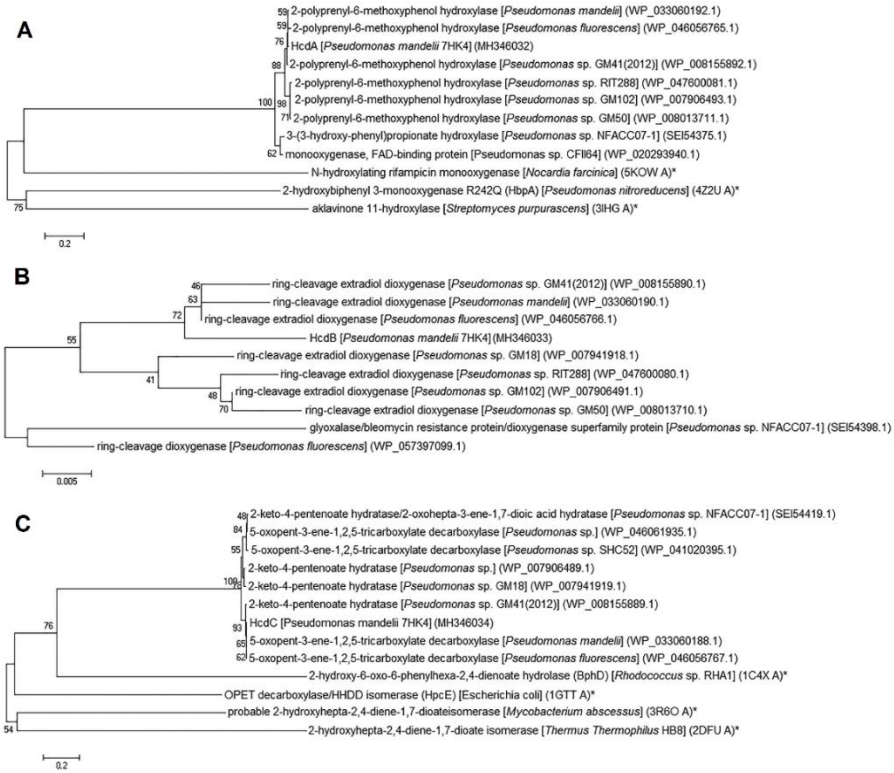

Figure S2. A. Phylogenetic tree of HcdA protein. Neighbour joining analysis was performed on the 8 closest homologues of HcdA and 3 other homologous proteins with known structure and/or function. B. Phylogenetic tree of HcdB protein. Neighbour joining analysis was performed on the 9 closest homologues of HcdB. C. Phylogenetic tree of HcdC protein. Neighbour joining analysis was performed on the 8 closest homologues of HcdC and 4 other homologous proteins with known structure and/or function. The numbers on the nodes indicate how often (no. of times, %) the species to the right grouped together in 1000 bootstrap samples. Bars represent the number of amino acid substitutions per site. Accession numbers are given in parentheses. Proteins with known structure and/or function are marked with an asterix (*).

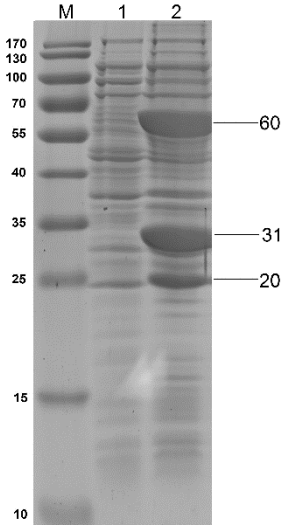

Figure S3. SDS-PAGE of *E. coli* BL21 cell-free extract, containing induced recombinant HcdA, HcdB and HcdC proteins (lane 2) and control cells without *hcdABC* genes (lane 1). M – molecular mass ladder (kDa). The arrows indicate HcdA, HcdB and HcdC proteins.

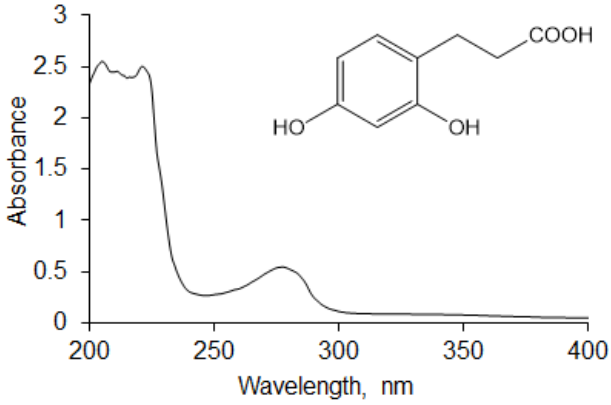

Figure S4. UV-Vis spectrum of 3-(2,4-dihydroxyphenyl) propionic acid.

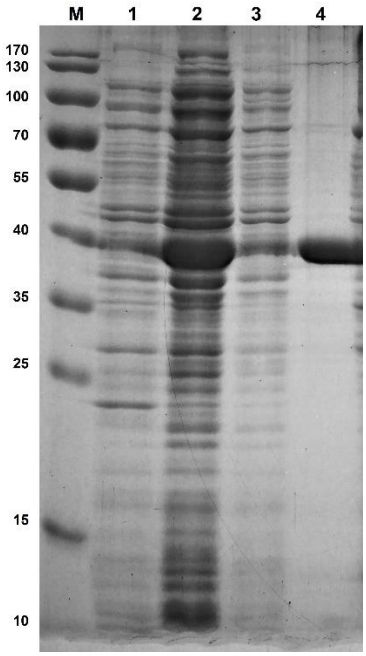

Figure S5. SDS-PAGE of His_6-tagged HcdE protein purified by affinity chromatography. Lane 1 – 3 µl of *E. coli* BL21 cell-free extract without *HcdE* gene, lane 2 – 5 µl of *E. coli* BL21 cell-free extract containing induced recombinant HcdE protein, lane 3 – 5 µl of *E. coli* BL21 cell-free extract containing induced recombinant HcdE protein after purification, lane 4 – 10 µl of eluted His_6-tagged HcdE protein. M – molecular mass ladder (kDa).

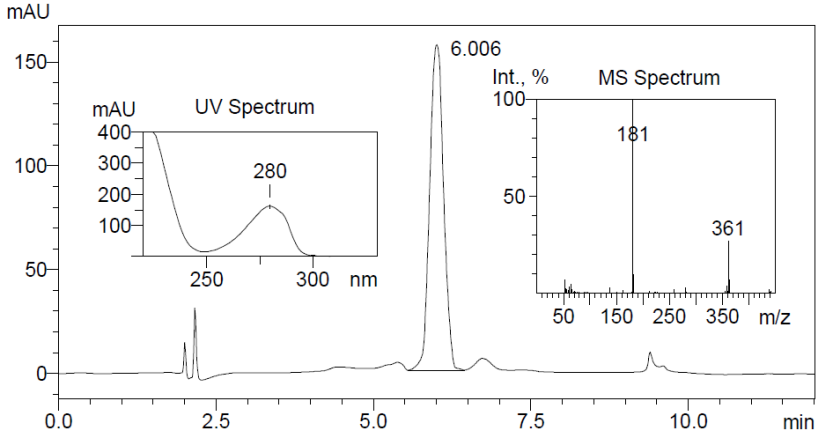

Figure S6. HPLC chromatogram of 3-(2,4-dihydroxyphenyl) propionic acid at 280 nm wavelength. 1 mM of compound was dissolved in acetonitrile. Corresponding UV and MS spectra of the

main peak were presented. The negative ions $[M-H]^-$ generated are at m/z 181 (3-(2,4-dihydroxyphenyl) propionic acid) and 361 (dimer of 3-(2,4-dihydroxyphenyl) propionic acid).

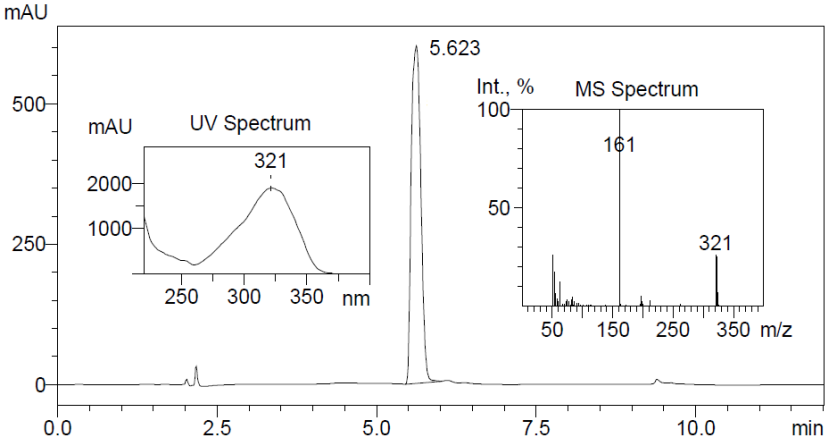

Figure S7. HPLC chromatogram of 7-hydroxycoumarin at 280 nm wavelength. 1 mM of compound was dissolved in acetonitrile. Corresponding UV and MS spectra of the main peak were presented. The negative ions $[M-H]^-$ generated are at m/z 161 (7-hydroxycoumarin) and 321 (dimer of 7-hydroxycoumarin).

THE LIST OF PUBLICATIONS

Articles

Krikštaponis A, Meškys R. Biodegradation of 7-Hydroxycoumarin in *Pseudomonas mandelii* 7HK4 via *ipso*-Hydroxylation of 3-(2,4-Dihydroxyphenyl)-propionic Acid. Molecules, **2018**, 23(10).

Krikštaponis A, Urbelis G, Meškys R. The First Step of Biodegradation of 7-Hydroxycoumarin in *Pseudomonas mandelii* 7HK4 Depends on an Alcohol Dehydrogenase-Type Enzyme. International Journal of Molecular Sciences, **2021**, 22, 1552.

Conference posters

Krikštaponis A, Meškys R. „Biodegradation of 7-hydroxycoumarin in *Pseudomonas mandelii* 7HK4“. The 15th International Conference of Lithuanian Biochemical Society. 26-29 June, 2018 in Dubingiai, Lithuania.

NOTES

Vilnius University Press
9 Saulėtekio Ave., Building III, LT-10222 Vilnius
Email: info@leidykla.vu.lt, www.leidykla.vu.lt
Print run copies 11